

Abstracts and Author Index

The Nexus of Histochemistry and Molecular Genetics

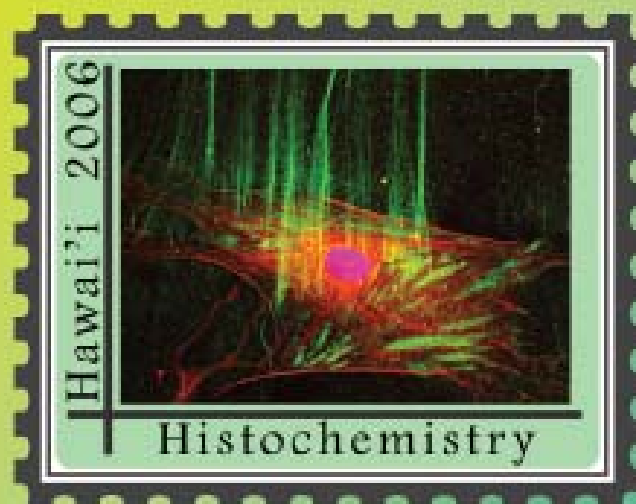
Real-time visualization of
signal-transduction in living cells
and tissues

7th Joint Meeting of The Histochemical Society &
The Japan Society of Histochemistry and Cytochemistry

Hilton Waikoloa Village, Big Island of Hawai'i
August 23-27, 2006

Organized by Joseph E. Mazurkiewicz & Toyoshi Fujimoto

See inside cover for instructions pn searching PDFs



THE NEXUS OF HISTOCHEMISTRY AND MOLECULAR GENETICS

Real-time visualization of signalling
transduction in living cells and tissues

To search a PDF, open the PDF in Adobe Acrobat Reader.
Choose "Edit" and then select "Search" ("Find" in Acrobat 6 or older).
Enter your search criteria and click enter.

Edited by

Joseph E. Mazurkiewicz
Albany Medical College, Albany, New York

Toyoshi Fujimoto
Nagoya University Graduate School of Medicine, Nagoya, Japan

Robin Kealoha Black
UH Hilo Conference Center, Hilo, Hawaii

University of Hawaii at Hilo Conference Center, Hilo, Hawaii
Judith Fox-Goldstein, Director
Jules Ung Sanderson, Conference Coordinator
Mary Ann Tsuchiyama, Assistant Director

Contents

Deciphering protein turnover, topology and transport in living cells	S01
LIPPINCOTT-SCHWARTZ, JENNIFER; LORENTZ, HOLGER; HAILEY, DALE; KIM, PETER AND PATTERSON, GEORGE	1
Application of live-cell fluorescent biosensors in studies of the control of specificity of signal transduction processes	S02
MEYER, TOBIAS	2
Visualization of PKC signaling	S03
SAITO, N.	3
Visualization of calcium signaling	S04
HIROSE, KENZO	4
Chemical and biophysical approaches to the study of protein trafficking and function in living cells	S05
HOWARTH, M. ¹ , LIN, C.W. ¹ , CHEN, T.C.S. ¹ , CHEN, I. ¹ , FERNANDEZ-SUAREZ, M. ¹ , SLAVOFF, S. ¹ , GERROW, K. ² , EL- HUSSEINI, A. ² AND TING, A.Y. ¹	5
Immuno-laser capture microdissection for analysis of RNA expression	S06
BASKIN, D. G.	6
“Exploitation of laser capture microdissection for the analysis of gene mutation and mRNA expression”	S07
TAKEKOSHI, S., EGASHIRA, N., YASUDA, M., UMEMURA, S., OSAMURA, R.Y.	7
Cytomolecular analysis of non-gynecologic liquid-based cytology preparations using laser microdissection technique	S08
NEMOTO, N. ^{1,2} , NAKANISHI, Y. ¹ , KOMATSU, K. ² , SEKI, T. ² , HONMA, T. ^{1,2} , HENMI, A. ¹ AND SUGITANI, M. ^{1,2}	8
The use of laser capture microdissection in vascular biology	S09
FEIG, JONATHAN E. ¹ , TROGAN, EUGENE ¹ AND FISHER, EDWARD A. ¹	9
Proteomic analysis of laser capture microdissected neurofibrillary tangles from Alzheimer’s disease	S10
MONTINE, T.	10
Nanoscale Fluorescence Microscopy	S11
HELL, S.W.	11
An overview of computational methods for three-dimensional microscopy	S12

CONCHELLO, JOSÉ-ANGEL	12
Single Plane Illumination Microscopy (SPIM) and the third dimension in the life sciences	S13
STELZER, E.H.K., KELLER, P.J., PAMPALONI, F. AND GREGER, K.	13
Deconvolution-Assisted Structured Illumination Wide-field Optical Sectioning Fluorescence Microscopy	S14
ROSA-MOLINAR, E. ¹ , TORRES-VASQUEZ, I. ¹ , SERRANO-VELEZ, J.L. ¹ , AND CONCHELLO, J-A. ²	14
Development of genetically-encoded functional indicators with expanded dynamic range and video-rate functional imaging using a spinning disc confocal system with a mercury arch lamp as a light source	S15
NAGAI, T. ¹ , TANI, T. ¹ AND MIYAWAKI, A. ²	15
NIR laser-based manipulation of functional molecules in living cells	S16
YAMAOKA, Y. AND TAKAMATSU, T.	16
Higher harmonic generation microscopy	S17
SUN, CHI-KUANG	17
Persistent CD deficiency-induced autophagic neuropathology in the absence of bax-dependent apoptosis	S18
SHACKA, J.J.* ¹ , KLOCKE, B.J. ¹ , SHIBATA, M. ² , UCHIYAMA, Y. ² AND ROTH, K.A. ¹	18
Molecular Mechanism of Autophagy	S19
OHSUMI, YOSHINORI	19
Overview of intracellular signal transduction system	S20
SASANO, HIRONOBU	20
Use of Reverse Phase Protein Microarrays for Signal Pathway Profiling of Human Cancer Specimens: Implications and Applications for Patient Tailored Therapy	S21
PETRICOIN, EMANUEL F.	21
Analysis of c-kit and PDGFRA gene mutations in gastrointestinal stromal tumors for their diagnosis and imatinib therapy	S22
HIROTA, S.	22
Multichannel data acquisition permits assessment of tumor heterogeneity in signalling pathway components.	S23
GARDNER, H., AND RHEINHARDT, J.	23
Three-dimensional time-lapse-imaging for signal molecules during T-cell activation	S24

SUZUKI, TAKESHI	24
Live imaging of intracellular signaling	S25
SAITO, N.	25
Things to think about when thinking about imaging: old concepts and new	S26
LEVENSON, RICHARD	26
Figure Preparation in a Nutshell	S27
PAQUETTE, S.M.	27
GFL neurotrophic factors	S28
JOHNSON, E.M.	28
Beyond Programmed Cell Death: New Insights Into Non-Apoptotic Death Pathways	S29
ROTH, K.A. AND SHACKA, J.J.	29
Autophagy and its relation to neurodegeneration	S30
UCHIYAMA, Y.	30
In vivo roles of caspase in neural cell death and development	S31
MIURA, MASAYUKI	31
Proteomics of Pathological Protein in Alzheimer's Disease	S32
MONTINE, THOMAS J. ¹ , BOUTTE, ANGELA ¹ , LIEBLER, DANIEL ² , MONTINE, KATHLEEN S. ¹ , AND WOLTJER, RANDALL ¹	32
Introduction to Workshop on Advancing in situ Hybridization to Visualize Molecular Events: Interactions of Advances and Standardization	S33
UNGER, E. R. ¹	33
In situ hybridization with quantum dot detection and confocal scanning microscopy for three-dimensional visualization of protein and mRNA: Applications in pituitary hormone research	S34
MATSUNO, A. ¹ , ITOH, J. ² , TAKEKOSHI, S. ³ , OSAMURA, R.Y. ³	34
Advances in electron microscopic in situ hybridization: Application in analysis of nucleolus rRNAs and "introns" of rRNA precursor RNA	S35
KOJI, T.	35
MISFISHIE: How standard FISH reporting standardizes results and why it is important	S36
TRUE, L.D. ¹ , DEUTSCH, E.W. ² , CAMPBELL, D. ² , PASCAL, L. ¹ , OUDES, A. ¹ , LIU, A.Y. ^{1,2} .	36
Automation for Standardized In Situ Hybridization Applications: Functional Genomic Research and Cancer Diagnostics	S37
GROGAN, THOMAS M. ^{1,2} AND NITTA, HIROAKI ²	37

Quantification of viability in organotypic spheroids of human malignant glioma for drug testing	S38
DE WITT HAMER, P.C., JONKER, A., ZWINDERMAN, A.H., LEENSTRA, S. AND VAN NOORDEN, C.J.F.	38
Dynamic Imaging of Tagged Receptors	S39
KAWATA, MITSUHIRO	39
FRET-FLIM reveals the organization of different receptor-ligand complexes in endocytic membranes	S40
WALLRABE H. ¹ , TALATI, RONAK ² , PERIASAMY, AMMASI ¹ , BARROSO, MARGARIDA ²	40
Associative Multi-dimensional Image Analysis Software for Modern Optical Microscopy	S41
ROYSAM, B.	41
Second-Harmonic Generation Imaging of the Colon	P01
HARADA, Y., NAKANO, K., YAMAOKA, Y., HITOMI, T., AND TAKAMATSU, T.	42
Difference of photoacoustic waves between various tissues	P02
YAMAOKA, Y. ^{1,2} AND TAKAMATSU, T. ¹	43
Local gene transfer to calcified tissue cells using prolonged infusion of a lentiviral vector	P03
WAZEN, R.M., MOFFATT, P. AND NANCI, A.	44
Chromosome-specific DNA repeat probes	P04
BAUMGARTNER, A. ^{1,2} , WEIER, J.F. ^{1,2} AND WEIER, H.U.G. ²	45
Method for Quantification of Proliferation in Tissue Sections using the Laser Scanning Cytometer	P05
KRULL, D.L., KEENER, M.J., BUTLER, L. AND PETERSON, R.A.	46
Immunomodulatory effects of macrolide antibiotics in sulfur mustard-exposed airway epithelial cells:	P06
GAO, X. ¹ , RAY, R. ² , XIAO, Y. ³ , BARKER, P.E. ³ , AND RAY, P. ¹	47
Effects of PBS composition on the sensitivity of signal detection under CLSM with Quantum Dot (Qdot)	P07
NIIOKA, M. ^{1,2} , ITOH, J. ² , KINOUE, T. ¹ AND WATANABE, T. ¹	48
Immunolocalization of various proteins in living mouse organs revealed by "in vivo cryotechnique"	P08
OHNO, S., TERADA, N., OHNO, N., SAITOH, S. AND FUJII, Y.	49

- Comparison of the z-axis resolutions achieved by immunofluorescence
microscopic imaging of tissue sections of different thicknesses: usefulness
of ultrathin cryosections for ultrahigh-resolution immunofluorescence
microscopy **P09**
TAKIZAWA, T.¹, MORI, M.¹, ISHIKAWA, G.², TAKESHITA, T.²,
GOTO, T.¹ AND ROBINSON, J.M.³ 50
- Production of mouse monoclonal antibodies against rat type IV collagen by
the mouse iliac lymph node method **P10**
SADO, Y., INOUE, S., TOMONO, Y. AND OMORI, H. 51
- Standardization of Immunohistochemistry for Formalin-Fixed, Paraffin-
Embedded Tissue Sections Based on the Antigen Retrieval Technique: **P11**
SHI, SHAN-RONG AND TAYLOR, CLIVE R. 52
- Immunohistochemical detection of antigen-specific antibody-producing
plasma cells in regional lymph nodes and spleen of rats immunized with
horseradish peroxidase **P12**
MIZUTANI, Y., SHIOGAMA, K., SHIMOMURA, R., KAMOSHIDA,
S., INADA, K. AND TSUTSUMI, Y. 53
- Antigen retrieval of surface layer proteins for post-embedding
immunolectron microscopy from *Tannerella forsythensis* by
microwaving and autoclaving with citraconic anhydride **P13**
MORIGUCHI, K.¹, IWAMI, J.², HIGUCHI, N.², MURAKAMI, Y.³,
MAEDA, H.⁴, YOSHIMURA, F.³, NAKAMURA, H.², KAMEYAMA,
Y.⁴ AND OHNO, N.¹ 54
- Cytochrome oxidase activity remains even after long fixation **P14**
UEDA, T.¹ AND ISHIKAWA, Y.² 55
- X-ray microanalysis of biological specimens by high voltage electron
microscopy **P15**
NAGATA, T.^{1,2} AND KAMETANI, K.³ 56
- Nanocrystal fluorophores for molecular genetic and cancer testing **P16**
XIAO, YAN, BLASIC, JOE, HOLDEN, MARCIA AND BARKER,
PETER E. 57
- Optical imaging of tumor progression in living systems **P17**
MOIN, KAMIAR¹, SAMENI, MANSOUREH¹, LINEBAUGH,
BRUCE¹, RUDY, DEBORAH¹, TUNG, CHING², AND SLOANE,
BONNIE¹ 58
- Multiplexing molecular markers with multispectral imaging **P18**
MANSFIELD, JAMES R.,¹ KERFOOT, CHRISTOPHER A.², AND
LEVENSON, RICHARD M.¹ 59

- X-ray microanalysis on the activity of acid phosphatase in mouse kidney **P19**
OLEA, M. T.¹, AND NAGATA, T.² 60
- Distribution of mitochondria in mouse spermatogenic cells, detected by the expression of pEYFP-Mito electroporated in vivo, and its possible relation to germ cell apoptosis **P20**
HISHIKAWA, Y.¹, AN, S.¹, SHIBATA, Y.¹, AND KOJI, T.¹ 61
- Genome Size and DNA Content of the X chromosomes, Autosomes and Limited Chromosomes of *Sciara coprophila* **P21**
RASCH, E.M. 62
- Circadian rhythm generation in a glioma cell line **P22**
FUJIOKA, A.¹, HONDA, E.², TAKASHIMA, N.^{1,3} AND SHIGEYOSHI, Y.¹ 63
- Functional analysis of the Ku70-binding site of Ku80 by GFP technology **P23**
KOIKE, M.¹, AND KOIKE, A.¹ 64
- Both Actin and Myosin Inhibitors Block or Slow Chromosome Motion in Mitotic PtK1 Cells: **P24**
SNYDER, J.A.¹ AND OLSOFKA, CLAIRE 65
- Ubiquitination of protamine in the sperm nucleus of rat and human **P25**
HARAGUCHI, CELINA M.¹, MABUCHI, TADASHI², HIRATA, SHUJI³, SHODA, TOMOKO³, HOSHI, KAZUHIKO³ AND YOKOTA, SADAKI¹ 66
- Effect of the *ams* mutation in the Ataxia and Male Sterility (AMS) mouse on photic injury to photo receptor cells **P26**
ARAKI, ASUKA¹, NAKANO, AKINOBU¹, ZHOU, LI¹, MARUYAMA, RIRUKE¹, OHIRA, AKIHIRO² AND HARADA, TAKAYUKI¹ 67
- Cholesterol depletion induces autophagy **P27**
CHENG, J., OHSAKI, Y., TAUCHI-SATO, K., FUJITA, A. AND FUJIMOTO, T. 68
- Cytoplasmic lipid droplets functions as a unique platform for degradation of apolipoprotein B **P28**
OHSAKI, Y., CHENG, J., FUJITA, A. AND FUJIMOTO, T. 69
- Effect of a plasticizer, di(2-ethylhexyl)phthalate on the liver peroxisomes of sweet water fishes **P29**
YOKOTA, SADAKI AND HARAGUCHI, CELINA M. 70
- All-trans-retinol induces rapid recruitment of TIP47 to lipid droplets in the retinal pigment epithelium **P30**

TSUIKI, E.¹, FUJITA, A.², OHSAKI, Y.², CHENG, J.², IRIE, T.³,
 SENOO, H.³, MISHIMA, K.¹, KITAOKA, T.¹, AND FUJIMOTO, T.^{2,71}

- Macromolecular synthesis in mitochondria of developing and aging mouse
 hepatocytes as revealed by electron microscopic radioautography **P31**
 NAGATA, T.^{1,2} 72
- Sequential appearance of Golgi-stacking proteins on newly-formed Golgi
 apparatus **P32**
 TAMAKI, H. AND YAMASHINA, S. 73
- Translocation of alkaline phosphatase during the process of restoration after
 colchicine treatment in cultures of rat liver cells **P33**
 CHIDA, K. AND TAGUCHI, M. 74
- Proteases induced intracellular Ca²⁺ dynamics of smooth muscles of
 arterioles via RARs1 and 2 **P34**
 SATOH, Y., MISAKI, T. AND SATINO, T. 75
- Genesis of secretory granule with Chromogranin A-GFP transfection: a
 cytochemical approach **P35**
 INOMOTO, C.¹, UMEMURA, S.¹, EGASHIRA, N.¹, MINEMATSU,
 T.¹, TAKEKOSHI, S.¹, ITOH, Y.², ITOH, J.², TAUPENOT, L.³,
 O'CONNOR, D.T.³, AND OSAMURA, R.Y.¹ 76
- ATP induced intracellular Ca²⁺ dynamics of mast cells but not exocytosis
P36
 NAKAMURA, Y., OOSAKA, M., SATINO, T. AND SATOH, Y. 77
- Immunoelectron microscopy of quick-frozen and physically fixed membranes
 revealed heterogeneous GM1 domains in the cell membrane **P37**
 FUJITA, AKIKAZU, CHENG, JINGLEI, AND FUJIMOTO, TOYOSHI
 78
- Focal contact adhesion to porous films; the affect on cell shape, adhesion,
 migration, growth and survival of human keratinocytes and fibroblasts
 in culture **P38**
 MCMILLAN, J.R.^{1,2}, QIAO, H.^{1,2}, TANAKA, M.¹, YAMAMOTO, S.¹,
 SHIMOMURA, M.¹ AND SHIMIZU, H.² 79
- Disturbed cell-cell attachment by overexpression of PKC α **P39**
 OHBA, M.¹, AKAHANE, T.¹, KOHNO, Y.², AND KUROKI, T.³ 80
- Immunocytochemical analysis of osteopontin function in osteoclast
 formation **P40**
 SUZUKI, K.¹, SODEK, J.² AND YAMADA, S.¹ 81
- Morphological variability of symbiotic bacteria, Buchnera, in bacteriocyte
 depending on the morph of the host insect **P41**

- NISHIKORI, K., KUBO, T., AND MORIOKA, M. 82
- Immunolocalization of NG2 proteoglycan in myofibroblasts and smooth muscle cells of mouse and human intestines **P42**
TERADA, N., OHNO, N., SAITO, S., FUJII, Y., AND OHNO, S. 83
- PACAP decreases ischemic neuronal cell death in the hippocampus **P43**
SHIODA, S.¹, NAKAMACHI, T.¹, OHTAKI, H.¹, DOHI, K.¹ 84
- Comparison of MR images and histochemical localization of intra-arterially administered microglia in the rat model of Alzheimer's disease **P44**
TOOYAMA, I.¹, SONG, YANG^{1,3}, MORIKAWA, SHIGEHIRO², MORITA, MASAHITO² AND INUBUSHI, TOSHIRO² 85
- Neuropeptide W –containing neuron network in the rat Brain **P45**
TAKENOYA F.^{1,2}, KAGEYAMA, H.¹, DATE, Y.³, NAKAZATO, M.³, SHIODA, S.¹ 86
- Galanin-like peptide promotes feeding behavior through activation of orexinergic neurons in the rat lateral hypothalamus **P46**
KAGEYAMA, HARUAKI¹, GUAN, JIAN-LIAN¹, TOSHINAI, KOJI², DATE, YUKARI², TAKENOYA, FUMIKO^{1,3}, NAKAZATO, MASAMITSU² AND SHIODA, SEIJI¹ 87
- Histochemical analysis of the nerve regeneration in the goldfish spinal cord **P47**
TAKEDA, A.¹ AND FUNAKOSHI, K.¹ 88
- Immunohistochemical characterization of Toll-like receptor 2 expression in mouse lumbar dorsal root ganglia. **P48**
RODELLA, L.F., BORSANI, E., RICCI, F., ALBERTINI, R., STACCHIOTTI, A. AND BIANCHI, R. 89
- Localization of fibroblast growth factor-1 (FGF1) in cholinergic neurons innervating the rat larynx **P49**
OKANO, H.^{1,2}, TOYODA, K.^{1,2}, BAMBA, H.², HISA, Y.², OOMURA, Y.³, IMAMURA, T.⁴, FURUKAWA, S.⁵, KIMURA, H.¹ AND TOOYAMA, I.¹ 90
- Expression of green fluorescent protein positive cells in the olfactory epithelium and vomeronasal organ of the GAD67-GFP knock-in mouse **P50**
WATANABE, M.¹, KANAYAMA, T.¹, NAKAMURA, Y.², YANAGAWA, Y.³, OBATA, K.⁴, OKI, K.¹, YABUMOTO, M.⁵, AND WATANABE, H.⁶ 91
- Endodermal origin of mouse thyroid C cells – Analysis of Cx43-lacZ and Mash1 mice **P51**
KAMEDA, Y. 92

- Distribution pattern of NT-3 and BDNF during the ontogeny of the retina in the lizard **P52**
 YANES C.¹, SANTOS, E.¹, ROMERO-ALEMAN, M.M.², CASAÑAS, N.¹, VIÑOLY, R.¹, DE PABLOS, E.¹ AND MÓNZON-MAYOR, M.² 93
- Aquaporin water channels in the olfactory mucosa **P53**
 TAKATA, K., ABLIMIT, A., MATSUZAKI, T., TAJIKA, Y., AOKI, T., HAGIWARA, H., SUZUKI, T. 94
- Immunohistochemical analysis of histamine H3 receptor (H3-R) in the stomach of the rat **P54**
 ABE, M.¹, AJIOKA, H.¹, KITANO, S.¹, NANRI, M.¹, KIRIMOTO, T.¹, HORIE, S.² AND OKA, T.¹ 95
- Protein 4.1G expression in Schwann cells of rodent peripheral nervous system **P55**
 OHNO, N., TERADA, N. AND OHNO, S. 96
- Effects of Steroid Hormones on Dendritic Morphogenesis of Cultured Hippocampal Neurons **P56**
 ITOSE, M., NISHI, M. AND KAWATA, M. 97
- Dynamic behavior of intranuclear aggregates of mutant and wild-type Ataxin1 **P57**
 KRAWCZYK, P.M., KROL, H., REITS, E., ATEN, J. A. 98
- Histone acetylation/deacetylation alters the balance between herpes simplex virus latency and reactivation **P58**
 SAWTELL, N.M.¹, HAAS, R.L.¹, AND THOMPSON, R.L.² 99
- Expression of alcohol dehydrogenase-1 and retinaldehyde dehydrogenase-1 in the rat anterior pituitary **P61**
 FUJIWARA, K. AND YASHIRO, T. 100
- Studies with leptin siRNA probes show that gonadotropes may depend on pituitary leptin for basal and gonadotropin releasing hormone (GnRH) stimulation of luteinizing hormone (LH) expression **P62**
 IRUTHAYANATHAN, M.J.J., CRANE, C., AKHTER, N., JOHNSON, B. AND CHILDS, G.V. 101
- E- and N- cadherin divergence during histogenesis of the rat anterior pituitary gland **P63**
 KIKUCHI, M., YATABE, M. AND YASHIRO, T. 102
- Embryonic development of collagen architecture in chicken adenohypophysis **P64**
 NISHIMURA, S., NAGATA, M., TABATA, S., AND IWAMOTO, H. 103

- EXPRESSION OF LEPTIN AND LEPTIN RECEPTOR IN BOVINE
ADENOHYPOPHYSEAL CELLS **P65**
OGASAWARA H., OHWADA, S., NAGAI, Y., TAKETA, Y.,
WATANABE, K., ASO, H., AND YAMAGUCHI, T. 104
- Distribution of neural cell adhesion molecule, NCAM, is additive to N-
cadherin and opposite to E-cadherin in the rat anterior pituitary cells **P66**
TAKAHASHI, K., KIKUCHI, M. AND YASHIRO, T. 105
- Differential Expression of Myostatin and Activin Receptor Type IIB in the
Bovine Anterior Pituitary Gland **P67**
TAKETA, Y., ASO, H., NAGAI, Y., OGASAWARA, H., HAYASHI, S.,
MIYAKE, M., WATANABE, K., OHWADA, S. AND YAMAGUCHI, T.
106
- Direct cellular expression of c-Fos in the rat anterior pituitary **P68**
TAKIGAMI, S.¹ AND YASHIRO, T.¹ 107
- Differential expression of L-serine synthetic enzyme 3-phosphoglycerate
dehydrogenase in the fetal and adult mouse eye **P69**
SAKAI, K.¹, FURUYA, S.² AND HASHIKAWA, T.¹ 108
- Immunohistochemical Demonstration of Monocarboxylate Transporters in
the in vitro and in vivo Rabbit Corneal Epithelium **P70**
SHINOMIYA, KATSUHIKO¹, KATSUTA, OSAMU¹, HORIBE,
YOSHIHIDE², FUJII, SHINOBU², KAWAZU, KOUICHI² AND
IKUSE, TOSHIMI¹ 109
- Capillary supply of slow and fast muscles and its remodelling after
denervation and reinnervation **P71**
ERZEN, I.¹, CEBASEK, V.¹, KUBINOVA, L.², JANACEK, J.² AND
RIBARIC, S.³ 110
- Comparison of early with late endothelial progenitor cells in tube forming
activity in vitro **P72**
MUKAI, N.^{1,2,3}, KOBAYASHI, A.¹, KUWANA, R.¹, AMAGASA, T.²,
AND MORITA, I.^{1,3} 111
- Heterogenous succinate dehydrogenase activities quantified in situ in muscle
fibers of lateral pterygoid muscle attached to bones **P73**
MIZUTANI, M.¹, NAKAE, Y.² AND OHNO, N.¹ 112
- Hyperplasia in DM cattle is due to failure of MSTN induction by HGF **P74**
HAYASHI, SHINICHIRO, ASO, HISASHI, OGASAWARA, HIDEKI,
MIYAKE, MASATO, WATANABE, KOUICHI, OHWADA, SHYUICHI
AND YAMAGUCHI, TAKAHIRO 113
- Immunoelectron microscopic analysis of CD11c-positive dendritic cells in
the periapical region of the rat periodontal ligament **P75**

- KANEKO, T.¹, ZHAO, L-Y.^{1,2}, OKIJI, T.³, AND SUDA, H.¹ 114
- Ultrastructural transformation of gastric parietal cells reverting from the active to the resting state of acid secretion revealed in isolated rat gastric mucosa model processed by high-pressure freezing **P76**
SUGANUMA, T., SAWAGUCHI, A., AOYAMA, F., OHASHI, M. AND IDE, S. 115
- Endothelin (ET) -1, Nitric oxide (NO) and inflammatory markers during sepsis are altered in the liver in a time-dependent manner **P77**
JESMIN, S.¹, ZAEDI, S.¹, MOWA, C.N.², MAEDA, S.¹, MIYAUCHI, T.¹ 116
- Histochemical studies on Al in the livers of mice administered with Al by immunostaining and X-ray microanalysis with high voltage electron microscopy **P78**
KAMETANI, K.¹ AND NAGATA, T.^{2,3} 117
- Dynamic changes of expression of molecules related to the epithelial-mesenchymal transition in the early phase of liver development **P79**
NAKATANI, K., SAKABE, M., AND NAKAJIMA, Y. 118
- Dlk-1 expression in the callipyge model of skeletal muscle hypertrophy; integrated immunohistochemical, transcriptomic and proteomic analysis. **P80**
WHITE, J.D.^{1,2}, GROUNDS, M.D.², TELLAM, R.³, VUOCOLO, T.³, MCDONAGH, M.⁴, KNIGHT, M.⁴, COCKETT, N.E.⁵ 119
- Subcellular localization of injected Technetium-99m Sestamibi in rat heart **P81**
ISHIKAWA, Y.¹, SATAKE, O.³, UEDA, T.², KURIHARA, T.¹ AND KAJINAMI, K.³ 120
- Silencing or blockage of VEGF in the cervix of pregnant rats down regulates levels of oxytocin **P82**
MOWA, C.N.¹, LI, T.², FOLKESSON, H.G.², JESMIN, S.³, JOHNSON, E.⁴, LOPEZ, M.⁵, USIP, S.², SMITH, D.⁵, PAPKA, R.E.² 121
- The microenvironment of human trophoblastic cells in early pregnancy influences cell surface carbohydrate structure expression and controls cell proliferation **P83**
SAITOH, E.^{1,2}, SUZUKI, A.², SUSUMU, N.², TANABE, K.¹ AND AOKI, D.² 122
- Identification of estrogen receptor BETA-positive intraepithelial lymphocytes and their possible roles in normal and tubal pregnancy oviducts **P84**
ULZIBAT, S.¹, HISHIKAWA, Y.¹, SHIBATA, Y.³, EJIMA, K.¹, AN, S., KITAJIMA, M.², FUJISHITA, A.², ISHIMARU, T.², KOJI, T.¹ 123

- Antagonism of Endothelin A receptor in diabetic erectile dysfunction
reverses down regulation of NO/NOS but not VEGF **P85**
JESMIN, S.¹, MOWA, C.N.², ZAEDI, S.¹, MAEDA, S.¹, MIYAUCHI,
T.¹ 124
- p53 Phosphorylation in Mouse Skin and In vitro Human Skin Model by
High-dose-Radiation Exposure **P86**
KOHNO, Y.¹, SUGASAWA, J.², KOIKE, A.², KOIKE, M.² 125
- Localization of myosin and actin in the skin, hair and whisker of rat **P87**
MORIOKA, K.¹, MATSUZAKI, T.² AND TAKATA, K.² 126
- Variation of caveolin-1 expression with photoaging and chronological aging
on chinese skin **P88**
NOBLESSE, E.¹, KURFURST, R.¹, BIGLIARDI-QI, M.², BIGLIARDI,
P.L.²; ZHIQIANG, C.³, SCHNEBERT, S.¹, AND BONTE, F.¹ 127
- Adipogenesis and adipogenesis in obesity revealed by a visualization
technique of living adipose tissue **P89**
NISHIMURA, SATOSHI¹, NAGASAKI, MIKA¹, NAGAI, RYOZO¹,
AND SUGIURA, SEIRYO² 128
- Dynamics of corticosteroid receptors and importins in living neural cells and
non-neural cells **P90**
NISHI, M., FUJIKAWA, K., AND KAWATA, M. 129
- Detection and utility of tumor-specific auto-antibody in sera of pulmonary
carcinoma patients **P91**
NAGASHIO, R.^{1,2}, MATSUMOTO, T.^{2,3}, KAGEYAMA, T.^{2,3}, SATO,
Y.^{2,3} AND NAKAJIMA, T.¹ 130
- High Resolution, high sensitivity BAC-FISH analyses of human
chromosomes **P92**
WEIER, H.-U.G.¹, BAUMGARTNER, A.^{1,2}, ZENG, H.¹, LU, C.-M.^{1,3},
AND WEIER, J.F.^{1,2} 131
- Detection of Total and Phosphorylated VEGFR2/KDR in Cells and Tissues **P93**
CHANG, W.S.¹, KAHOU, N.S.¹, MAK, J.², BAGRI, A.² AND PEALE,
F.¹ 132
- The Expression of FOXL2 in Human Pituitaries **P94**
EGASHIRA, N.¹, TAKEI, M.², TERAMOTO, A.², OSAMURA, R.Y.¹
133
- The Improvement of immunohistochemical detection for pituitary
transcription factor in human pituitary adenoma **P95**
KAJIYA, H.¹, TAKEKOSHI, S.¹, MINEMATSU, T.¹, EGASHIRA, N.¹,
TAKEI, M.^{1,2}, TERAMOTO, A.², OSAMURA, R.Y.¹ 134

- Differential expression of barrier-to-autointegration factor in papillary thyroid carcinoma cells **P96**
MURATA, S.¹, OHNO, N.², TERADA, N.², HARAGUCHI, T.³, IWASHINA, M.¹, MOCHIZUKI, K.¹, NAKAZAWA, T.¹, KONDO, T.¹, NAKAMURA, N.¹, YAMANE, T.¹, IWASA, S.¹, OHNO, S.², AND KATO, R.¹ 135
- Low copy DNA repeats on human chromosome 1 **P97**
ZENG, H.¹, GUAN, J.¹, LU, C.-M.¹, BAUMGARTNER, A.^{1,2}, WEIER, J.F.^{1,2}, AND WEIER, H.-U.G.¹ 136
- Usefulness of HNF-1 β as an immunocytochemical diagnostic marker of ovarian clear cell adenocarcinoma in ascites specimens **P98**
HIGASHIGUCHI, A.¹, SUZUKI, A.¹, HIRASAWA, A.¹, TAMADA, Y.¹, SUSUMU, N.¹, SUZUKI, N.², AOKI, D.¹ AND SAKAMOTO, M.³ 137
- A Molecular Correlate to the Gleason Grading System for Prostate Adenocarcinoma **P99**
TRUE, L.^{1,2}, COLEMAN, I.³, HAWLEY, S.⁴, HUANG, A.³, GIFFORD, D.³, COLEMAN, R.³, BEER, T.⁶, GELMANN, E.⁷, DATTA, M.⁸, MOSTAGHEL, E.^{3,5}, KNUDSEN, B.⁴, LANGE, P.², VESSELLA, R.², LIN, D.², HOOD, L.⁹, AND NELSON, P.^{1,2,3,5} 138
- Establishment of new diagnostic marker peptides for neuroendocrine tumor of the lung **P100**
MATSUMOTO, TOSHIHIDE¹, NAGASHIO, RYO^{2,3}, KAGEYAMA, TAIHEI¹, SATO, YUISHI^{1,3}, KAMEYA, TORU⁴ 139
- Utility of LC-1 antibody which reacts with carcinoma cells and cancer stromal fibroblasts of the lung **P101**
SATO, Y.^{1,3}, NAGASHIO, R.^{1,2}, MATSUMOTO, T.³, KAGEYAMA, T.³ 140
- Elevated expression of fatty acid synthase (FAS) in human aberrant crypt foci (ACF) **P102**
PRETLOW, THERESA P., KEARNEY, KATHLEEN E. AND PRETLOW, THOMAS G. 141
- Multi-dimensional stromal-colon cancer co-cultures: Developing models for drug response. **P103**
DAWSON, D.M.¹, CHASE, R.M.², NAVARRE, W.³ 142
- Analysis of hhit gene expression and loss of heterozygosity in colonic mucosa of IBD and colorectal carcinoma patients **P104**
WIERZBICKI, P.¹, KARTANOWICZ, D.¹, STANISLAWOWSKI, M.¹, WIERZBICKI, M.¹, SOKOLOWSKA, I.¹, ADRYCH, K.², WYPYCH, J.², SMOZYNSKI, M.², MYSLIWSKI, A.¹, KMIEC, Z.¹ 143

- Expression of secretory phospholipase A2 mRNA and protein in the oral mucosal disorder related to dendritic cell migration. **P105**
KOMIYAMA, K.¹, TSURUTA, T.², MUKAE, S.¹, AND OKAZAKI, Y.¹
144
- Aglyconic mucin core proteins in a case of extramammary Paget's disease **P106**
SMITH, R. F. AND SMITH, A.A. 145
- SSTR2A is expressed in clinically non-functioning pituitary adenomas. **P107**
TAKEI, MAO^{1,2}, KAJIYA, HANAOKO², MINEMATSU, TAKEO²,
EGASHIRA, NOBORU², TAKEKOSHI, SUSUMU², TAHARA,
SHIGEYUKI¹, TERAMOTO, AKIRA¹ AND OSAMURA, ROBERT Y.²
146
- Computerized Morphometric Analysis of Immunostained Prion Protein in Tissues and Cells **P108**
MAXIMOVA, O.A.¹, POMEROY, K.L.¹, VASILYEVA, I.², BACIK, I.¹, JOHNSON, B.¹, TAFFS, R.E.¹, CERVENAKOVA, L.²,
PICCARDO, P.¹, AND ASHER, D.M.¹ 147
- Feasibility Study for Automating Multi-targeted Colorimetric Molecular Histochemical Protocols for HER-2 Diagnosis **P109**
NITTA, HIROAKI¹, FARRELL, MICHAEL¹, KERNAG, CASEY¹,
ASHWORTH-SHAPE, JULIA¹, BIENIARZ, CHRISTOPHER¹,
CARPENTER, ANNE¹, PESTANO, GARY A.¹, WALK, ERIC¹,
MILLER, PHIL¹, AND GROGAN, THOMAS M.^{1,2} 148
- Evidence for HIV transgene modulation and immunocytochemical localization in a HIV-1 model of AIDS **P110**
DENARO, F.J.^{1,4}, MAZZUCHELLI, R.^{2,3}, CURRELI, S.², BRYANT, J.⁴, RIVA, A.³, GALLI, M.³, GALLO, R.C.², AND ZELLA, D.² 149
- X-chromosome inactivation in invasive cytotrophoblasts from human placenta **P111**
WEIER, J.^{1,2}, NGUYEN, H.¹, MAK, W.³, FERLATTE, C.¹,
BAUMGARTNER, A.^{1,2}, WEIER, H.² AND FISHER, S.^{1,4,5} 150
- The expression of proinflammatory cytokines in radicular cysts **P112**
KARTANOWICZ, D.¹, LOS, D.², DIJAKIEWICZ, M.², MYŚLIWSKI, A.¹ AND KMIEC, Z.¹ 151
- Novel features of the palatine tonsils in IgA nephropathy. - A role of the mucosal immune system **P113**
NAGURA, H.^{1,2}, HOTTA, O.³, TAGUMA, Y.³ AND HOZAWA, K.^{4,5} 152
- Melatonin: a novel protective agent against drug's oxidative injury **P114**
BONOMINI, F.¹, TENGATTINI, S.¹, REITER, R.J.², REZZANI, R.¹
AND BIANCHI, R.¹ 153

- Mitochondrial mosaics in the liver of patients with Pearson en Alpers-Huttenlocher syndromes **P115**
ROELS, F.¹, VERLOO, P.², SENECA, S.³, MEERSSCHAUT, V.⁴, EYSKENS, F.⁵, DE CONO, N.², SMET, J.², MARTIN, J.J.⁶, PRAET, M.¹ AND VAN COSTER, R.² 154
- Protective effect of red wine polyphenolic compounds, Provinols™, against drug nephrotoxicity through its antioxidant and anti-apoptotic properties **P116**
TENGATTINI, S.¹, BONOMINI, F.¹, PECHÁNOVÁ, O.², ANDRIANTSITOHAINA, R.³, BIANCHI, R.¹ AND REZZANI, R.¹ 155
- Subcutaneous injection of epigallocatechin gallate into dystrophin-deficient mdx mice ameliorates muscular dystrophy **P117**
NAKAE, Y.¹, HIRASAKA, K.², GOTO, J.², NIKAWA, T.², SHONO, M.³, YOSHIDA, M.⁴, AND STOWARD, P.J.⁵ 156
- Clinicopathological examination of four cases of human allograft recipients (a kidney, a liver, a heart, and a part of aorta) **P118**
TANNO, MASATAKA¹, HAYAKAWA, KINNYA², IZUMI, HIROSI, KUME, KEIKO, FUKUMURA, YUKI AND SUDA, KOICHI³ 157
- Morphological alterations of submandibular glands caused by Cyclosporin A in Rat **P119**
SAGA, T., NISHIMURA, H., KITASHIMA, S., YAKEISHI, A., YOSHIDA, M., YAMAKI, K. 158
- Index 159

S01

DECIPHERING PROTEIN TURNOVER, TOPOLOGY AND TRANSPORT IN LIVING CELLS

LIPPINCOTT-SCHWARTZ, JENNIFER; LORENTZ, HOLGER; HAILEY,
DALE; KIM, PETER and PATTERSON, GEORGE
Cell Biology and Metabolism Branch, NICHD, NIH, Bethesda, MD

Abstract: The development of fluorescent proteins as molecular tags over the past decade has spurred a revolution by allowing complex biochemical processes to be correlated with the functioning of proteins in living cells. Fluorescent proteins such as green fluorescent protein (GFP) from the jellyfish *Aequorea victoria* and its variants can be fused to virtually any protein of interest to analyze protein geography, movement and chemistry in living cells. As such, they have provided an important new tool for understanding protein function, filling an urgent need now that the genome sequence of many organisms is complete. Here, experimental protocols using photoactivatable GFP that allow in cellula pulse-chase analysis of proteins undergoing degradation or selective delivery to different organelles will be presented. In addition, a new fluorescent-based protease protection assay for determining the topology of transmembrane and luminal proteins associated with a wide variety of cellular compartments (including the ER, Golgi apparatus, autophagosomes and peroxisomes) and protein complexes will be described.

S02

APPLICATION OF LIVE-CELL FLUORESCENT BIOSENSORS IN STUDIES OF THE CONTROL OF SPECIFICITY OF SIGNAL TRANSDUCTION PROCESSES

MEYER, TOBIAS

*Department of Molecular Pharmacology, Stanford University School of Medicine, Stanford,
CA 94305 (tobias1@stanford.edu)*

Abstract: Quantitative fluorescence imaging provides powerful measurement opportunities for understanding cellular signaling pathways and networks. I will discuss in my talk different currently useful fluorescence biosensors and imaging strategies and will present some of our recent results in applying fixed cell and live cell imaging to investigate the spatial and temporal control of cellular signaling systems. I will first focus on a strategy that we developed to rapidly perturb phosphoinositide signaling pathways using chemically-induced enzyme activation that led to new insights into the roles of PI(45)P2 and PI(345)P3 lipid second messengers in cell migration and endocytosis. I will then focus on fluorescence-imaging based siRNA screens that led to the discovery of STIM proteins that sense Ca²⁺ in the endoplasmic reticulum and control Ca²⁺-influx into cells and will discuss genome-wide siRNA studies on the control of growth factor-induced cell proliferation and cell metabolism that led to new insights into the overall organization of cellular signaling systems.

S03

VISUALIZATION OF PKC SIGNALING

SAITO, N.

Laboratory of Molecular Pharmacology, Biosignal Research Center, Kobe University, Kobe, Japan (naosaito@kobe-u.ac.jp)

Abstract: Protein kinase C (PKC) is a key enzyme in various intracellular signaling pathways and multiple subtypes of PKC are suggested to have subtype-specific functions. We have reported that each PKC subtype shows spatio-temporally different targeting in response to various stimuli by using live-imaging of GFP-tagged PKCs.

By single molecule imaging technique, GAMMAPKC-GFP is localized on the plasma membrane only less than 1 sec, although the imaging under confocal microscopy shows the PKC localization on the membrane more than 1 min. These findings suggest that PKC repetitively and shortly localizes on the plasma membrane when activated and that the number of the repetitive translocation determines the duration of PKC activation. The mutation in C1B domain of GAMMAPKC significantly reduced the duration of membrane localization of a single molecule of GAMMAPKC-GFP. These results suggested that the digitized signaling by PKC at a single molecule level is efficient for the rapid ON/OFF regulation of PKC signaling.

In brain cerebellar slice from GAMMAPKC-GFP bitransgenic mice, activation of metabotropic glutamate receptor induced a single transient translocation of GAMMAPKC-GFP from the cytoplasm to plasma membrane in the dendrite of Purkinje cells. This transient GAMMAPKC translocation was simultaneously observed throughout the Purkinje cell dendrites. In contrast, trans-synaptic parallel fiber stimulation induced GAMMAPKC-GFP translocation which was not restricted at the distal dendrites, propagated forwardly along the dendritic tree, and reached to the proximal trunk close to the soma. The translocation propagated at 4 to 15 MICROM/sec and the time course of the propagation was similar to that of Ca²⁺ waves observed in the Purkinje cells. This finding suggests that PKC signals activated locally by parallel fiber input could propagate to the soma through dendrites in living Purkinje neurons.

These findings strongly suggest the importance of spatio-temporal activation of the specific PKC subtype in various cell responses.

S04

VISUALIZATION OF CALCIUM SIGNALING

HIROSE, KENZO

Department of Cell Physiology, Nagoya University Graduate School of Medicine, Nagoya, Japan. (kenzo@med.nagoya-u.ac.jp)

Abstract: Ca^{2+} signaling pathways control many fundamental cellular functions. Since the discovery of the spatio-temporal complexity of the intracellular Ca^{2+} dynamics, great attention has been paid to the mechanisms and roles of its complexity: how is the spatial and temporal complexity realized, and for what does the complexity work? To challenge these problems, we have developed techniques for visualization of dynamics of signal molecules which work upstream or downstream of Ca^{2+} . For visualization of IP_3 , a second messenger that mobilizes the intracellular Ca^{2+} stores, we produced a fluorescent IP_3 probe named GFP-PHD consisting of green fluorescent protein (GFP) and pleckstrin homology domain of phospholipase $\text{C}\delta 1$. With GFP-PHD, we found that IP_3 oscillations accompany Ca^{2+} oscillations in MDCK cells. Analysis of spatial dynamics showed the existence of IP_3 waves accompanying intracellular and intercellular Ca^{2+} waves. Thus GFP-PHD revealed complex spatio-temporal dynamics of IP_3 underlying complex Ca^{2+} dynamics. To understand how temporal patterns of Ca^{2+} concentration changes control gene transcription, we focused on Ca^{2+} dependent transcription factor, NFAT. We analyzed time courses of nuclear import and export of NFAT by continuously imaging GFP-tagged NFAT in living cells. We found the time course is best explained by a model in which a rapid Ca^{2+} -dependent dephosphorylation of NFAT proceeds in the cytoplasm followed by slower nuclear import. Thus, the dephosphorylated NFAT functions as a working memory of pulsatile Ca^{2+} signals. Ca^{2+} oscillations therefore induce a build-up of dephosphorylated NFAT in the cytoplasm, allowing effective nuclear translocation. We have also developed a series of fluorescent molecular probes including probes for nitric oxide, kinase activity of myosin light chain kinase and glutamate, all of which are under the control of Ca^{2+} signaling. These probes are thus invaluable tools to uncover the dynamic feature of Ca^{2+} signaling which realizes complex biological functions.

S05

CHEMICAL AND BIOPHYSICAL APPROACHES TO THE STUDY OF PROTEIN TRAFFICKING AND FUNCTION IN LIVING CELLS

HOWARTH, M.¹, LIN, C.W.¹, CHEN, T.C.S.¹, CHEN, I.¹, FERNANDEZ-SUAREZ, M.¹, SLAVOFF, S.¹, GERROW, K.², EL-HUSSEINI, A.² and TING, A.Y.¹

¹Department of Chemistry, Massachusetts Institute of Technology, Cambridge, MA 02139, USA; ²Department of Psychiatry, the Brain Research Center, University of British Columbia, Vancouver, British Columbia V6T 1Z3, Canada mhowarth@mit.edu

Abstract: Our lab develops new methodology for studying protein structure, function, and trafficking in the live cell context. I will describe new methods to label cellular proteins with non-genetically-encoded probes such as organic fluorophores, photoaffinity tags, and quantum dots. I will show how these can be used for single-particle tracking of AMPA receptors on the surface of neurons. I will also describe methodologies for detecting protein-protein interactions and for measuring enzyme activation with high spatiotemporal resolution in living cells.

S06

IMMUNO-LASER CAPTURE MICRODISSECTION FOR ANALYSIS OF RNA EXPRESSION

BASKIN, D. G.

*Veterans Affairs Puget Sound Health Care Medical Center, University of Washington, Seattle,
WA USA (baskindg@u.washington.edu)*

Abstract: Laser capture microdissection (LCM) following immunocytochemical staining is a powerful microscopic preparative technique for obtaining tissue sample enriched in RNA from a specific cell type for analysis by real time quantitative PCR. Protocols for Immuno-LCM essentially involve immunostaining of a tissue specimen followed by LCM picking of cells and extraction of RNA from the pool of picked cells. The principle difficulty in Immuno-LCM is preservation of high quality RNA during fixation, tissue processing, and immunostaining. Protocols have been developed for Immuno-LCM of RNA extracted from paraformaldehyde, paraffin embedded (PFPE) tissue slices. This technique is widely used for obtaining RNA from archived pathology material. The use of PFPE tissue for Immuno-LCM appears to be most useful for situations in which tissue and RNA transcripts are very abundant. It has, however, severe limitations for cell biological studies, particularly for mRNA transcripts that are low in copy number such as those for many receptors. In such situations, and where formaldehyde fixation is incompatible with obtaining undegraded RNA, Immuno-LCM on frozen unfixed tissue offers an alternative approach. Immuno-LCM often can be successfully applied to unfixed frozen tissue slices that are dipped in ethanol (which is compatible with immunocytochemistry of many antigens) and rapidly immunostained to minimize RNA extraction. These procedures produce improved results if precautions are taken to minimize degradation of RNA. We have developed protocols for performing Immuno-LCM on rat brain neurons that are identified by immunostaining, and then picked by laser capture microdissection and analyzed by real-time quantitative PCR. For example, we have shown that mRNA for the neural transcription factor c-fos is highly elevated in hindbrain catecholamine neurons after rats are treated with satiety hormones. Protocols and controls for Immuno-LCM will be discussed. (*Supported by the Department of Veterans Affairs Medical Research Service and NIH*)

S07

“EXPLOITATION OF LASER CAPTURE MICRODISSECTION FOR THE ANALYSIS OF GENE MUTATION AND MRNA EXPRESSION”

TAKEKOSHI, S., EGASHIRA, N., YASUDA, M., UMEMURA, S., OSAMURA, R.Y.

Department of Pathology, Tokai University School of Medicine, Japan.

Abstract: Laser capture microdissection (LCM) has been developed to provide a powerful method to isolate defined populations of cells from heterogeneous histological tissue sections or cytologic preparations for molecular analyses under direct visualization. This talk focuses on the usefulness of LCM for DNA mutation analysis and gene expression analysis in pathological lesion. The mutation of the p53 tumor suppressor gene is one of the most frequent genetic alterations observed in human cancers. LCM-selected tissues procured from colorectal adenocarcinoma and breast tumor with LCM were analyzed by single-strand conformation polymorphism (SSCP) and direct sequence after PCR amplification for p53 exons 5, 6, 7, and 8. As a result, in the LCM-microdissected samples, the mutation could be confirmed to tissue-cell specific lesions. On the other hand, the combined-use of LCM and DNA microarray technique is useful method for the monitor of gene expression in pathological lesions. Carbon tetrachloride (CCl₄) induced fatty liver through the generation of carbon trichloride radicals by cytochrome P-450 enzymes. CCl₄- induced fatty changes occur at the centri lobular regions of the liver because cytochrome P450 enzymes localize in that area and fewer content of anti-oxidative enzymes such as glutathione peroxidase. The unfixed frozen cryosections were prepared for LCM. The RNA was extracted from captured-tissues and amplified. Amplified-RNAs were converted to labeled cDNA to obtain probes that were hybridized onto DNA microarrays. As a results, the expression of 46 genes, including cytochrome P-450 enzymes, were increased in CCl₄-injured lesion. In contrast, the administration of CCl₄ decreased the expression of 24 genes including anti-oxidative enzyme such as glutathione S-transferase. These results suggest that the alterations of gene expression by CCl₄ stimulate the radical generation and lipid peroxidation, resulting in the exacerbated fatty change in the liver. In conclusion, LCM technique is useful for mutation analysis and the observation of the changes of gene expression for specific pathological lesion.

S08

CYTOMOLECULAR ANALYSIS OF NON-GYNECOLOGIC LIQUID-BASED CYTOLOGY PREPARATIONS USING LASER MICRODISSECTION TECHNIQUE

NEMOTO, N.^{1,2}, NAKANISHI, Y.¹, KOMATSU, K.², SEKI, T.², HONMA, T.^{1,2}, HENMI, A.¹ and SUGITANI, M.^{1,2}

¹Department of Pathology, Nihon University, School of Medicine, and ²Pathology Division Nihon University Itabashi Hospital, Tokyo, Japan (nemo@med.nihon-u.ac.jp)

Abstract: Laser assisted microdissection technique is an essential method to obtain the pure target cell samples from heterogeneous cell populations. This technique has widely been accepted because of its reliability and easy handling by well developed sophisticated software. In this workshop, we will talk about cytomolecular analysis of non-gynecologic liquid-based cytology (LBC) preparations using laser microdissection technique (LSI 337 Cell Robotics and PALM- MBIII). LBC preparations of non-gynecologic specimens (breast tumor scrapings, urine, body fluid) were processed for cytomorphological examination and molecular analysis for HER2, cytokeratins and p53 after microdissection. In addition, we examined the influence of long-term storage of the specimens in the preservation of cell morphology and molecular analysis. Regarding the morphological analysis, the LBC preparations were good enough to evaluate cell morphology by Papanicolaou staining. For molecular analysis, p53 mutation was satisfactorily demonstrated in the microdissected urine samples (about 50 tumor cells) by PCR-SSCP. Cytokeratin mRNA and HER2 mRNA were also satisfactorily detected by molecular analysis in the microdissected cell samples, which were stored for more than two weeks in the preservative solutions for LBC. The HER2 mRNA levels were well correlated with the expression of HER2 protein and with HER2 DNA levels demonstrated by FISH. In conclusion, a combination of LBC preparation and laser microdissection technique would be a powerful and useful tool for both cytological evaluation and molecular analysis of non-gynecologic cytology specimens.

S09

THE USE OF LASER CAPTURE MICRODISSECTION IN VASCULAR BIOLOGY

FEIG, JONATHAN E.¹, TROGAN, EUGENE¹ and FISHER, EDWARD A.¹

¹Department of Medicine and Cell Biology, Marc and Ruti Bell Vascular Biology and Disease Program, New York University School of Medicine, New York, New York. (jonathan.feig@med.nyu.edu)

Abstract: Macrophage foam cells (foam cells) are integral in the development of atherosclerotic plaques. Gene expression analysis of lesional foam cells in homogenized arterial specimens is complicated by the cellular heterogeneity of plaques and the presence of lesions of various degrees of severity. To overcome these limitations, we tested the ability of laser capture microdissection (LCM) and real-time quantitative reverse transcription PCR to selectively analyze RNA from lesional foam cells of apolipoprotein E (apoE)-deficient mice. Proximal aortic tissue sections were immunostained for macrophage specific CD68/macrosialin by a rapid protocol. Alternating sections from each animal were used to isolate RNA either from entire sections (analogous to isolation from whole tissue) or by LCM selection of CD68-positive cells. Compared with whole sections, CD68 mRNA levels were greatly enriched (33.6-fold) in the laser-captured lesional foam cells. To illustrate the ability of this method to measure changes in lesional foam cell gene expression, we applied these techniques to our regression model of atherosclerosis. Compared to unregressed lesions, there were 3- to 6-fold increases in mRNA for liver X receptor α and cholesterol efflux factors ABCA1 and SR-BI in foam cells. Expression levels of the inflammatory markers VCAM or MCP-1 were reduced by 75%, but there was induction at the mRNA and protein levels of chemokine receptor CCR7, an essential factor for dendritic cell migration. Remarkably, when CCR7 function was abrogated *in vivo*, lesion size and foam cell content were substantially preserved. In summary, by selectively enriching foam cell RNA, LCM provides a powerful approach to study the *in situ* expression and regulation of atherosclerosis-related genes. Furthermore, it will allow for finer discrimination of changes in levels of genes that can ultimately be shown to play a significant role in the regression of atherosclerosis as well as in other vascular diseases.

S10

PROTEOMIC ANALYSIS OF LASER CAPTURE MICRODISSECTED NEUROFIBRILLARY TANGLES FROM ALZHEIMER'S DISEASE

MONTINE, T.

*Departments of Pathology and Neurological Surgery, University of Washington, Seattle, WA
(tmontine@u.washington.edu)*

Abstract: We obtained neurofibrillary tangles (NFTs) by laser capture microdissection (LCM) from pyramidal neurons in hippocampal sector CA1 in patients with Alzheimer disease (AD) and then prepared these for analysis by liquid chromatography (LC)-tandem mass spectrometry, and then searched peptide databases. We identified 72 proteins in LCM NFTs by multiple unique peptides; of these, 63 had previously unknown association with NFTs. One of these discovered proteins was glyceraldehyde-3-phosphate dehydrogenase (GAPDH). We validated by immunohistochemistry that GAPDH co-localized with the majority of NFTs as well as plaque-like structures in AD brain and was co-immunoprecipitated by antibodies to paired helical filament (PHF) tau, but not tau, from AD temporal cortex. Biochemical characterization of GAPDH showed that it, along with phosphorylated tau and A β peptides, was present in detergent-insoluble fractions from AD temporal cortex but not from age-matched controls. Simultaneously, another group identified the gene for GAPDH as a potential genetic susceptibility factor for AD. These data are the first proteomic investigation of NFTs and an example of how techniques of proteomics can be coupled with LCM to aid in discovery.

S11

NANOSCALE FLUORESCENCE MICROSCOPY

HELL, S.W.

Max Planck Institute for Biophysical Chemistry, Goettingen, Germany (hell@mpi.de)

Abstract: The resolution of a microscope using lenses and visible light has been limited by diffraction to ~ 200 nm. We show that this barrier can be broken through reversible saturable optical (fluorescence) transitions (RESOLFT). First put forward as Stimulated Emission Depletion (STED) [1,3] and Ground State Depletion (GSD) microscopy [2, 3], RESOLFT concepts overcome diffraction by a saturated transition between two marker states, effected with a light featuring an intensity zero. Abbe's equation is extended to $\Delta x \approx \lambda / 2n \sin \alpha \sqrt{1 + I/I_{sat}}$ [4-6]. I_{sat} is the intensity required for saturating the transition and I is the one applied [4] Δx can be continuously decreased by increasing I/I_{sat} [1-6]. We report on STED-microscopy with fluorescence spot sizes down to 16 nm, i.e. $\sim \lambda / 50$ [6]. STED also allows fluorescence correlation spectroscopy with subdiffraction probing volumes [7]. Populating the marker's triplet state [2,3] as well as the 'switching' between conformational states [4,5] in GFP-like proteins entail ultralow which should enable nanoscale resolution even with a lamp.

S12

AN OVERVIEW OF COMPUTATIONAL METHODS FOR THREE-DIMENSIONAL MICROSCOPY

CONCHELLO, JOSÉ-ANGEL

Associate Member, Molecular, Cell, and Developmental Biology Program, Oklahoma Medical Research Foundation Oklahoma City, OK 73104, USA (jose-conchello@omrf.ouhsc.edu)

Abstract: Computational optical sectioning microscopy (COSM) has become an accepted alternative as well as a complement to purely optical methods for three-dimensional (3D) microscopy such as confocal scanning, multiphoton fluorescence excitation, and structured illumination microscopies. Several methods for COSM have been developed over the years. All these methods have the goal to undo the degradations introduced by the process of image formation and recording. Thus the methods are derived based on a mathematical model for this process. A thorough model accounting for all sources of degradation is prohibitively complex in terms of the computer demands, both in CPU time and memory. Thus, all algorithms are derived from simplified models. In general, the more precise the model, the better the results that it affords, but also the higher the computational cost. This talk presents a brief overview of the most recent developments in algorithms for COSM based on more complete models for image formation.

S13

SINGLE PLANE ILLUMINATION MICROSCOPY (SPIM) AND THE THIRD DIMENSION IN THE LIFE SCIENCES

STELZER, E.H.K., KELLER, P.J., PAMPALONI, F. and GREGER, K.

Cell Biology and Biophysics Unit, European Molecular Biology Laboratory (EMBL), Heidelberg, Germany. (stelzer@embl.de)

Abstract: Novel technologies are required for three-dimensional cell biology and biophysics. By three-dimensional we refer to experimental conditions that avoid hard and flat surfaces and favour unconstrained sample dynamics (Keller, Pampaloni, Stelzer, 2006). Light-sheet-based microscopes are particularly well suited for studies of sensitive three-dimensional biological systems. Their application can be illustrated with examples from the biophysics and three-dimensional cell cultures. Three-dimensional approaches reveal new aspects of a system and enable experiments in a more physiological, clinically more relevant context. A new implementation of the theta principle (Stelzer, Lindek 1994) takes advantage of parallel recording. This high-resolution light microscope (Huisken, Swoger, Del Bene, Wittbrodt, Stelzer 2004) is designed to generate images of large samples (embryos, three-dimensional cell cultures) down to the sub-cellular level. The fundamental principle of EMBL's SPIM is the detection of fluorescence light perpendicular to the illumination axis. The illumination system provides the excitation light from the side of an object and hence excites fluorophores within a single plane. The illuminating light sheet overlaps with the focal plane of a regular fluorescence microscope. SPIMaging provides optical sectioning directly. Photo bleaching outside the thin volume of interest is completely avoided and photo toxicity is thus dramatically reduced. Millimetre-sized specimens can be observed in their entirety and as a function of time since a SPIM performs well with long working distance lenses. The specimen can be rotated to further increase the resolution and the information content of the data. Stacks recorded along different angles are combined in post-processing steps to yield high-resolution images of complete specimens (Swoger, Huisken, Stelzer 2003). The 3D resolution is then dominated by the lateral resolution and becomes isotropic. Since the SPIM provides an excellent signal to noise ratio image image processing procedures such as deconvolution work extremely well.

S14

DECONVOLUTION-ASSISTED STRUCTURED ILLUMINATION WIDE-FIELD OPTICAL SECTIONING FLUORESCENCE MICROSCOPY

ROSA-MOLINAR, E.¹, TORRES-VASQUEZ, I.¹, SERRANO-VELEZ, J.L.¹, and CONCHELLO, J-A.²

¹*Biological Imaging Group, University of Puerto Rico-Rio Piedras, San Juan, PR and*

²*Molecular, Cell, and Developmental Biology Program, Oklahoma Medical Research Foundation, Oklahoma City, OK (ed@hpcf.upr.edu)*

Abstract: The resolution of conventional optical wide-field fluorescence microscopes is limited by the diffractive properties of light and by the numerical aperture of the objective lens, and, as a result, the axial resolution of whole-mount preparations of biological specimens is less than optimum. We will describe how we used deconvolution-assisted structured illumination wide-field optically sectioning fluorescence microscopy (dSIM) to examine whole-mount preparations of the spinal cord for the purpose of describing the three-dimensional (3-D) morphology of spinal motor neurons innervating the anal fin muscles in the Western Mosquitofish, *Gambusia affinis affinis*. Small strips of nylon filter paper coated with red-fluorescent 3,000 MW dextran Texas Red[®] were implanted into the musculature of the anal fin. dSIM revealed the 3-D morphology of small multipolar motor neurons (means range from 7.7 to 11.9 μm) distributed in spinal cord segments associated with trunk vertebrae 8-16 (Tk8-16). The cell bodies and dendritic fields of these multipolar motor neurons overlap and are extensive. We also noted the 3-D morphology of commissural neurons axons that ascend, descend, and bifurcate throughout Tk8-16. The results presented will show that dSIM improves the axial resolution in whole-mount preparations of the spinal cord, thus allowing the visualization of the multipolar motor neurons and commissural neurons for anatomically realistic 3-D reconstruction. This work was supported by NIH/NS390405-06.

S15

DEVELOPMENT OF GENETICALLY-ENCODED FUNCTIONAL INDICATORS WITH EXPANDED DYNAMIC RANGE AND VIDEO-RATE FUNCTIONAL IMAGING USING A SPINNING DISC CONFOCAL SYSTEM WITH A MERCURY ARCH LAMP AS A LIGHT SOURCE

NAGAI, T.¹, TANI, T.¹ and MIYAWAKI, A.²

¹Research Institute for Electronic Science, Hokkaido University, Japan, ²Brain Science Institute, RIKEN, Japan(tnagai@es.hokudai.ac.jp)

Abstract: In addition to the microscopy techniques, probing tools are also essential to visualize biological phenomena. Green fluorescent protein and its color variants from *Aequorea victoria* as well as red-emitting variant from *Anthozoa* (GFPs) revolutionized our ability to uncover the complicated detail of protein dynamics and gene activation. In addition, combination of GFPs with fluorescence resonance energy transfer (FRET) technique allows us to develop fluorescent indicators, by which we can visualize localized molecular events in their natural environment within a living cell in real-time and space. To date, increasing number of indicators that report concentrations of second messenger molecules and activation of signaling components have been developed and successfully visualized the dynamic molecular signaling. While most indicators have cyan- and yellow-emitting fluorescent proteins (CFP and YFP) as FRET donor and acceptor, their poor dynamic range often prevents detection of subtle but significant signals. Here, by using new construction methods, we developed FRET-based Ca²⁺ and active caspase-3 sensors that show drastic and much bigger change in the ratio of YFP/CFP in accordance with Ca²⁺ concentration (600% dynamic range) and caspase-3 activation (900% dynamic range), respectively. The new indicators enable visualization of subcellular dynamics of Ca²⁺ and caspase-3 activation with better spatial and temporal resolutions than before. Our study will provide an important guide for the development and improvement of indicators using GFP-based FRET. In addition, we will introduce the use of mercury arch lamp as a light source for video-rate confocal imaging using a spinning disc. We demonstrate the usefulness of this method for long term live imaging.

S16

NIR LASER-BASED MANIPULATION OF FUNCTIONAL MOLECULES IN LIVING CELLS

YAMAOKA, Y. and TAKAMATSU, T.

Department of Pathology and Cell Regulation, Kyoto Prefectural University of Medicine, Japan (ttakam@koto.kpu-m.ac.jp)

Abstract: Proteins are well organized spatially and temporally in living cells. As a method for investigation of their spatiotemporal functions, CALI (chromophore-assisted laser inactivation) has been proposed. In this method, laser irradiation generates reactive oxygen species (ROS) thus inactivating the functions of target proteins tagged with chromophores. However, because CALI usually employs blue light which is often absorbed by intracellular materials, nonspecific photodamage results. To avoid this damage, we developed the new method of “multiphoton excitation-evoked CALI (MP-CALI)”. Differing from standard CALI, MP-CALI employs a near infrared (NIR) femtosecond pulse laser as an excitation light source. Because multiphoton excitation occurs inside a limited, subfemtoliter volume, it is possible to inactivate a specific protein in a smaller and deeper region than excited by conventional CALI, without unnecessary photodamage.

Experiments were performed on HeLa cells stably transfected with cDNA encoding Cx43 fused with EGFP (Cx43-EGFP). While currents of gap junction plaques consisting of Cx43-EGFP were measured, a single point in the plaque was irradiated with an 850-nm femtosecond pulsed laser with a laser irradiance of 2.7 MW/cm² for 380 ms. During laser irradiation (MP-CALI), the gap junction current decreased from 1.1 nA to 0.2 nA (substantial residual current), without damaging the cell membrane. The residual current after MP-CALI was due to remaining functional gap junctions out of the focal plane. In addition, the Cx43-EGFP signal at the irradiated region recovered with time, indicating that the cells were viable after MP-CALI. These results indicate that multiphoton excitation inactivates the function of a protein tagged with EGFP without causing nonspecific photodamage to the living cell. We think that MP-CALI is very useful for detailed spatiotemporal investigation of proteins in living cells. We also discuss other applications.

S17

HIGHER HARMONIC GENERATION MICROSCOPY

SUN, CHI-KUANG

*Department of Electrical Engineering and Graduate Institute of Electro-Optical Engineering,
National Taiwan University, Taipei 10617, Taiwan. (sun@cc.ee.ntu.edu.tw)*

Abstract: Optical higher harmonic generations, including second-harmonic-generation (SHG) and third-harmonic-generation (THG) processes are known to leave no energy deposition to the interacted matters due to the virtual-transition characteristic. In contrast to the absorption- induced-fluorescence processes that require energy deposition and electron transitions, the higher harmonic generation processes provide the optical noninvasive nature desired for microscopy applications, especially for long-term observation of the dynamic changes of live samples, including small animals and clinical patients. Different from single-photon and multi-photon fluorescence, no cell damage and photobleaching effect is expected from the optical harmonic-generation process itself due to the fact that there is no real electron-transition involved and the total generated harmonic photon energy has to be equal to the total annihilated photon energy. With a nonlinear nature similar to the multi-photon excited fluorescence, the generated SHG intensity depends on the square of the incident light intensity, while the generated THG intensity depends on the third power of the incident light intensity. These nonlinear dependencies allow localized excitations to enable intrinsic optical sectioning and a high three-dimensional resolution similar or better than that of the two-photon fluorescence microscopy. In this presentation, we review the recent development of higher harmonic generation microscopy, which provide high-penetration least-invasive intravital optical microscopic images. Contrast mechanisms of higher harmonic generation microscopy will be discussed, with a focus on intravital molecular imaging. Examples of small animal imaging, including noninvasive embryonic studies, will be presented.

S18

PERSISTENT CD DEFICIENCY-INDUCED AUTOPHAGIC NEUROPATHOLOGY IN THE ABSENCE OF BAX-DEPENDENT APOPTOSIS

SHACKA, J.J.^{1*}, KLOCKE, B.J.¹, SHIBATA, M.², UCHIYAMA, Y.² and ROTH, K.A.¹

¹University of Alabama at Birmingham, Birmingham, AL, USA; ²Osaka University Graduate School of Medicine, Osaka, Japan. shacka@uab.edu

Abstract: Neuronal ceroid lipofuscinoses (NCL) are a group of pediatric neurodegenerative diseases caused by genetic disruptions in lysosome function. Cathepsin D is a major lysosomal protease and its targeted deletion in mice induces extensive neuropathology, including markers of apoptosis and autophagic stress concomitant with an increased accumulation of undigested lipopigment. The neuropathology exhibited in CD-deficient mouse brain is similar to that observed in human NCL. Since the relative contributions of apoptosis and autophagy in NCL remain elusive, combined Bax- and CD-deficient mice were generated to determine the importance of Bax-dependent apoptosis for CD deficiency-induced neuropathology. Morphological analysis of CD-deficient brains (as determined by H&E stain) indicated large numbers of neurons with condensed, hyperchromatic nuclei and also neurons with marked cytoplasmic swelling that contained undigested, lipofuscin-like autofluorescent material. Brains of CD-deficient mice also showed robust neurodegeneration, as measured by DeOlmos silver stain. Increased immunoreactivity for cleaved caspase-3 and LC3-II, biochemical markers for apoptosis and autophagic vacuoles, respectively were also detected in CD-deficient brains by immunohistochemistry and by western blot analysis. The targeted deletion of Bax significantly inhibited CD deficiency-induced activation of caspase-3 and decreased numbers of neurons with apoptotic morphology. However, combined Bax and CD deficiency did not prevent neuropathology induced by CD deficiency, as evidenced by similar amounts of autofluorescence, levels of LC3-II and DeOlmos silver-stained, degenerating neurons. Together these results suggest the importance of autophagic stress for NCL-induced neurodegeneration, effects that are persistent even in the absence of Bax-dependent apoptosis. Ongoing studies will also be discussed that are aimed at determining the contribution of altered signaling pathways to CD-deficient neuropathology.

S19

MOLECULAR MECHANISM OF AUTOPHAGY*Progress in Molecular Mechanism of Autophagy*

OHSUMI, YOSHINORI

National Institute for Basic Biology, Okazaki, Japan

Abstract: Lysosome/vacuole is a lytic compartment responsible for intracellular bulk protein degradation. Since discovery of lysosome by cell fractionation procedure, electron microscopy was the most effective method for autophagy, presented dynamic aspects of vacuolar system and defined autophagy as a major route for intracellular components to the lysosome. However, for long time not much had been uncovered on the molecular mechanism of autophagy, because of several difficulties of biochemical analysis.

Eighteen years ago I found yeast cells induce bulk protein degradation in the vacuole under starvation conditions, and the whole process is topologically the same as macroautophagy in higher eukaryotes. It provided an ideal system to elucidate the molecules involved in autophagy through genetical and molecular biological analyses. The most critical event in autophagy is the sequestration of a portion of cytoplasm by membrane sac, resulting a double membrane structure, autophagosome. We found that 17 *ATG* genes are required for the autophagosome formation. Most of these genes are conserved from yeast to human and plants. Analysis of these genes revealed that Atg proteins are divided into several functional units. Most striking findings were two ubiquitin-like conjugation systems essential for autophagy. Atg12 forms a conjugate with Atg5 via consecutive reactions of Atg7 and Atg10. Atg8, another UBL molecule, forms a conjugate with a membrane phospholipids, phosphatidylethanolamine. Atg5 and Atg8 localize on the isolation membrane and the autophagosome, respective, providing good molecular markers to monitor the autophagy in vivo. Others consists of a protein kinase and its regulators, and an autophagy specific PI3 kinase complex. However, we don't know precise roles of Atg proteins during autophagy. Present stage of molecular dissection of machinery of autophagy will be presented and future perspective will be discussed.

S20

OVERVIEW OF INTRACELLULAR SIGNAL TRANSDUCTION SYSTEM

SASANO, HIRONOBU

Department of Pathology, Tohoku University School of Medicine, Sendai, Japan

Abstract: Various functions of the cells are regulated by external factors such as cytokines, hormones and growth factors. These factors are all involved in regulating cell proliferation, apoptosis, angiogenesis, differentiation, aging and others in both physiological and pathological status. Especially in cancer tissues, abnormalities of these intracellular pathways play important roles in their pathogenesis, development and subsequent biological behaviors. These external factors generally exert their effects by binding to the specific receptor molecules located on the cell surface, activating complicated cascades of intracellular pathways especially through sequential kinase signaling with redundancy and cross talk, and eventually result in communication with the nucleus of the cells. Therefore, the overall efficacy of intracellular signal transduction system may be determined by both quantitative and qualitative characteristics of the factors described above, transmembrane receptor proteins and intracellular or cytoplasmic secondary messenger proteins including kinases proteins. These signal transduction system plays especially important roles in human malignancy, such as neoplastic cell proliferation, metastasis or others and could therefore become the important targets of antineoplastic therapy. In cancer cells, the components of these intracellular signals may be altered by oncogenes and/or tumor suppressor genes through overexpression and/or genetic mutations, which cause abnormal intracellular signaling, suppression of apoptosis, promotion of metastasis and dysregulated cell proliferation. In this presentation, these intracellular signal transduction pathways will be briefly reviewed.

S21

USE OF REVERSE PHASE PROTEIN MICROARRAYS FOR SIGNAL PATHWAY PROFILING OF HUMAN CANCER SPECIMENS: IMPLICATIONS AND APPLICATIONS FOR PATIENT TAILORED THERAPY

PETRICOIN, EMANUEL F.

Center for Applied Proteomics and Molecular Medicine, George Mason University, 10900 University Blvd, MS 4E3, Room 181A Discovery Hall, Manassas, VA 20110, email: epetrico@gmu.edu

Abstract: The field of molecular medicine is moving beyond genomics to proteomics as most molecularly targeted therapeutics target protein activity not gene expression. The challenge and opportunity within proteomics is much more than just developing a list of all the proteins, but is to characterize the information flow within the cell and the organism mediated through and by, protein pathways and networks. Elucidation of these networks hold the promise for biomarker discovery to detect disease earlier and with greater predictive value as well as target discovery and rationally targeted medicine. Patient-tailored therapy will rely on new proteomic approaches to discover and profile the ongoing intracellular molecular networks within the patients tissue. A new type of protein microarray, the reverse phase array, has been developed for multiplexed phospho-specific signal pathway profiling using clinical material of patients treated before, during and after therapy. From just a few thousand cells taken from a patient biopsy specimen and procured via laser capture microdissection, over 125 specific signaling events can be monitored. Since these phospho-specific events are most often a functional read-out of the drug target itself, these profiles can generate a “theranostic” fingerprint where both a diagnostic and therapeutic target are the same entity. Example case studies will be presented that demonstrate the ability of this approach to generate data that can be used for de novo target discovery as well as tailoring therapy. Once the circuitry of the cell is elucidated, we can take advantage of the interdependent feed-forward and negative feedback loops that underpin and regulate the information flow. A rational approach to targeting multiple points within key “nodes” within the signaling pathways reveals the potential for combinatorial targeted therapy specified for each patient.

S22

ANALYSIS OF C-KIT AND PDGFRA GENE MUTATIONS IN GASTROINTESTINAL STROMAL TUMORS FOR THEIR DIAGNOSIS AND IMATINIB THERAPY

HIROTA, S.

Hyogo College of Medicine, Nishinomiya, Hyogo, Japan. (hiros@hyo-med.ac.jp)

Abstract: Gastrointestinal stromal tumors (GISTs) are the most common mesenchymal tumors of human gastrointestinal tract. We found that KIT, a receptor tyrosine kinase encoded by protooncogene c-kit, is expressed by practically all GISTs. Now, KIT expression is the most reliable marker for GIST diagnosis. We also found that somatic mutations of c-kit gene are detectable in approximately 90 % of sporadic GISTs. Most mutations are present at exon 11, but a minority of GISTs have either at exon 9, at exon 13, or at exon 17. About half of sporadic GISTs without c-kit gene mutations (~5% of sporadic GISTs) were demonstrated to have somatic mutations of platelet-derived growth factor receptor alpha (PDGFRA) gene that encodes another receptor tyrosine kinase. The PDGFRA gene mutations are located at exon 12 or at exon 18. Since these mutations observed in c-kit and PDGFRA genes result in constitutive activation of KIT or PDGFRA without ligand stimulation, they are considered to be causes of GISTs. Although the KIT immunohistochemistry is essential for GIST diagnosis, the alternative diagnostic procedure such as mutational analyses of c-kit and PDGFRA genes may be required to diagnose immunohistochemically KIT-negative rare GISTs definitely.

Imatinib was developed as a selective tyrosine kinase inhibitor, and is now being used for the treatment of metastatic or unresectable GISTs by blocking constitutively activated KIT or PDGFRA. It shows a remarkable therapeutic effect on most GIST patients, but the effect of imatinib is different in various types of c-kit and PDGFRA gene mutations. Moreover, the secondary resistance against imatinib is often acquired by the second mutation of the identical genes. Mutational analyses of c-kit and PDGFRA genes are also significant for prediction of the drug effectiveness including other molecular target drugs.

S23

MULTICHANNEL DATA ACQUISITION PERMITS ASSESSMENT OF TUMOR HETEROGENEITY IN SIGNALLING PATHWAY COMPONENTS.

GARDNER, H., and RHEINHARDT, J.

Tissue Biomarker Group, Biomarker Development, Novartis Institutes for Biomedical research, Cambridge MA USA (humphrey.gardner@novartis.com)

Abstract: Commonly, abundance of protein signalling intermediates such as phosphoepitopes of kinases is reported by H score of immunohistochemical stains. Correlation between the abundance of different signalling pathway components as well as outcome is often computed by rank correlation analysis or by turning H scores into binary values based on their median value for each analyte, followed by chi square tests. This approach is necessary when using multiple slides, each one stained for a different analyte, but has the inevitable disadvantage that correlation between the abundance of different signalling intermediates cannot be assessed on a cell by cell basis, and any information about heterogeneity within a tumor is lost. We have attempted to address this problem by simultaneous immunostaining for multiple analytes using Qdot fluorophores, followed by visualisation of the data in 3D space and statistical approaches to identifying subsets of tumor cells with different signalling phenotypes within each tumor sample. This approach allows us to quantify heterogeneity per se, as well as having the potential to identify tumor cell phenotypes which may be associated with different natural histories.

S24

THREE-DIMENSIONAL TIME-LAPSE-IMAGING FOR SIGNAL MOLECULES DURING T-CELL ACTIVATION

SUZUKI, TAKESHI

Department of Anatomy and Cell Biology, Gunma University Graduate School of Medicine, Maebashi, Japan (suzutake@showa.gunma-u.ac.jp)

Abstract: T-cells are activated by conjugation with antigen presenting cells (APCs) that display the specific antigen on the surface with MHC molecules. During T-cell activation, the supramolecular activating cluster (SMAC) is made at the contact area between the conjugated cells, i.e., T-cell and APC. I investigated the movements of signal molecules such as PKC during T-cell activation by three-dimensional live-cell-imaging. PKC have C1 domain that specifically binds to DAG, and the recruitment of PKC molecules to specific membrane region is considered to be regulated by DAG. During T-cell activation by APC, only PKC- θ accumulates at the center of SMAC (cSMAC). It has been thought that other molecules of PKC family expressed in T-cell such as PKC- δ do not accumulate anywhere during T-cell activation. This indicates a possibility that an unknown system may work for specific recognition of PKC- θ other than recruiting machinery by C1-DAG binding function. This PKC- θ -specific accumulation machinery should be recognized by a region along the PKC- θ molecule itself. To determine the region responsible for cSMAC accumulation, we prepared the GFP-labeled PKC- θ and - δ . PKC- θ -GFP accumulated compactly at cSMAC after conjugation with APC for more than 10 min. Surprisingly, PKC- δ -GFP also accumulated transiently along the entire contact-area after conjugation for very short term (about 1 min). Expression of chimera molecules of them revealed that the cSMAC-targeting is regulated by v3 region of PKC- θ other than C1-DAG binding machinery. Three-dimensional time-lapse-imaging has made it possible for us to analyze the movement of molecules at immunological synapses in detail. Most of this work was done at the National Jewish Medical and Research Center (Denver, CO) in cooperation with Dr. Abraham Kupfer (Johns Hopkins University, Baltimore, MD).

S25

LIVE IMAGING OF INTRACELLULAR SIGNALING

SAITO, N.

Laboratory of Molecular Pharmacology, Biosignal Research Center, Kobe University, Kobe, Japan (naosaito@kobe-u.ac.jp)

Abstract: I have focused on the function of multifunctional protein, protein kinase C (PKC) in neuronal signal transduction. PKC consists of multiple subtypes and is suggested to have subtype-specific functions. Subtype-specific function of PKC, however, has not been elucidated due to its low substrate-specificity.

Green fluorescent protein (GFP) enabled us to monitor intracellular movement of intracellular signaling molecules in living cells. Live imaging of PKC subtype revealed that each PKC subtype shows spatio-temporally different targeting in response to various stimuli. This subtype- and stimulus-specific targeting of PKC strongly suggested that the various targeting of a PKC subtype may be the molecular basis of the multiple functions of PKC in cellular signaling. I will discuss the importance of spatio-temporal activation of the specific isozyme of PKC in various cell responses using single molecule imaging or transgenic mice.

S26

THINGS TO THINK ABOUT WHEN THINKING ABOUT IMAGING: OLD CONCEPTS AND NEW

LEVENSON, RICHARD

CRI, Woburn, MA (rlevenson@cri-inc.com)

Abstract: Overview: This first part of the session on image acquisition and publishing will address some of the essentials of good imaging technique, and will also touch upon photonic crimes and misdemeanors. Multispectral imaging, an extension of conventional approaches to both brightfield and fluorescence microscopy, will be discussed as well.

Successful imaging requires understanding of issues concerning color, linearity and spatial resolution. The acquired images then need to be displayed and analyzed. The former involves questions of appropriate or acceptable manipulation. The latter brings up quandaries of quantitation. How can one know that quantitative numbers bear a relationship to real properties of the sample or its molecular constituents? After these problems are appropriately dealt with, images must be saved in useful formats. Choices include the faithful but ungainly TIFF and the unreliable but svelt jpeg.

Finally, a technique becoming well known in fluorescence confocal microscopy, but just being applied to brightfield microscopy: spectral imaging. Coupled with appropriate software tools, spectral imaging brings increased sensitivity, freedom from autofluorescence and the ability to perform high degrees of multiplexing—even for chromogenic immunohistochemistry. Single-cell multiplexing in tissue is possible, along with improved quantitation due to spectral imaging's ability to distinguish signals without crosstalk. With new capabilities come new demands on quality control, standards, calibration, and understanding of imaging issues and responsibilities.

S27

FIGURE PREPARATION IN A NUTSHELL

PAQUETTE, S.M.

Journal of Histochemistry & Cytochemistry, Univ. of Washington Med. School, Seattle, WA, USA

Abstract: How you choose to present your figures in a manuscript drastically effects what steps you must take in preparing them for publication, but you may not know how you wish to present your figures, nor which publisher you will be working with, until after you have begun writing your manuscript. You may already have captured your images or received files from colleagues once you've begun writing, and obtaining new files that meet a publisher's requirements could be difficult and time-consuming. This can result in a 'what comes first?' problem - the manuscript, or the figures? In order to produce figures that you can easily edit and that are likely to meet most publishers' guidelines, you should keep general guidelines for review and publication in mind whenever gathering any image or data that might be used as a figure, always use the highest resolution possible, keep original, unedited, source files handy, use the appropriate file-types and formats for a given image type, and determine the general layout and labeling of each figure before you ever open an image editing program. We will briefly go over some definitions used in image-editing and publication, and using examples, we will illustrate some techniques that can be used to produce figures that will meet the needs of not only print but also online publication.

S28

GFL NEUROTROPHIC FACTORS

JOHNSON, E.M.

Washington University Medical School, St. Louis, MO, USA. (eugene.johnson@wustl.edu)

Abstract: There are four members in the family of neurotrophic factors called GDNF family ligands (GFLs). In addition to the first member described glia cell line-derived neurotrophic factor (GDNF), other members include neurturin, (NRTN), artemin (ARTN), and persephin (PSPN). In this lecture I will review the history of the discovery of these factors and the discovery and organization of the receptors which mediate their actions. The receptors involve complexes generated by four selective binding subunits (GFR α s) and the common signaling molecule, the receptor tyrosine kinase, Ret. These factors play critical *physiological* roles as proliferative or trophic factors on several populations of neuronal precursor populations and mature neurons, and on certain non-neuronal cells. The physiological roles of this family of molecules will be reviewed by summarizing the phenotypes of the knockouts of the ligands and the receptors. There is also considerable interest in the *pharmacological* effects of the factors. The actions of these factors on various neuronal and non-neuronal cell types, in culture, will be described as well as the actions in various animals models of nervous system injury and neurodegenerative disease. Lastly, I will briefly discuss past and present clinical trials involving these agents and speculate on future directions of both basic and clinical research involving this family of molecules.

S29

BEYOND PROGRAMMED CELL DEATH: NEW INSIGHTS INTO NON-APOPTOTIC DEATH PATHWAYS

ROTH, K.A. and SHACKA, J.J.

University of Alabama at Birmingham, Birmingham, AL, USA (kroth@path.uab.edu)

Abstract: Apoptotic (Type I) death is the most common form of programmed cell death in the embryonic mammalian nervous system however, autophagic (Type II) death also occurs during nervous system development and is seen in a variety of neurodegenerative conditions. Autophagic death is defined morphologically by the aberrant accumulation of autophagic vacuoles in a degenerating cell that may in addition, display morphological features of apoptosis. We have used two different neuronal cell death models to explore the interrelationship between autophagic and apoptotic cell death pathways. In the first in vivo model, cathepsin D (CD)-deficient mice display extensive accumulation of autophagosomes and lysosomes in neurons resulting in both apoptotic and autophagic cell death. To determine the significance of the apoptotic death pathway in the neurodegeneration observed in the CD-deficient brain, we generated mice deficient in effectively blocked caspase-3 activation and apoptosis in the CD-deficient nervous system. However, these mice still exhibited extensive neuronal autophagic vacuole accumulation and neurodegeneration indicating that non-apoptotic death pathways play a major role in the CD-deficient neuropathological phenotype. To further define the pathways regulating neuronal autophagic death, we used an in vitro model of neuronal lysosomal dysfunction produced by chloroquine exposure which results in accumulation of autophagic vacuoles, caspase-3 activation and death. We found that genetic or pharmacological inhibition of apoptotic death provided incomplete protection from chloroquine-induced neuron death. In comparison, low concentrations of the plecomacrolide antibiotic Bafilomycin A1 provided greater protection from chloroquine-induced death than either a broad caspase inhibitor or Bax deficiency. Since Bafilomycin A1 did not inhibit chloroquine-induced autophagic vacuole formation or staurosporine-induced apoptosis, the precise mechanism of Bafilomycin A1 mediated neuroprotection requires further investigation. These studies indicate an unexpected degree of complexity in neuron death regulation.

S30

AUTOPHAGY AND ITS RELATION TO NEURODEGENERATION

UCHIYAMA, Y.

Osaka University Graduate School of Medicine, Suita, Osaka, Japan
(uchiyama@anat1.med.osaka-u.ac.jp)

Abstract: Autophagy is a highly regulated process involving the bulk degradation of cytoplasmic macromolecules and organelles in eukaryotic cells via the lysosomal/vacuolar system. While it is induced under starvation, differentiation, and normal growth control, the participation of autophagy has also been demonstrated in various neurodegenerative disorders. Moreover, it has been shown that autophagy can trigger a form of cell death distinct from apoptosis in neurons. We have recently shown that autophagy is involved in the pathogenesis of Batten disease/ lysosomal storage disorders.

Conditional knockout mice of *Atg7*, an essential gene for autophagy in yeast, has been generated and analyzed. That is, *Atg7* is essential for ATG conjugation systems and autophagosome formation, amino acid supply in neonates, and starvation-induced bulk degradation of proteins and organelles in mice. It is also evident that hepatocytes possess multiple cellular abnormalities which include concentric membranous structures and deformed mitochondria, and accumulation of ubiquitin-positive aggregates. Thus, the important role of autophagy is noted in starvation response and the quality control of proteins and organelles in quiescent cells. We have also analyzed mice lacking *Atg7* in the central nervous system which exhibit behavioral deficit, such as abnormal limb-clasping reflexes and reduction of coordinated movement, and died within 28 weeks after birth. It is interesting that massive loss of neurons is detected in the cerebral and cerebellar cortices of the mice, while polyubiquitinated proteins accumulate in autophagy-deficient neurons as inclusions. This may indicate that autophagy is involved in the degradation of ubiquitinated proteins. At present, the correlation between ubiquitinated proteins or ubiquitin aggregates and neuron death still remains unknown. However, analysis of these ubiquitin aggregates is very important to further understand neurodegenerative disorders.

S31

IN VIVO ROLES OF CASPASE IN NEURAL CELL DEATH AND DEVELOPMENT

MIURA, MASAYUKI

Department of Genetics, Graduate School of Pharmaceutical Sciences, University of Tokyo, 7-3-1 Hongo, Bunkyo-ku, Tokyo 113-0033, Japan . (miura@mol.f.u-tokyo.ac.jp)

Abstract: Caspase activity is required not only for cell death but also for various physiological functions, including sperm individualization, erythrocyte differentiation, keratinocyte differentiation, neural stem cell differentiation, T-cell and B-cell proliferation, and Langerhans cell migration. Loss of maternal and zygotic Dark (Dapaf-1/HAC-1) function in *Drosophila* results in extra macrochaetes on the scutellum. We examined whether caspases are actually activated in the *scabrous*-expressing proneural clusters that contain SOP cells in wing imaginal discs. Generally, an anti-active caspase antibody is used to stain dying cells. However, it is very hard to detect low or mild levels of caspase activity in cells by this method. To determine the caspase activity *in vivo*, we created the fluorescence resonance energy transfer (FRET)-based caspase indicator SCAT3. Interestingly, FRET abolishment was weakly occurred in broad area of wild-type wing discs, suggesting that caspase was mildly activated in wing discs. Careful examination of wing discs showed no dead cells in the *scabrous*-expressing proneural clusters, suggesting caspase works as a non-apoptotic molecule in proneural clusters. By using a genetic screening, we identified a candidate of novel substrate, which, through cleavage by caspases can regulate *Drosophila* neural precursor development. Isoform of Shaggy, *Drosophila* GSK-3 β and essential for the negative regulation of Wingless signaling, is cleaved by the Dark-dependent caspase. This cleavage converts it to an active kinase, which contributes to the formation of neural precursor (SOP) cells. Our results suggest a novel role for caspases in modulating cellular differentiation through cleavage of substrate that is independent of apoptosis.

S32

PROTEOMICS OF PATHOLOGICAL PROTEIN IN ALZHEIMER'S DISEASE

MONTINE, THOMAS J.¹, BOUTTE, ANGELA¹, LIEBLER, DANIEL²,
MONTINE, KATHLEEN S.¹, and WOLTJER, RANDALL¹

¹University of Washington, Seattle, WA, USA and ²Vanderbilt University, Nashville, TN, USA
(tmontine@u.washington.edu)

Abstract: Several neurodegenerative diseases, including Alzheimer's disease (AD), are proposed to derive from pathological protein that share a number of potentially inter-related biochemical features including misfolding, decreased solubility in detergents, aggregation into amyloid or inclusions, and extensive post-translational modifications. We have employed liquid chromatography coupled with electrospray ionization and tandem mass spectrometry as a means of discovering those proteins that adopt a pathological phenotype in AD. Our first set of experiments investigated laser capture microdissected (LCM) neurofibrillary tangles (NFTs) from hippocampal sector CA1 of patients with AD. Our approach discovered 77 proteins associated with LCM NFTs identified by 2 or more unique peptides; 63 of these were not previously co-localized to NFTs. Among these, we validated that GAPDH co-localized with NFTs, bound to paired helical filament tau, and was present in the detergent-insoluble fraction. Our next set of experiments used the same approach to investigate the detergent-insoluble proteome in AD temporal cortex. We discovered 125 proteins identified by 2 or more unique peptides in the sarkosyl-insoluble fraction from patients with AD and validated 15 or 15 with immunological detection. When compared among patients with prodromal AD and age-matched controls, widespread detergent-insolubility was observed in prodromal AD except for tau, which demonstrated detergent-insolubility only in established AD. Use of novel software called P-Mod mapped selective oxidation within the detergent-insoluble proteome. These results demonstrate the power of proteomic-based discovery tools in the comprehensive assessment of pathological protein in neurodegenerative diseases.

S33

INTRODUCTION TO WORKSHOP ON ADVANCING IN SITU HYBRIDIZATION TO VISUALIZE MOLECULAR EVENTS: INTERACTIONS OF ADVANCES AND STANDARDIZATION

UNGER, E. R.¹

¹*Division of Viral and Rickettsial Diseases, National Center for Infectious Diseases, Centers for Disease Control and Prevention, Atlanta, GA 30333, United States of America (eunger@cdc.gov)*

Abstract: Visualizing molecular events within a morphologic context remains the goal of all in situ hybridization methods. The sensitivity and resolution that can be achieved with these methods have increased, making in situ hybridization a method of central importance in basic research as well as in clinical diagnostics. Increased reliance on a method brings with it an increased requirement for the results to be reproducible with good inter-laboratory comparability. The goal of this workshop is to address technical advances and the results obtained as well as the latest approaches to standardization. Two different advances in technique will be presented: Quantum dot detection and confocal scanning microscopy for three-dimensional visualization of protein and mRNA as applied to pituitary hormone research and electron microscopic in situ hybridization as applied to the analysis of nucleolus rRNAs and "introns" of rRNA precursor RNA. Two different efforts to standardize ISH will be presented: The MISFISHIE project [Minimum Information Specification For In Situ Hybridization and Immunohistochemistry Experiments] a standard for reporting immunohistochemistry and FISH studies and automation for standardized *in situ* hybridization applications in functional genomics research and cancer diagnostics

The findings and conclusions in this report are those of the authors and do not necessarily represent the views of the funding agency

S34

IN SITU HYBRIDIZATION WITH QUANTUM DOT DETECTION AND CONFOCAL SCANNING MICROSCOPY FOR THREE-DIMENSIONAL VISUALIZATION OF PROTEIN AND MRNA: APPLICATIONS IN PITUITARY HORMONE RESEARCH

MATSUNO, A.¹, ITOH, J.², TAKEKOSHI, S.³, OSAMURA, R.Y.³

¹Dept. of Neurosurgery, Teikyo University Ichihara Hospital, 3426-3 Anesaki, Ichihara, Chiba 299-0111, Japan; ²Teaching & Research Support Center, Tokai University School of Medicine, Boseidai, Isehara, Kanagawa 259-1100, Japan; ³Dept. of Pathology, Tokai University School of Medicine, Boseidai, Isehara, Kanagawa 259-1100, Japan, (akirakun@med.teikyo-u.ac.jp)

Abstract: We have elucidated the intracellular localization of pituitary hormone and its mRNA using electron microscopic in situ hybridization and immunohistochemistry [1-3]. This method has very high resolution, and provides two-dimensional images of subcellular localization of pituitary hormone and its mRNA in a pituitary cell. Using preembedding method, growth hormone (GH) messenger RNA are localized as osmium black on RER. GH protein is identified mainly on the secretory granules with colloidal gold particles, and is also identified in the cisternae of RER. However, electron microscopic in situ hybridization and immunohistochemistry method cannot tell the localization of mRNA and protein three-dimensionally.

Confocal laser scanning microscopy can visualize the localization of protein three-dimensionally. Recently, nanocrystals such as Quantum dot (Qdot) are available for confocal laser scanning microscopic observation. We apply Qdot for the simultaneous detection of intracellular localization of mRNA and its encoded protein in rat pituitary cells. Successfully we can visualize GH and its mRNA, prolactin and its mRNA with Qdot 605 and 655 [4,5]. This method is useful because it can provide the spatial and three-dimensional relationship between mRNA and protein.

Electron microscopic in situ hybridization and immunohistochemistry has advantage of high resolution. Meanwhile, in situ hybridization and immunohistochemistry using Qdots and confocal laser scanning microscopy has merit that it can provide three dimensional images. Thus, both methods are useful for understanding the relationship between protein and mRNA simultaneously in two or three dimensions.

S35

ADVANCES IN ELECTRON MICROSCOPIC IN SITU HYBRIDIZATION: APPLICATION IN ANALYSIS OF NUCLEOLUS RRNAS AND “INTRONS” OF RRNA PRECURSOR RNA

KOJI, T.

*Nagasaki University Graduate School of Biomedical Sciences, Nagasaki, Japan.
(tkoji@net.nagasaki-u.ac.jp)*

Abstract: For a better understanding of cell-type specific gene expression, nuclear localization of specific gene transcripts is essential. Although advance in light-microscopical (LM) in situ hybridization (ISH) enabled us to analyze cytoplasmic distribution of mRNAs easily, our technology for nuclear distribution of specific gene transcripts remained still immature. As a model system to explore it, we attempted to localize 28S rRNA and 18S rRNA in the nucleolus of mouse Sertoli cells. As probes, 34-mer synthetic oligodeoxynucleotides (oligo-DNA) complementary to a part of 28S or 18S rRNA were labeled with thymine-thymine (T-T) dimer or digoxigenin (Dig). When both rRNAs were simultaneously localized in a paraffin section of mouse testis by LM-ISH, using FITC labeled anti-(T-T dimer) and TRITC labeled anti-Dig, uneven distribution in the nucleolus was found. However, the resolution was not high enough to discriminate the site of each rRNA precisely. Thus, we next conducted pre-embedding electron microscopic ISH (EM-ISH) to localize them in the nucleolus. Briefly, the paraformaldehyde-fixed frozen sections of mouse testis were hybridized with the above probes in the presence of nucleic acid mixture in place of formamide, then the haptens were detected enzyme-immunohistochemically, osmified, embedded into Epon resin and cut into ultra-thin sections. Very interestingly, 28S rRNA was found predominantly in a vicinity of fibrillar center (FC) while 18S rRNA was distributed more widely distributed surrounding FC. To clarify the difference in the distribution of both rRNAs as well as other “intron” parts of pre-rRNA quantitatively, we performed “post-embedding” double-localization EM-ISH with different sizes of colloidal gold in LR White-embedded mouse testis. Consequently, the similar pattern of rRNA distribution was confirmed, and further the signal for “intron” parts was scattered almost evenly throughout the nucleolus. These results indicate that there are different pathways in rRNA processing within nucleoli even though originated from the same precursor molecule.

S36

MISFISHIE: HOW STANDARD FISH REPORTING STANDARDIZES RESULTS AND WHY IT IS IMPORTANT

TRUE, L.D.¹, DEUTSCH, E.W.², CAMPBELL, D.², PASCAL, L.¹, OUDES, A.¹, LIU, A.Y.^{1,2}.

¹University of Washington, Seattle, WA, USA; ²Institutes for Systems Biology, Seattle, WA, USA. (*ltrue@u.washington.edu*)

Abstract: Background: A goal of the biomedical literature is to report results in sufficient detail so that the study can be independently replicated. To ensure that a sufficient level of detail is provided, a minimum information specification is needed for reporting data. A data content specification has already been widely accepted - MIAME. However, no specification exists for in-situ hybridization (FISH) or immunohistochemistry (IH) experiments. In this study, we developed and evaluated a specification for FISH/IH studies. This specification details the minimum information that should be provided when reporting results.

Design: A specification that consists of 6 sections - Design (e.g. number of cases and stains), Processing (e.g. tissue type, fixative), Probe/Antibody Data, Staining Protocol, Imaging Data, and Image Characterization - was developed. This specification does not stipulate a specific format for data reporting. A selection of FISH/IH articles from the past 5 years was assessed for compliance with the 6 specification sections. Each reviewer assessed each of 32 articles. Compliance with each MISFISHIE subsection was rated on a scale of 0 to 10. 10 indicates that all information the reviewer needed to reproduce the experiment was provided; scores <10 correspond to how incomplete the information was that the reviewer thought necessary to reproduce the work.

Results: Only 4 papers (13%) were deemed totally MISFISHIE. 28% were non-compliant in one section. 31% did not comply in two sections. 90% complied with Design and Specimen Processing sections. 75% complied with Probe/Antibody Information and Staining Protocol sections. Only 16% of articles were compliant with Imaging Data.

Conclusions: Many papers lack sufficient detail for independent investigators to reproduce the studies with complete confidence. We propose that investigators and journal editors evaluate in-situ-hybridization and immunohistochemical studies using the MISFISHIE specification.

S37

AUTOMATION FOR STANDARDIZED IN SITU HYBRIDIZATION APPLICATIONS: FUNCTIONAL GENOMIC RESEARCH AND CANCER DIAGNOSTICS

GROGAN, THOMAS M.^{1,2} and NITTA, HIROAKI²

¹Department of Pathology, The University of Arizona, ²R&D Discovery, Ventana Medical Systems, Inc., Tucson, Arizona, USA. (tgrogan@ventanamed.com)

Abstract: *In situ* hybridization (ISH) is becoming a very important application for post-genomic research and clinical diagnostics. However, due to the lack of standardization of ISH protocols, ISH still remains a most technically challenging molecular biology technique. The reproducibility of manual ISH assays is dependent on individual's experience and reagent preparation. However, the development of ready-to-use reagents and software-based instrumentation for automated ISH applications can standardize ISH protocols. In particular, automation can give precise control of reaction conditions, such as temperature and pH. For functional genomic research, collaboration studies utilizing ISH techniques can be globally conducted and ISH results can be reproduced at any laboratory equipped with the instrumentation. For cancer diagnostics, tissue biopsies from any patient can be tested with standardized ISH protocols for detecting target genes or gene expression at any clinical laboratory in the world. A combination of ISH and immunohistochemistry on the same slide is a further technically challenging application. When a colorimetric protocol for gene and protein double staining, such as for HER-2/*neu* or EGFR, can be performed by automation, it would be a valuable and accurate test for cancer diagnostics. However, the performance of ISH assays is still influenced by the quality of tissue sections, probe designs, and signal detection reagents. Most importantly, tissue fixation methods (fixatives and fixation length) need to be better defined for further improvement of ISH results. Thus, automating ISH applications can significantly improve the advancement of functional genomics research and the quality of patient care. Our next challenge is to develop the chemistry and instrumentation for rapid ISH applications to provide robust results in a timely fashion.

S38

QUANTIFICATION OF VIABILITY IN ORGANOTYPIC SPHEROIDS OF HUMAN MALIGNANT GLIOMA FOR DRUG TESTING

DE WITT HAMER, P.C., JONKER, A., ZWINDERMAN, A.H.,
LEENSTRA, S. and VAN NOORDEN, C.J.F.

*Academic Medical Center, University of Amsterdam, Amsterdam, The Netherlands.
(c.j.vannoorden@amc.uva.nl)*

Abstract: The prognosis for patients with glioblastoma multiforme (GBM) remains poor, despite surgical resection, radiotherapy and temozolomide chemotherapy. To screen for novel therapeutics established cell lines or primary cell cultures are used. However, the correlation between in vitro and in vivo responsiveness is poor. The organotypic spheroid (OS) model provides a more complex biological system, that maintains cell-cell interactions, extracellular matrix and cellular heterogeneity. We found that the cancer genomic profiles of 5 original GBM tumors and their OSs compared better than that of their primary cell culture, thus proving that the OS model is a more representative model of GBM. Accurate and reproducible quantification of therapeutic responses in the OS model has been lacking. For this purpose, lactate dehydrogenase (LDH) activity was demonstrated in cryostat sections of spheroids. Calibrated digital image acquisition of the stained cryostat sections enabled demarcation of LDH-active and LDH-inactive tissue areas by thresholding at specific absorbance values. The viability index (VI) was calculated as ratio of LDH-active areas and total spheroid tissue areas. Duplicate staining and processing on the same tissue showed good correlation and therefore reproducibility. Sodium azide incubation of spheroids induced reduction in VI to almost zero. We also determined sample size requirements for a valid screening strategy: how many spheroids per experimental group and how many sections per spheroid are required to detect one-third reduction in the VI after treatment? Because of the large biological variation of the VI (20%), at least 12 spheroids per group and 1 section per spheroid are required. We conclude that quantification of viability in cryostat sections of OSs from malignant glioma can be performed reliably and reproducibly with this approach, but high-throughput screening does not appear to be feasible using OSs although relatively efficient experiments can be planned.

S39

DYNAMIC IMAGING OF TAGGED RECEPTORS

KAWATA, MITSUHIRO

Kyoto Prefectural University of Medicine, Kyoto, Japan(mkawata@koto.kpu-m.ac.jp)

Abstract: Steroid hormones enter cells by penetrating directly across the plasma membrane of the target cells and bind to intracellular receptor proteins. Liganded receptors translocate either intracellularly or intranuclearly and form large protein complexes with cofactors to induce or repress gene transcription.

Two types of steroid hormone receptors (glucocorticoids and sex steroids) dynamism is presented here by using real-time imaging with fluorescence recovery after photobleaching (FRAP) and fluorescent resonance energy transfer (FRET.) Glucocorticoid receptor (GR) and mineralocorticoid receptor (MR) are localized in the cytoplasm in the absence of the ligand and they translocate to the nucleus after ligand binding. FRET demonstrated that importin α is involved in GR/MR translocation from the cytoplasm to the nucleus and GR and MR dimerize within the nucleus. FRAP showed that the movement of ligand-bound GR/MR is restricted in the nucleus. Upon estradiol treatment ER α and ER β are relocalized to show discrete pattern, and they are localized at the same discrete cluster. FRET clearly showed the interaction of ER α and ER β . In the presence of the estradiol, however, the discrete staining pattern of ER α and ER β are mostly overlapped with Brg-1, indicating that most of the ERs clusters are involved in the chromatin remodeling machinery. FRAP showed that nuclear ER α and ER β are dynamic and mobile in the absence of the ligand, but its mobility is slightly decreased after the ligand treatment. When ATP is deleted from the culture medium, even liganded ER α significantly loses its free mobility in the nucleus. Nuclear matrix which is scaffolding sites within the nucleus is composed of actin and actin-related peptides. Treatment by detergent causes complete loss of ER α in the unliganded condition, but liganded ER α stick to the nuclear matrix. Nuclear matrix is an important factor to determine the dynamism of unliganded and liganded ER α .

S40

FRET-FLIM REVEALS THE ORGANIZATION OF DIFFERENT RECEPTOR-LIGAND COMPLEXES IN ENDOCYTOTIC MEMBRANES

WALLRABE H.¹, TALATI, RONAK², PERIASAMY, AMMASI¹, BARROSO, MARGARIDA²

¹University of Virginia - Keck Center for Cellular Imaging, VA and ²Albany Medical Center – Center for Cardiovascular Sciences, NY

Abstract: Fluorescence Resonance Energy Transfer (FRET)- and Fluorescence Lifetime Imaging (FLIM)-based assays determine the organization of receptor-ligand complexes (polymeric IgA-receptor, pIgA-R; transferrin receptor, TFR; low-density lipoprotein-receptor, LDL-R) in endocytic membranes of MDCK cells. Differently-fluorophore labeled (Donor -D- or Acceptor -A-) pIgA-R ligands, holo-transferrin (Tfn) and/or LDL were internalized into polarized or non-polarized epithelial MDCK cells, imaged using confocal microscopy and processed for FRET and/or FLIM analysis. A two-parameter confocal FRET assay demonstrates whether receptor-ligand complexes are randomly distributed or clustered. 2-Photon FLIM investigates the effect of the different endocytic environments (e.g. pH, protein composition) on the organization of the receptor-ligand complexes. Our results show that clusters containing different receptor-ligand complexes show different levels of organization from random to a mixed clustered/random to a clear clustered organization in distinct endocytic compartments. Changes in the lifetime distribution of Tfn-TFR complexes localized to different endocytic compartments suggest that these complexes may be exposed to different micro-environments and/or organized in distinct higher-order distributions. Different organizations of receptor-ligand complexes may represent protein sorting and pH-induced conformational changes as they occur during the endosomal trafficking in polarized cells. Clusters containing LDL-LDL-R complexes undergo a clustered to random organization which may reflect the release of the LDL from its receptor. Analysis of receptor organization in endocytic membranes will provide insights into protein sorting, biogenesis of membrane microdomains and endosomal organization and dynamics.

S41

ASSOCIATIVE MULTI-DIMENSIONAL IMAGE ANALYSIS SOFTWARE FOR MODERN OPTICAL MICROSCOPY

ROYSAM, B.

*Department of Electrical, Computer and Systems Engineering, NSF Center for Subsurface Sensing & Imaging Systems, Rensselaer Polytechnic Institute, New York, USA.
(roysam@ecse.rpi.edu)*

Abstract: Modern optical microscopy is a powerful tool for biological investigations at the sub-cellular, cellular, and tissue levels. Confocal and multi-photon microscopes have made three-dimensional (3-D) imaging of multiple structures and functional markers routine. Burgeoning libraries of organic and inorganic fluorophores enable multiplexed labeling of diverse structural and functional markers. Time-lapse imaging of living tissue is enabled by sensitive detectors, fluorescent proteins, multi-photon imaging, and controlled-environment chambers. By combining these techniques, processes such as signaling and molecular transport can be recorded in the spatio-temporal context of intact tissue. In this regard, imaging is advantageous compared to arrays and flow-based methods, in which spatial organization is unavoidably disrupted. Overall, optical microscopy yields a wealth of multi-dimensional data capturing 3-D structure, dynamics, chemistry, and physics.

This talk describes robust automation technologies to translate multi-dimensional image data into concise and informative quantitative measurements. A particular focus is on quantifying complex histological units such as the neurovascular stem-cell niche, and dynamic systems such as a developing embryo. For these systems, it is necessary to segment multi-fluor data to extract multiple types of compartments, surfaces, and signals. From these, it is necessary to compute spatial relationships and interactions among multiple structures and functional markers, and temporal relationships associated with structural dynamics and molecular processes. All of this requires processing of large volumes of image data.

The FARSIGHT system is specifically designed for the multi-dimensional imaging capabilities of modern optical microscopy, and the complex image analysis needs of contemporary cell/tissue biology. The system exploits properties of fluorescence images to segment compartments, surfaces, curves, and signals from images. It computes standard morphometric data for each of these entities. Finally, it computes a set of associative statistical measurements of relationships among these entities. This system can be adapted to diverse cytological and histological studies by modifying simple association scripts.

P01

SECOND-HARMONIC GENERATION IMAGING OF THE COLON

HARADA, Y., NAKANO, K., YAMAOKA, Y., HITOMI, T., and TAKAMATSU, T.

Department of Pathology and Cell Regulation, Kyoto Prefectural University of Medicine, Kyoto, Japan (yoharada@koto.kpu-m.ac.jp)

Abstract: Nonlinear microscopical techniques using second-harmonic generation (SHG) signals are hopeful implements for noninvasive analysis of biomedical specimens. The purpose of this study was to characterize normal fresh colonic structure without exogenous labels using nonlinear microscopy, because collagen fibrils, being nonsymmetric, have nonlinear susceptibilities. We developed an experimental system of nonlinear laser scanning microscopy for SHG and two-photon excitation fluorescence (TPEF). Near-infrared femtosecond laser was employed for excitation. Bright SHG signals were detected in the submucosa, the lamina propria, and the serosa of freshly-prepared colonic tissue. Conventional histological analysis confirmed that bright signals corresponded to collagen fibrils. TPEF images of colonic tissue showed that the mucosa and the submucosa had the intrinsic fluorescence. Our results indicated that second-harmonic imaging was a useful tool for characterization of fresh colonic structures without fixation or staining.

P02

DIFFERENCE OF PHOTOACOUSTIC WAVES BETWEEN VARIOUS TISSUES

YAMAOKA, Y.^{1,2} and TAKAMATSU, T.¹

¹Department of Pathology and Cell Regulation, ²Department of Methodologies for Medical Research, Kyoto Prefectural University of Medicine, Japan (yamaoka@koto.kpu-m.ac.jp)

Abstract: Recently, photoacoustic tomography (PAT) has been developed for imaging of thick tissues. To produce photoacoustic waves, the tissues are illuminated by nanosecond (ns) pulse laser. Because light is absorbed heterogeneously in tissues, measuring the photoacoustic wave due to laser-induced thermoelastic expansion enables us to obtain the structure of tissues depending on their optical absorption. Usually, the obtained structure is believed to be reflected by the structure of blood vessels. However, photoacoustic waves are generated from not only blood vessels but also other tissues. In addition, how various tissues generate photoacoustic waves is not clear. In this study, to clarify the generation mechanism of laser-induced acoustic waves in tissues, we measured the photoacoustic waves from various types of tissues.

Various tissues such as blood vessel, esophagus, liver and kidney taken from F344 rats were illuminated by ns light pulses at 532 nm and 1064 nm (Continuum Corp. Minilite). As a result, we found that the obtained signal is different from various tissues about not only the intensity but also the phase of the photoacoustic waves. This result indicates that the distinction of tissues by laser-induced photoacoustic waves is possible.

P03

LOCAL GENE TRANSFER TO CALCIFIED TISSUE CELLS USING PROLONGED INFUSION OF A LENTIVIRAL VECTOR

WAZEN, R.M., MOFFATT, P. and NANJI, A.

Laboratory for the Study of Calcified Tissues and Biomaterials, Faculty of Dentistry, Université de Montréal, Montreal, QC, Canada. rima.wazen@umontreal.ca

Abstract: Gene transfer offers the potential for sustained expression of therapeutic proteins in specific target tissues. However, in the case of calcified tissues, delivery of viral vectors remains problematic and has been essentially limited to anatomical sites accessible by injections such as joints and synovial spaces.

Our aim was to test the efficiency of lentiviral vectors (LVs) on osteogenic cells in vitro, and determine the feasibility of directly transducing resident bone cells in vivo.

Materials and Methods: LVs encoding for green fluorescent protein (GFP) and ameloblastin (AMBN), a protein associated with mineralization not found in bone, under the control of the EF-1 α promoter, were produced. The transduction efficiency of the viral constructs and the effect of the transgene on the synthetic activity of osteogenic cells were evaluated in vitro using the MC3T3 and primary calvaria-derived cultures. For in vivo delivery, holes were created in the bone of the rat hemimandible and tibia. One-day osmotic minipumps were connected to these holes and used to deliver the LV. Tissues were embedded in paraffin and sections were processed for immunohistochemical detection of GFP and AMBN.

Results: Our data show that the transgene was expressed in MC3T3 and primary calvaria-derived cultures. Following infusion, a variety of cell types, near the infusion site, including osteoblasts and osteocytes, successfully expressed the transgene.

Conclusion: Our study shows that osteogenic cells can be transduced with LVs to express cytoplasmic and secreted proteins, and establishes the feasibility of directly infecting cells in bone tissue using continuous infusion. This proof of principle represents a mandatory first step towards local gene transfer studies in models of bone formation, repair and pathological loss. Supported by the Canadian Institutes of Health research.

P04

CHROMOSOME-SPECIFIC DNA REPEAT PROBES

BAUMGARTNER, A.^{1,2}, WEIER, J.F.^{1,2} and WEIER, H.U.G.²

¹*Dept. of Obstetrics, Gynecology and Reproductive Sciences, University of California, San Francisco, CA, USA;* ²*Life Sciences Division, University of California, E.O. Lawrence Berkeley Natl. Lab., Berkeley, CA, USA. (baumgartnera@obgyn.ucsf.edu)*

Abstract: Fluorescence in situ hybridization (FISH) has gained increasing popularity as a highly sensitive technique to study cytogenetic changes in the research environment as well as in the clinical laboratory. Today, hundreds of commercially available probes serve the basic needs of the biomedical research community. Widespread applications, however, are often limited by the lack of appropriately labeled, specific nucleic acid probes. We describe two rapid approaches to the preparation of chromosome-specific probe DNAs and readily available methods to label the probes with the reporter molecules of choice. Notably, the techniques allow preparation of highly specific DNA repeat probes suitable for enumeration of chromosomes in interphase cell nuclei or tissue sections without a need for chromosome enrichment by flow cytometry and sorting or molecular cloning. Examples of production of DNA repeat probes specific for either human chromosome 17 or 18 also demonstrate that the entire process from probe concept and design to successful hybridization can be completed in the laboratory in just a few days without a need for highly specialized equipment.

P05

METHOD FOR QUANTIFICATION OF PROLIFERATION IN TISSUE SECTIONS USING THE LASER SCANNING CYTOMETER

KRULL, D.L., KEENER, M.J., BUTLER, L. and PETERSON, R.A.
Safety Assessment, GlaxoSmithKline RTP, NC, USA (david.l.krull@gsk.com)

Abstract: Immunohistochemical labeling of proliferating cells in tissue sections has been common practice in pre-clinical drug development studies. In order to obtain a proliferation index, positive and negative cells are manually counted by a pathologist with the aid of imaging software such as ImageProPlus[®]. This method is time-consuming and may introduce bias. We have developed a method to obtain a proliferation index of selected cell types within tissue sections that were immunohistochemically labeled with antibodies against Ki-67 and Topoisomerase II alpha. Sections of monkey liver and urinary bladder were immunohistochemically labeled with and developed using a DAB chromagen. A second marker, Cytokeratin AE1/AE3, was applied to the urinary bladder and developed using liquid permanent red. A fully automated workspace was optimized on the iCyte[®] Laser Scanning Cytometer using scatter and fluorescence detection. DAB labeled cells were counted by measuring the signal in the inverted scatter channel (primary event contour) produced by an argon ion laser. Hematoxylin stained nuclei (primary contour) were counted by measuring the signal in the inverted scatter 2 channel produced by a HeNe laser. Eosin staining around nuclei was also measured (peripheral contour) in the scatter channel produced by an argon ion laser. This enabled us to evaluate hepatocytes only and to avoid unwanted positive staining hepatic sinusoidal cells. This technique was also applied to sections of monkey and rat urinary bladder. The cytokeratin marker enabled evaluation of the proliferation index of the urinary bladder epithelium. This method was also used in an investigational rat study that evaluated the effect of uracil on urothelial proliferation. The group mean percentage of Ki-67-positive urothelial cells in this study was increased in rats that received dietary uracil (12.3 x control diet values). This automated method of quantification on the LSC will increase efficiency, reduce bias and free up pathologist time.

P06

IMMUNOMODULATORY EFFECTS OF MACROLIDE ANTIBIOTICS IN SULFUR MUSTARD-EXPOSED AIRWAY EPITHELIAL CELLS:

Utilization of quantum dots for immunocytochemical analysis of iNOS

GAO, X.¹, RAY, R.², XIAO, Y.³, BARKER, P.E.³, and RAY, P.¹

¹Walter Reed Army Institute of Research, Silver Spring, MD, USA; ²United States Army Medical Research Institute of Chemical Defense, APG, MD, USA; ³National Institute of Standards and Technology, Gaithersburg, MD, USA. (xiugong.gao@na.amedd.army.mil)

Abstract: Sulfur mustard (SM), a vesicant chemical warfare agent, causes airway injury due to a massive release of destructive enzymes and mediators of inflammation. Inducible nitric oxide synthase (iNOS) is one of the important inflammatory mediators. However, iNOS is difficult to detect in airway epithelial cells by Western blotting and conventional immunocytochemical methods primarily due to its very low basal level expression. Results from real time RT-PCR experiments indicated that the iNOS mRNA level was $10^3 - 10^5$ times lower than that of some proinflammatory cytokines. In this study, we used quantum dots, a novel nano-scale material, as fluorophore in the immunocytochemical detection of iNOS. As a result of the high stability, intensity, and signal to noise ratio of the fluorescence signal, iNOS was easily detectable in both unexposed control and SM-exposed small airway epithelial cells (SAEC) and normal human bronchial/tracheal epithelial (NHBE) cells. Exposure to 100 μ M of SM dramatically increased iNOS expression in the two cell types. When roxithromycin, a representative macrolide antibiotic, was added into the culture medium at 100 μ M immediately before SM exposure, iNOS expression was reduced substantially (comparable to basal level). Other commonly used macrolides including azithromycin, clarithromycin and erythromycin also effectively decreased iNOS expression in SM-exposed SAEC and NHBE cells. Thus, the current study provides *in vitro* evidence of the immunomodulatory effects of macrolide antibiotics in SM-exposed airway epithelial cells. In this method, the output is quantitative, and multiple samples (up to 30) can be analyzed simultaneously on the *BenchMark XT IHC/ISH* platform (Ventana). Therefore, this method can be employed for high throughput screening of anti-inflammation drugs.

P07

EFFECTS OF PBS COMPOSITION ON THE SENSITIVITY OF SIGNAL DETECTION UNDER CLSM WITH QUANTUM DOT (QDOT)

NIIOKA, M.^{1,2}, ITOH, J.², KINOUE, T.¹ and WATANABE, T.¹

¹Department of Community Health, ²Department of Teaching and Research Support Center, Tokai University School of Medicine, Japan. (niioka@is.icc.u-tokai.ac.jp)

Abstract: Confocal laser scanning microscopy (CLSM) is a powerful tool to detect the co-localization of two or more signals in one cell at the same time. However, it is often difficult to detect low abundance antigens by using conventional immunofluorescence technique. To use Qdot (Invitrogen Corp.) secondary antibody conjugates or Qdot streptavidin conjugates can provide substantial benefits in the detection of low abundance targets. Even so, we found that the incubation and washing buffer affected the result of signal detection by using CLSM.

Liver tissue was obtained from recovery phase of cirrhotic rats induced by 12-week CCl₄ treatment and frozen sections were prepared. To detect the desmin-positive (stellate cells) and MMP-9-positive cells, Qdot conjugated second antibody or Qdot conjugated streptavidin were applied to the tissue samples according to the manufacturer's protocol. Positive signals were detected under CLSM (Carl Zeiss, Inc.). Three types of PBS incubation and washing buffer were prepared; 1) PBS (+) (80mM Na₂HPO₄, 21mM NaH₂PO₄, 1454mM NaCl), 2) PBS (-) (81mM Na₂HPO₄, 14.7mM KH₂PO₄, 26.8mM KCl, 1369mM NaCl), 3) modified PBS (-) (203mM Na₂HPO₄, 14.7mM KH₂PO₄, 26.8mM KCl, 1369mM NaCl). To use PBS (-) increased the sensitivity to detect both desmin- and MMP-9-positive cells. Moreover, to use modified PBS (-) dramatically improved both signals. Only a few positive signals were detected by using conventional fluorescence conjugated antibody. The desmin positive cells (stellate cells) did not express MMP-9 in the recovery phase of rat liver cirrhosis.

Effects of PBS composition on the sensitivity of Qdot have never been to studies so far. To use modified PBS (-) buffer not only increases the sensitivity but also saves expensive antibodies.

P08

IMMUNOLocalIZATION OF VARIOUS PROTEINS IN LIVING MOUSE ORGANS REVEALED BY "IN VIVO CRYOTECHNIQUE"

OHNO, S., TERADA, N., OHNO, N., SAITOH, S. and FUJII, Y.
University of Yamanashi, Chuo, Yamanashi, Japan. (sohno@yamanashi.ac.jp)

Abstract: Preservation of tissue components is necessary for describing functioning morphology of living animal organs. Therefore, we need freezing organs *in vivo* and examining immunolocalization of their components. All experiments using animals were approved by the University Committee in accordance with the Guidelines for Animal Experimentation in University of Yamanashi. We applied "in vivo cryotechnique" to immunohistochemistry of various mouse organs. (i) Serum proteins in nephrons: It was performed on anesthetized mouse kidneys under normal, experimentally hyperflow or heart-arrest conditions. Under the normal and heart-arrest conditions, albumin and immunoglobulin (Ig) light chains were immunolocalized in blood vessels. However, under the hyperflow condition, they were immunolocalized in Bowman's space and proximal tubular cells. (ii) Visualization of injected fluorescent probes: Goat FITC-IgG was injected into livers, which were frozen with isopentane-propane cryogen (-193°C). The double immunostaining with anti-mouse IgG antibody visualized its colocalization with the injected FITC-IgG. (iii) Protein leakage at blood-brain barriers: Albumin and IgG were immunolocalized in cerebellar blood vessels of living mice. However, their leakage through blood capillaries was revealed in the resected cerebellum as a model of anoxia. (iv) Disruption of blood-testis barriers: In normal seminiferous tubules, albumin was immunolocalized as arch-like patterns around some spermatogonia in basal compartments. Twenty-four or 48hrs after cadmium-treatment, it was also detected in adluminal compartments, indicating functional disruptions of blood-testis barriers. (v) Light-exposed retina of living mice: Immunoreactivity of phosphorylated rhodopsin was recognized at outer segments of photoreceptor cells, exposed to day-light. In 12hrs' dark-adapted retina, it was completely abolished. Even with light for 10sec after dark-adaptation, it was not yet detected. However, in 30sec, it was definitely recovered. In conclusion, ischemic or anoxic effects can be minimized by the "in vivo cryotechnique", which is quick enough to capture transient physiological processes and to maintain any proteins *in vivo*.

P09

COMPARISON OF THE Z-AXIS RESOLUTIONS ACHIEVED BY IMMUNOFLUORESCENCE MICROSCOPIC IMAGING OF TISSUE SECTIONS OF DIFFERENT THICKNESSES: USEFULNESS OF ULTRATHIN CRYOSECTIONS FOR ULTRAHIGH-RESOLUTION IMMUNOFLUORESCENCE MICROSCOPY

TAKIZAWA, T.¹, MORI, M.¹, ISHIKAWA, G.², TAKESHITA, T.², GOTO, T.¹ and ROBINSON, J.M.³

¹Molecular Anatomy, ²Obstetrics & Gynecology, Nippon Medical School, Tokyo, Japan; ³Physiology & Cell Biology, Ohio State University, Columbus, USA. (t-takizawa@nms.ac.jp)

Abstract: Ultrathin cryosections of cells and tissues (50-100 nm thick) have seldom been used as substrates for immunofluorescence microscopy (IFM). We recently introduced a new application for ultrathin cryosections as excellent substrates for IFM, as well as immunoelectron microscopy (for review see *J Histochem Cytochem* 51: 707, 2003). In the current study, we compared the z-axis resolutions achieved by IF microscopic imaging of human placental tissue sections of different thicknesses (ultrathin cryosections, optical sections of cryostat sections, and conventional cryostat sections). We used these images to determine the distribution of caveolin-1 and CD31 in endothelial cells of full-term, human placenta. IFM was carried out as described previously (*Methods Mol Med* 121: 351, 2006). Confocal images of ultrathin cryosections and cryostat sections were collected with an Olympus IX81 microscope equipped with a FV1000 confocal scan unit. Conventional images of the same cryostat sections were collected with an IX81 microscope equipped with a DP70 CCD camera. Endothelial cells were major sites of caveolin-1 and CD31 expression. Using ultrathin cryosections, the precise subcellular distribution of individual caveolae that were arranged immediately beneath the cell surface could be resolved in human placental endothelial cells. In contrast, individual caveolae were not readily discernible in cryostat sections by conventional IFM because of out-of-focus fluorescence signal. An improvement in the z-axis resolution of caveolae occurred when the same cryostat sections were observed by confocal microscopy. However in optical sections, the out-of-focus fluorescence signal was not completely eliminated and many caveolae remained stacked in the volume of the optical sections. Similar differences in the z-axis resolution of CD31 were observed. Our results show that ultrahigh-resolution IFM using ultrathin cryosections is particularly valuable for determining the precise subcellular distributions of and interactions between specific macromolecules in complex structures.

P10

PRODUCTION OF MOUSE MONOCLONAL ANTIBODIES AGAINST RAT TYPE IV COLLAGEN BY THE MOUSE ILIAC LYMPH NODE METHOD

SADO, Y., INOUE, S., TOMONO, Y. and OMORI, H.
Shigei Medical Research Institute, Okayama, Japan (sado@shigei.or.jp)

Abstract: We have established a novel method of preparing hybridomas producing mouse monoclonal antibodies and denoted "the mouse iliac lymph node method" (*Acta Histochem. Cytochem.* 39, Advance publication). Lymphocytes from enlarged iliac lymph nodes from two mice injected intramuscularly at the tail base with an emulsion of antigen and Freund's adjuvant are used for cell fusion. It has advantages: (1) a single injection of the antigen emulsion is sufficient, (2) the lymph nodes are ready for use 14 days after injection, and (3) a high yield of positive hybridomas is obtained. This method was applied to the production of mouse antibodies against rat type IV collagen.

We have already reported a rat model of anti-GBM nephritis induced by rat nephritogenic monoclonal antibodies (*Kidney Int.* 66: 177-186, 2004). Antibodies belonging to rat IgG2a and IgG2b have strong nephritogenicity to WKY/NCrj rats, and those belonging to rat IgG1 have weak nephritogenicity. This result indicates that the antibody subclasses are very important to the induction of nephritis. Although mouse antibodies are from different species, we tried to develop mouse monoclonal antibodies reacting with rat renal glomerular basement membrane (GBM) in order to have clues to analyze the nephritis. C57BL/6 and BALB/c mice were immunized with an emulsion of rat fraction containing the NC1 domains of type IV collagen. Their B cells from enlarged iliac lymph nodes were fused with mouse SP2 myeloma cells, and mouse IgG1, IgG2a, and IgG2b monoclonal antibodies could be established. They were able to stain rat renal basement membranes intensively. Injection of the IgG1 and IgG2a antibodies were able to induce nephritis in WKY rats, but that of the IgG2b was not. This result demonstrates that the new method is surely useful for production of antibodies against rat type IV collagen.

P11

STANDARDIZATION OF IMMUNOHISTOCHEMISTRY FOR FORMALIN-FIXED, PARAFFIN-EMBEDDED TISSUE SECTIONS BASED ON THE ANTIGEN RETRIEVAL TECHNIQUE:

From Experiments to Hypothesis

SHI, SHAN-RONG and TAYLOR, CLIVE R.

Department of Pathology, University of Southern California Keck School of Medicine, Los Angeles, California

Abstract: Standardization of immunohistochemistry (IHC) for archival formalin-fixed, paraffin-embedded (FFPE) tissue sections has become increasingly important due to the emergence of a new field of pathology that requires demonstration of the differential expression of various prognostic markers for individualized cancer treatment. From a practical point of view, one of the most difficult issues in the standardization of IHC for FFPE tissue is the adverse influence of formalin upon antigenicity, and the great variation in fixation/processing procedures. Our previous studies have demonstrated a potential approach to standardization of IHC for FFPE tissue based on optimal antigen retrieval (AR), to achieve a maximal degree of retrieval that provides a comparable level of IHC staining among various FFPE tissue sections that have been fixed in formalin from 4 hours to 7 days. On this basis the following hypothesis is proposed: "The use of optimized AR protocols permits retrieval of specific proteins (antigens) from FFPE tissues to a defined and reproducible degree (expressed as R%), with reference to the amount of protein present in the original fresh/unfixed tissue". This hypothesis may be explained mathematically. Suppose the amount of a protein in a fresh cell/tissue = Pf, and that Pf produces an IHC signal in fresh tissue of J (Pf). When the IHC signal of FFPE is J (Pffpe), then the retrieved rate of AR (R%) is calculated as: $AR \text{ rate } (R\%) = \frac{J (Pffpe)}{J (Pf)} \times 100\%$, the amount of protein in the FFPE tissue of Pffpe = Pf x R%. In a situation where optimized AR is 100% effective, then Pffpe = Pf if the IHC signal is of equal strength in fresh tissue and FFPE tissue.

Further studies are demanded to test this hypothesis. A research design using cell/tissue models is presented to test limitations of this hypothesis, based upon correlation of accurate quantitative biochemical measurements with IHC staining results.

P12

IMMUNOHISTOCHEMICAL DETECTION OF ANTIGEN-SPECIFIC ANTIBODY-PRODUCING PLASMA CELLS IN REGIONAL LYMPH NODES AND SPLEEN OF RATS IMMUNIZED WITH HORSERADISH PEROXIDASE

MIZUTANI, Y., SHIOGAMA, K., SHIMOMURA, R., KAMOSHIDA, S., INADA, K. and TSUTSUMI, Y.

*Department of Pathology, Fujita Health University School of Medicine, Aichi, Japan.
ymizutan@fujita-hu.ac.jp*

Abstract: The peroxidase-labeled antigen method is a technique that visualizes antigen-specific antibody-producing plasma cells on a tissue section. Antigen-specific antibody-producing plasma cells are localized with the use of biotin- or enzyme-labeled antigen. Establishment of this method enables us to analyze pathological conditions from the new viewpoint that allows us to observe antigen-specific antibody-producing plasma cells in the specific lesions. This method was reported in 1968 by two groups, include of Straus and a research group of Averameas et al. But it has never been applied thereafter. In this experiment, we attempted to repeat this method using the lymph node and spleen of rats immunized with horseradish peroxidase (HRP). Rats were immunized subcutaneously with HRP three times in footpad. After immunization, rats were euthanized by diethyl ether, and then inguinal lymph nodes and spleen were sampled. These organs were fixed in 4% paraformaldehyde solution, and then frozen sections were prepared. These sections were incubated with 1 µg/ml HRP solution. Anti-HRP antibody-producing plasma cells were visualized by incubating with diaminobenzidine and hydrogen peroxide. Sections were double stained with HRP and a cocktail of anti-rat IgG, IgA and IgM polyvalent antibody, and we analyzed the proportion of anti-HRP antibody-producing plasma cells in total plasma cells. In frozen sections of the lymph node and spleen, anti-HRP antibody-producing plasma cells were visualized as brown reaction products. Double staining for HRP binding and rat immunoglobulins revealed that the proportion of anti-HRP antibody-producing plasma cells in total plasma cells was about 40% in the inguinal lymph node, and about 10% in the spleen.

P13

ANTIGEN RETRIEVAL OF SURFACE LAYER PROTEINS FOR POST-EMBEDDING IMMUNOELECTRON MICROSCOPY FROM TANNERELLA FORSYTHENSIS BY MICROWAVING AND AUTOCLAVING WITH CITRACONIC ANHYDRIDE

MORIGUCHI, K.¹, IWAMI, J.², HIGUCHI, N.², MURAKAMI, Y.³, MAEDA, H.⁴, YOSHIMURA, F.³, NAKAMURA, H.², KAMEYAMA, Y.⁴ and OHNO, N.¹

Departments of ¹Anatomy, ²Endodontics, ³Microbiology and ⁴Pathology, School of Dentistry, Aichi-Gakuin University, Nagoya, Aichi 464-8650, Japan. (keiichi@dpc.aichi-gakuin.ac.jp)

Abstract: Tannerella forsythensis (*Bacteroides forsythus*), an anaerobic Gram-negative periodontopathogen has unique bacterial protein profiles containing major proteins with apparent molecular weights of more than 200-kDa, shown by sodium dodecylsulfate-polyacrylamide gel electrophoresis (SDS-PAGE). It is also known to have a typical surface layer (S-layer) consisting of regularly arrayed subunits outside the outer membrane, revealed by electron microscopy. In this study, we used citraconic anhydride (Immunosaver; Nisshin EM Co., Ltd. Tokyo, Japan) as a medium in heating antigen retrieval. Therefore, we examined the relation between high molecular weight proteins and S-layer in electron microscopic immunolabeling with chemical fixation, 4%paraformaldehyde-0.05%glutaraldehyde and reduced osmium tetroxide postfixation, and antigen retrieval procedure, microwaving for 15 min at 100 °C and autoclaving for 15 min at 132 °C with 1% citraconic anhydride. Envelope and soluble fractions were separated by ultracentrifugation of the whole cell extracts for 60 min at 143,000 x g. The envelope fraction was subjected to SDS-PAGE. One of the major proteins with a size of 270-kDa was used as an antigen for preparing a specific antiserum. Fixed cells were dehydrated and embedded in LR White. Ultrathin sections were treated by inserting them in drops of antisera 500-fold diluted with 1% bovine serum albumin (BSA)-phosphate buffered saline (PBS) for 12h. The sections were incubated in goat-rabbit IgG conjugated with 20nm gold diluted 50-fold in BSA-PBS for 1h. Immunogold particles were more enhanced at the outermost cell surface where the S-layer was present than the ordinary method without microwaving, autoclaving and citraconic anhydride. In conclusion, antigen retrieval by microwaving and autoclaving with citraconic anhydride was effective at the post-embedding immunogold electron microscopy.

P14

CYTOCHROME OXIDASE ACTIVITY REMAINS EVEN AFTER LONG FIXATION

UEDA, T.¹ and ISHIKAWA, Y.²

¹Department of Anatomy, Kanazawa Medical University, Japan, ²Medical Research Institute, Kanazawa Medical University, Japan (tadashi@kanazawa-med.ac.jp)

Abstract: Seligman et al. developed DAB method in 1968. They indicated that both DAB and osmium could strongly visualize the site of reaction product by electron microscopy. Since then, DAB method is widely used. However, we recently found that we could observe the reaction product of Cytochrome Oxidase(CyOx) without osmium. Even though the reaction product was weak as compared with osmium black, it was recognized moderately. It has been traditionally accepted that it is better to use short fixation for cytochemistry. In the case of cytochrome oxidase, fixation time is used for less than 30min. This present study reanalyzes the technique for DAB method, especially the fixation time. The cardiac muscles of mice were used. Tissues were fixed with 2.5% glutaraldehyde for 10min-7days. Tissue sections were made, and then were incubated the reaction medium, which consisted of 3,3'-diaminobenzidine, catalase, cytochrome C, 0.1M phosphate buffer, pH 7.4. As a control, 10mM NaN₃ or 1mM KCN was added in the standard medium. In the fixation for 10min, the CyOx activity was strong in myocardial cell. Also the fixation for 1 day, the activity of the reaction product appeared normal. Even in the fixation for 7days, the CyOx activity almost remained. However, some mitochondria diminished the activity. In the control medium, none of the mitochondria appeared the reaction products. These results suggest that CyOx activity is not sensitive to fixation, and it remains in the prolonged fixation in cardiac muscle.

P15

X-RAY MICROANALYSIS OF BIOLOGICAL SPECIMENS BY HIGH VOLTAGE ELECTRON MICROSCOPY

NAGATA, T.^{1,2} and KAMETANI, K.³

¹Department of Anatomy and Cell Biology, Shinshu University School of Medicine, Matsumoto, ²Department of Anatomy, Shinshu Institute of Alternative Medicine, Nagano; ³Department of Instrumental Analysis, Shinshu University, Matsumoto, Japan. (E-mail: nagatas@po.cnet.ne.jp)

Abstract: We applied high voltage electron microscopy to X-ray microanalysis of biological specimens. We first quantified the end products of histochemical reactions such as Ag in radioautographs, Ce in acid phosphatase reaction and Au in colloidal gold immunostaining. Then, we analyzed various trace elements such as Zn, Ca, S, Cl, K and P which originally existed in cell organelles of various cells using both conventional chemical fixation and cryo-fixation followed by cryo-sectioning and freeze-drying, or freeze-substitution or freeze-drying and dry-sectioning. We also analyzed such elements as Al which was absorbed into cells. As the results, the P/B ratios of the end products containing such elements as Ag, Ce and Au, or endogenous elements such as Zn, S and Cl, and exogenous elements such as Al, increased with the increase of the accelerating voltages from 100 to 400KV, reaching a peak, and decreased. Applying the accelerating voltages at the highest P/B ratios, which are specific for respective elements, we could quantify the silver contents in radioautograms, acid phosphatase activity due to aging, various endogenous trace elements were found in various cells such as Zn in Paneth cell granules of mouse duodenum, Ca in human ligaments and rat mast cells in freeze-dried cryo-sections, S in mouse colonic goblet cells, several elements such as S, K, Cl, P and Ca in freeze-dried cryo-sections of the duodenum, proximal and distal colons of aging mice, Al in the pinocytotic vesicles of the duodenums, the lysosomes of hepatocytes and Kupffer cells of the livers and the uriniferous tubule cells of the kidneys of mice fed with Al containing water. From the results, it was shown that X-ray microanalysis using semi-thin sections observed by high voltage transmission electron microscopy at 200-400 KV was very useful resulting in high P/B ratios for quantifying and analyzing various trace elements in biological specimens.

P16

NANOCRYSTAL FLUOROPHORES FOR MOLECULAR GENETIC AND CANCER TESTING

XIAO, YAN, BLASIC, JOE, HOLDEN, MARCIA and BARKER, PETER E.
Biochemical Science Div., Nat'l Inst of Standards and Technology, Gaithersburg, MD 20899

Abstract: Rational design cancer drugs that target specific molecular lesions have shown great promise when appropriate patient are identified. As the therapeutic costs and specificity of patient in which such drug may be effective, universally available physical standards and reference materials become increasingly important when the drug, its molecular target and molecular stratification of patients are well-defined. Approximately one-third of breast cancers have over expression of HER2/ERBB2/neu gene and cognate HER2 receptor. For such patients, Herceptin may be effective. Because of the cost of drug and the risk of side effects, accurate diagnostic measurements of HER2 gene (by FISH) and receptor (by IHC) are crucial. To address benchmarking of FISH, IHC and other diagnostic modalities, NIST has developed background materials and methods for HER2 metrology. We created the HER2 BAC clone as FISH probe¹, and designed anti-HER2 chicken antibody for IHC study. To improve signal quantitation, we have incorporated quantum dot fluorophores into measurement of HER2 analytes at both the FISH and IHC levels in batch model reference material preparations with DNA and antibody probes and methods developed at NIST^{1, 2}. To further improve HER2 metrology, we have applied z-plane corrections to fluorescent signals with 3D quantitative analysis of quantum dot fluorescence supplemented by deconvolution algorithms. These methods and materials will go into interlaboratory validations soon. This model system for rational design cancer drugs illustrates a general approach to improving metrology of complex molecular genetic diagnostic tests through quantitative technology development in the process of generating stable, highly-certified fixed biological substrates coordinated for measurements at the gene, mRNA, protein and receptor levels of analysis.

P17

OPTICAL IMAGING OF TUMOR PROGRESSION IN LIVING SYSTEMS

MOIN, KAMIAR¹, SAMENI, MANSOUREH¹, LINEBAUGH, BRUCE¹, RUDY, DEBORAH¹, TUNG, CHING², and SLOANE, BONNIE¹

¹Wayne State University School of Medicine, Detoit, USA; ²Massachusetts General Hopital, Harvard University, Boston, USA. (kmoin@med.wayne.edu)

Abstract: Despite the awareness that proteolysis is essential for cancer progression, and that proteases represent potential drug targets, clinical trials for cancer treatment with inhibitors of MMPs have failed. Moreover, a broad and comprehensive strategy to identify potential protease targets has not been employed. We hypothesize that proteases are valid therapeutic/prevention targets in cancer and that imaging of proteolysis and its inhibition will provide a means to confirm this hypothesis. We have developed functional optical imaging techniques to monitor tumor progression and tumor-host interactions based on proteolytic activity, both *in vitro* and *in vivo*.

In vitro, we have used a 3-dimensional assay system to study tumor-stromal interactions, utilizing confocal microscopy. We have found that both pericellular and intracellular proteolysis occur during tumor invasion. Furthermore, there is significant interaction between tumor and stromal cells. Our results indicate that tumor cells actively recruit stromal cells and that these cells contribute significantly to tumor proteolysis. In addition, our most recent results show that the degree and the ratio of intracellular to pericellular proteolysis may be dependent on the density of the surrounding medium. It appears that in a low-density environment there is less overall proteolysis that is mostly intracellular.

In vivo, we have utilized quenched fluorescent probes that are activated by proteases. We have found that upon injection of these probes into tumor bearing mice, the probes are activated at the tumor site and the resulting fluorescence can be detected thereby revealing the position/size of the tumor *in vivo*. The probes are not specific to any particular tumor type. However, since there is increased expression of proteases in tumors, the resulting fluorescent products do accumulate at the tumor site. Our preliminary observations suggest that utilization of such probes will provide both a sensitive method for cancer diagnosis and a means to monitor therapeutic efficacy.

P18

MULTIPLEXING MOLECULAR MARKERS WITH MULTISPECTRAL IMAGING

MANSFIELD, JAMES R.,¹ KERFOOT, CHRISTOPHER A.², and LEVENSON, RICHARD M.¹

¹CRi, Woburn, MA; USA, ²Mosaic Laboratories, Lake Forest, CA, USA. (rlevenson@cri-inc.com)

Abstract: Background: Multi-analyte immunohistochemistry, whether in brightfield or fluorescence, has many potential applications in pathology. However, accurate assessment of two or more co-localized antigens, especially using brightfield microscopy has been hindered by the difficulty in discriminating and quantifying overlaying labels. Multispectral imaging (MSI) can resolve overlapping chromogens and generate quantitative images of individual analytes. MSI can also separate fluorophores from ubiquitous autofluorescence background, allowing more sensitive and quantitative studies. There are two immediate applications for MSI in immunohistochemistry: the first is in the study of ER and PR expression in breast cancer; the second is the imaging of QDMap™ immunofluorescence labels.

Design: Samples doubly labeled for ER and PR were prepared using DAB, VulcanRed and hematoxylin. Automated tools were developed to quantitate nuclear percent-positivity and degree of co-localization of dual nuclear markers. Immunofluorescent samples were all prepared using QDMap™ staining on Discovery XT automated staining systems. All samples were imaged using the CRi Nuance™ multispectral imaging system.

Results: Spectral unmixing of DAB and VulcanRed chromogens from the hematoxylin counterstain was achieved, resulting in a quantitative assessment of both ER and PR positive labeling as well as a quantitative assessment of degree of co-localization. QDMap™-labeled samples were imaged and the fluorophores separated from tissue autofluorescence. The unmixed QDot™ images were compared to standard methods, with MSI providing a large increase in sensitivity. In addition, separation of fluorophore from autofluorescence resulted in a more quantitative analysis of fluorescence intensity.

Conclusions: The use of multispectral imaging methods combined with automated spectral analysis tools can easily separate and quantitate multiple chromogens and counterstains in a single tissue sample even when the antigens are co-localized. These methods form an ideal complement to automated staining platforms and new multiplex labeling strategies, and together constitute clinically viable techniques that hold great potential to further characterize and subtype cancers.

P19

X-RAY MICROANALYSIS ON THE ACTIVITY OF ACID PHOSPHATASE IN MOUSE KIDNEY

OLEA, M. T.¹, and NAGATA, T.²

¹Rizal Technological University, Mandaluyong City, Philippines; ²Shinshu University School of Medicine, Matsumoto, Japan. (E-mail <mel_ole@hotmail.com>)

Abstract: Acid phosphatase(AcP) is one of the hydrolases contained in the lysosome and has been characterized as a marker enzyme for this cell organelle. The use of this enzyme as a marker for cell death and/or cell undergoing lysis has been established. In rat kidney, AcP has been localized in Type II and Type IV of the proximal tubule cells. Hence, the present study was undertaken to determine possible correlation between the enzyme activity and the maturational development of the animal. In this study, we used 6 groups of ddY strain mice, aged at postnatal day 1, week 1 and 2, and month 1, 2 and 10. For the cytochemical demonstration of the enzyme activity, the lanthanide-based method for the ultrastructural localization of AcP was employed.

The results showed that the fine localization of AcP was demonstrated in the proximal tubule cells, particularly of the second segment of the kidneys of mice at various ages. Dense reaction deposit as a result of AcP activity with cerium was observed in the lysosomes in all animals. The final deposits of the enzyme reaction products appeared electron dense and homogeneous in the proximal uriniferous tubule cells of all mice. However, in other cells it appeared heterogeneous. The presence of cerium in the deposits was confirmed qualitatively by X-ray microanalysis. In the recorded spectra, peak label La = 4.84 KeV and Lb = 5.26 KeV from element cerium was recorded. The main spectral line of cerium at La = 4.84 KeV was used in the quantitative computation of the peak-to-background (P/B) ratio. The computed average ratio of the different ages of the animals studied decreased significantly from 1 week after birth and progressively until the 10th month. The difference was significant at $p < 0.05$.

P20

DISTRIBUTION OF MITOCHONDRIA IN MOUSE SPERMATOGENIC CELLS, DETECTED BY THE EXPRESSION OF PEYFP-MITO ELECTROPORATED IN VIVO, AND ITS POSSIBLE RELATION TO GERM CELL APOPTOSIS

HISHIKAWA, Y.¹, AN, S.¹, SHIBATA, Y.¹, and KOJI, T.¹

¹*Nagasaki University Graduate School of Biomedical Sciences, Nagasaki, Japan, (yhish@net.nagasaki-u.ac.jp.)*

Abstract: During spermatogenesis, mitochondria change their structure and distribution, and have a central role in the regulation of germ cell apoptosis; the apoptosis is closely associated with redistribution of Bax and release of cytochrome c from mitochondria. It is also known that estrogen modulates various biological aspects in male reproductive organs through binding to estrogen receptor (ER). Interestingly, it has been reported that ERBETA is localized to mitochondria, suggesting that estrogen could directly affect mitochondrial functions through ERBETA. However, the precise mechanism of mitochondrial distribution and their functions related to apoptosis during spermatogenesis was largely unknown. Therefore, we investigated the change in the mitochondrial distribution and their function related to apoptosis-regulated proteins such as Bax and cytochrome c, and ERBETA in germ cells. We used a vector that encodes a fusion protein of enhanced yellow fluorescent protein and mitochondrial targeting sequence of cytochrome c oxidase (pEYFP-Mito). pEYFP-Mito was transfected directly into mouse testis by *in vivo* electroporation, and observed by laser scanning microscopy. Bax, cytochrome c, and ERBETA were detected immunohisto-chemically. As a result, pEYFP-Mito was found in the spermatogonia after 1 day, and was found in spermatogonia and spermatocytes after 7 to 90 days, consistently. pEYFP-Mito was localized in both a speckled cytoplasmic pattern and a whole cytoplasmic pattern in the cytoplasm of these germ cells. In the latter case, Bax and cytochrome c were also distributed throughout the whole cytoplasm, which was usually associated with apoptotic germ cells. Furthermore, ERBETA was localized in spermatogonia and spermatocytes and found to colocalize with speckled cytoplasmic pattern of pEYFP-Mito transfected germ cells. These results demonstrate that *in vivo* electroporation of pEYFP-Mito was a useful tool for examining the mitochondrial distribution during spermatogenesis, as well as the specific pattern of mitochondria to whole cells, which may be essential for the germ cell apoptosis.

P21

GENOME SIZE AND DNA CONTENT OF THE X CHROMOSOMES, AUTOSOMES AND LIMITED CHROMOSOMES OF *SCIARA COPROPHILA*

RASCH, E.M.

East Tennessee State University, Johnson City, TN USA (emrasch@worldnet.att.net)

Abstract: The unique chromosome biology of the dark winged fungus gnat *Sciara coprophila* (Lintner) has fascinated and puzzled investigators for more than 80 years. Male meiosis exhibits a monopolar spindle, non-random segregation of paternally imprinted chromosomes and non-disjunction of the maternal X chromosome. The unusual mechanism of sex determination requires selective elimination of one or two X chromosomes during early embryogenesis, Supernumerary (L) chromosomes which are retained only by germ line cells also are eliminated from the soma at very early cleavage divisions. Distinctive DNA puffs on the large, polytene larval salivary gland chromosomes are sites of selective DNA amplification. As a foundation for future genome studies to explore these many unusual phenomena, we have used DNA-Feulgen cytophotometry to determine genome size from hemocyte nuclei of male (X0) and female (XX) larvae and adults. The 2C-values for somatic cells of adult females of *Sciara* is ~0.57 pg DNA and ~0.52 pg DNA for adult males, or roughly equivalent to 500-550 Mbp of DNA. The DNA content of the X chromosome is ~ 0.05 pg DNA and the autosomal complement is ~ 0.45 pg DNA. Measurements of DNA levels for individual sperm from adults showed that the DNA contribution of the germ line-limited (L) chromosomes constitutes as much as 35% of the DNA of the male gamete. A parallel study using *Sciara ocellaris* (Comstock), a related species lacking L chromosomes, confirmed the presence of 2 X chromosomes in the sperm of this latter species. Supported in part by grants from NIH (14644) and NSF (DEB 77-03257 and DEB 00-80921) and research funds from the James H. Quillen College of Medicine.

P22

CIRCADIAN RHYTHM GENERATION IN A GLIOMA CELL LINE

FUJIOKA, A.¹, HONDA, E.², TAKASHIMA, N.^{1,3} and SHIGEYOSHI, Y.¹

¹Department of Anatomy and Neurobiology; ²Institute of Life Science, Kinki University School of Medicine, Osaka-Sayama, Osaka, Japan; ³Course of Medical Biosignaling, The Public Relations Committee, Graduate School of Medicine, Faculty of Medicine, Osaka University, 2-2 Yamadaoka Suita, Osaka, Japan (fujioka@med.kindai.ac.jp)

Abstract: In mammals, the principal circadian oscillator resides in the hypothalamic suprachiasmatic nucleus. However, the basic components and the ability to generate a circadian rhythm are also characteristic of most peripheral tissues and some cell lines. We showed that the rat C6 glioma cell line displayed circadian oscillations of reporter luciferase bioluminescence driven by the mouse *Per2* promoter and of clock and clock-related gene transcripts, after exposure to dexamethasone (Dex). The C6 glioma cell line has therefore the potential to be a useful tool in investigations of the underlying molecular machinery of the circadian clock. In our present study, we have used the sensitive 2-D-DIGE coupled to MS for the identification of proteins which periodically expressed and regulated the circadian oscillations of genes in nucleus. Nuclear extracts from C6 cells harvested every 4 hours for 2 days after the Dex administration were labeled with Cy5 fluorescent dye. An internal pool was generated by combining equal amounts of each nuclear extract and labeled with Cy3. The nuclear extracts, together with a pool aliquot, run in a single gel. Proteins were visualized using a fluorescence scanner and analyzed the differences in the amount across multiple samples with a DeCyder software. Then we identified those proteins with MALDI-TOF MS. With the nuclear extracts, we found a number of proteins showing diurnal fluctuation in the amount. We also found that some proteins show rhythmic phosphorylation.

P23

FUNCTIONAL ANALYSIS OF THE KU70-BINDING SITE OF KU80 BY GFP TECHNOLOGY

KOIKE, M.¹, and KOIKE, A.¹

¹*DNA Repair Gene Research, National Institute of Radiological Sciences, 4-9-1 Anagawa, Inage-ku, Chiba 263-8555, Japan. (m_koike@nirs.go.jp)*

Abstract: Ku plays a key role in multiple nuclear processes, e.g., DNA repair, transcription regulation, and replication. It is believed that heterodimerization between Ku70 and Ku80 is essential for Ku-dependent DNA repair, although its role is poorly understood. We previously identified the Ku70-binding site of Ku80. In this study, to understand the role of heterodimerization in the function of Ku, we generated and/or analyzed cell lines stably expressing the EGFP-tagged-wild-type human Ku80, its Ku70-binding mutant, its NLS-dysfunctional mutant, or its double mutant in Ku80-deficient cells. Our results show that the Ku70-binding site of Ku80 is required for the stabilization of Ku70 in the cytoplasm and for the nuclear translocation of Ku80 through its heterodimerization with Ku70. In addition, our results suggest that the nuclear translocation of Ku80 through the Ku70-binding site as well as through the NLS of Ku80 play, at least in part, a role in Ku80-dependent DNA repair. Furthermore, our results suggest the possibility that Ku80 has a DNA DSB repair function independent of Ku70 in the nuclei, in addition to that dependent on Ku70. In conclusion, the Ku70-binding site of Ku80 is required for the stabilization of Ku70 in the cytoplasm, for the nuclear translocation of Ku80, and for Ku80-dependent DNA repair.

P24

BOTH ACTIN AND MYOSIN INHIBITORS BLOCK OR SLOW CHROMOSOME MOTION IN MITOTIC PtK1 CELLS:

Is An Actomyosin System a Back-up To the Microtubule/Motor Protein Complex That Could Account for the Fidelity of Chromosome Segregation in Mitosis?

SNYDER, J.A.¹ and OLSOFKA, CLAIRE

Department of Biological Sciences, University of Denver, Denver, CO 80208/USA.

¹jsnyder@du.edu (303) 871-3537. FAX (303) 871 3471 (Poster)

Abstract: Our objective has been to use a myosin inhibitor to test its ability to block or slow chromosome motion in PtK₁ cells during mitosis. Using antibodies and stains to actin, myosin, tubulin and DNA, immunocytochemical analysis has revealed that both actin and myosin were identified in the mitotic PtK₁ spindle (Robinson and Snyder, (2005). *Protoplasma*: **225**: 113-122). With the advent of a new innovative fixative, we could simultaneously fix and identify both actin and tubulin cytoskeletal elements in mitotic PtK₁ spindles (Robinson and Snyder, (2004). *J. Histochem. Cytochem.* **122**:1-5). We have shown that actin poisons, particularly cytochalasin J, slowed or blocked prometaphase chromosome congression, detached several to many chromosomes from the spindle, and changed microtubule architecture in the spindle; such that microtubules lost compression and splayed from the spindle domain. Ultrastructural analysis revealed loss of kinetochore structure (Wrench and Snyder, (1997). *Cell Motil. Cytoskel.* **36**:112-124); these results suggested microfilaments interact with kinetochore fibers, and may connect along this subclass of microtubules from the centrosomes to the kinetochore. Our recent findings investigated the role of 2, 3-butanedione monoxime (BDM), a myosin poison and its effect on mitotic PtK₁ cells. Using antibodies and stains, as described above, we have been able to confirm that BDM had the same effect on the progression of mitosis, spindle architecture and chromosome position. Our new BDM studies (20 to 40 μm BDM treatment) on myosin localization, coupled with tubulin and chromosome localization, showed dislocation of chromosomes to the periphery of the spindle, chromosome detachment, and the splaying of interpolar microtubules from the spindle domain. We concluded from this study that an actomyosin system is present in the spindle and may act as a “back-up” system to assure fidelity in chromosome segregation during mitosis. (Supported by the Barton L. Weller Endowed Chair to JAS.)

P25

UBIQUITINATION OF PROTAMINE IN THE SPERM NUCLEUS OF RAT AND HUMAN

HARAGUCHI, CELINA M.¹, MABUCHI, TADASHI², HIRATA, SHUJI³, SHODA, TOMOKO³, HOSHI, KAZUHIKO³ and YOKOTA, SADAHI¹

¹Biology Laboratory, ²Department of Biochemistry and ³Department of Gynecology and Obstetrics, Interdisciplinary Graduate School of Medicine and Engineering, University of Yamanashi, Chuo-shi, Yamanashi, 409-3898, Japan

Abstract: DNA of sperm nucleus is compactly folded by protamine (PT) instead of histones. Soon after fertilization, PT is replaced by egg histones and presumably degraded quickly. It is still unclear whether PT is degraded by ubiquitin-proteasome system. To answer to this question, we investigated the ubiquitination of PT in spermatids and spermatozoa using quantitative immunoelectron microscopy and biochemical methods. Labeling density for polyubiquitinated proteins in spermatids started to increase at steps 10 to 12 and it reached the maximum in mature spermatozoa. Labeling density for PT changed similarly, suggesting that PT was ubiquitinated. Then, we immunostained sperm heads after extraction of DNA and PT. Labeling for polyubiquitin and PT were almost lost, suggesting the ubiquitination of PT. Next, we analyzed basic proteins prepared from mature sperm of rat and human for ubiquitin signals using Western blotting after acetic acid-urea PAGE. In basic proteins prepared in the presence of iodoacetamide at the beginning of extraction, polyubiquitin (pUb) signals were detected in protein bands migrated more slowly than PT and these bands also stained for PT, whereas a main PT band was not stained for pUb, indicating clearly that some population of PT molecules was polyubiquitinated. It is known that protamine, unlike histones and transition proteins, remains in the gel after incubation with SDS. After such treatment, the slowly-migrated bands as well as PT remained in the gel, showing clearly that these bands contained PT. Next, we observed the molecular mass of the slowly-migrated bands by gel-filtration on Sephacryl S-200. Fractions ranged between the latter half of BSA peak (66 kDa) and the latter half of carbonic anhydrase (29 kDa) were stained for PT as well pUb, showing that the molecular mass of PT was increased by its polyubiquitination. All together, we have demonstrated first time that PT is polyubiquitinated.

P26

EFFECT OF THE *AMS* MUTATION IN THE ATAXIA AND MALE STERILITY (*AMS*) MOUSE ON PHOTIC INJURY TO PHOTO RECEPTOR CELLS

ARAKI, ASUKA¹, NAKANO, AKINOBU¹, ZHOU, LI¹, MARUYAMA, RIRUKE¹, OHIRA, AKIHIRO² and HARADA, TAKAYUKI¹

Departments of ¹Pathology and ²Ophthalmology, Shimane University School of Medicine, Izumo 693-8501, Japan (asuka@med.shimane-u.ac.jp)

Abstract: To elucidate the cellular basis of atrophy of the *AMS* retina, we investigated how the *ams* mutation affected the process of apoptosis induced by photic injury to photo receptor cells. **Methods:** The *AMS* and control mice were kept in a cage with its inner wall lined with tinfoil and they were exposed to light from a 20W fluorescent tube placed just above a cage for the indicated period of time. All experiments using animals were approved by the University Committee in accordance with the Guidelines for Animal Experimentation in Shimane university. Morphological examinations of the retina including TUNEL and immunohistochemical analyses were performed. **Results:** 1. The retina of the 11 week-old *ams* homozygous mouse was found to be thinner than that of the age-matched control mouse. In addition, apoptotic cells were observed in the outer nuclear layer (ONL) of the *AMS* retina, while only a slight degree of staining for TUNEL was observed. 2. Many cells that were either weakly or strongly positive for TUNEL were observed throughout the *AMS* ONL at 12 hours after the 6-hour light exposure or soon after either the 12- or 24-hour light exposure. In contrast, only a small number of weakly TUNEL-positive cells were observed in the control mouse retina at only 12 hours after the 24-hour light exposure. 3. A decrease in the total number of the nuclei and an increase in the number of apoptotic cells was observed light microscopically in the *AMS* ONL, not at 1 day but at 7 days after the 24-hour light exposure. 4. Cells which were immuno-positive for activated caspase-3 were only seldom observed after light exposure. **Conclusion:** The *ams* mutation was thus found to make photo receptor cells vulnerable to photic injury. However, the process of apoptosis seems to be different from that of typical apoptosis, which we observed in the *AMS* cerebellar granule cells, because of the appearance of many TUNEL-weak-positive cells and the absence of the activated caspase-3-positivet cells, despite the presence of apoptotic cells which can easily be recognized by either light or electron microscopic observations.

P27

CHOLESTEROL DEPLETION INDUCES AUTOPHAGY

CHENG, J., OHSAKI, Y., TAUCHI-SATO, K., FUJITA, A. and FUJIMOTO, T.

Department of Anatomy and Molecular Cell Biology, Nagoya University Graduate School of Medicine, Nagoya 466-8550, Japan (chengjinglei@hotmail.com)

Abstract: Autophagy, or self-eating, is a mechanism to digest the cell's own components, and its importance in many physiological and pathological processes is becoming recognized. Atg proteins are known to execute the engulfing process, but there are still many uncertainties about the molecular mechanism that switches on autophagy.

In the present study, we found that cholesterol depletion induces macroautophagy. The cellular cholesterol was depleted in human fibroblasts and Huh7 hepatoma cells by three different protocols: 1) 5 mM methyl- β -cyclodextrin in DME, 60 min, 2) 10 μ g/ml nystatin in DME, 60 min, 3) 20 μ M mevastatin and 200 μ M mevalonolactone in DME with 1-10% lipoprotein-deficient serum, 3 days. By any protocol, marked increase of LC3-II was detected by immunoblotting and by immunofluorescence microscopy. The induction of LC3-positive membranes was also observed by GFP-LC3. The increase of LC3-II was blocked by 10 mM 3-methyladenine, implying that the process is dependent on the PI3-kinase (type III) activity. The above changes were more extensive than those caused by amino acid starvation, i.e., incubation in Hepes-buffered Hanks solution for 2 hrs. By electron microscopy, an increase of autophagic vacuoles was observed after cholesterol depletion and the vacuoles were indistinguishable from those after amino acid starvation.

The result indicates that acute or semi-acute decrease of cholesterol activates autophagy. Cholesterol depletion has been used extensively to study the membrane raft. Notably PI(4,5)P₂, a substrate of PI3-kinase, has been reported to concentrate in the detergent-resistant membrane, and to be decreased and/or dispersed by cholesterol depletion. Further dissection of the phenomenon should elucidate whether and how raft functions are related to the regulation of autophagy.

P28

CYTOPLASMIC LIPID DROPLETS FUNCTIONS AS A UNIQUE PLATFORM FOR DEGRADATION OF APOLIPOPROTEIN B

OHSAKI, Y., CHENG, J., FUJITA, A. and FUJIMOTO, T.

Department of Anatomy and Molecular Cell Biology, Nagoya University Graduate School of Medicine, Nagoya 466-8550, Japan (yohsaki@med.nagoya-u.ac.jp)

Abstract: Lipid esters stored in cytoplasmic lipid droplets (CLDs) of hepatocytes are utilized to synthesize very low-density lipoproteins (VLDL), into which apolipoprotein B (ApoB) is integrated cotranslationally.

In the present study, by using Huh7 cells, derived from human hepatoma and competent for VLDL secretion, we found that ApoB is highly concentrated around CLDs. Based on the characteristic crescent or circular shapes, we called the ApoB labeling around CLDs as "ApoB-crescents". ApoB-crescents were also identified in another hepatoma-derived cell line, HepG2, and in primary human hepatocytes, although the frequency was lower than in Huh7 cells. ApoB-crescents were seen in less than 10% of Huh7 cells under normal conditions, but the ratio increased to nearly 50% after 12 h of proteasomal inhibition by ALLN. Electron microscopy showed ApoB to be localized to a cluster of electron-lucent particles 50–100 nm in diameter adhering to CLDs. ApoB, proteasome subunits, and ubiquitinated proteins were detected in the CLD fraction, and this ApoB was ubiquitinated. Interestingly, proteasome inhibition also caused increases in autophagic vacuoles and ApoB in lysosomes. The lysosomal ApoB was not derived from secreted and endocytosed VLDL. ApoB-crescents began to decrease after 12–24 h of proteasomal inhibition, but the decrease was blocked by an autophagy inhibitor, 3-methyladenine. Inhibition of autophagy alone caused an increase in ApoB-crescents.

These observations indicate that both proteasomal and autophagy/lysosomal degradation of ApoB occur around CLDs, and that the CLD surface functions as a unique platform for convergence of the two pathways.

P29

EFFECT OF A PLASTICIZER, DI(2-ETHYLHEXYL)PHTHALATE ON THE LIVER PEROXISOMES OF SWEET WATER FISHES

YOKOTA, SADAHI and HARAGUCHI, CELINA M.

Biology Laboratory, Interdisciplinary Graduate School of Medicine and Engineering, University of Yamanashi, Chuo-shi, Yamanashi, 409-3898, Japan

Abstract: Proliferation of liver peroxisomes (POs) is induced by many kinds of chemicals which are released to the environment. Proliferation of mussel liver POs is being used for the evaluation of sea water pollution by petroleum products. In previous study, we investigated the proliferation of crayfish liver POs by a plasticizer, di(2-ethylhexyl)phthalate (DEHP). At DEHP concentration lower than 0.01 mg/ml, no significant increase of POs was observed, suggesting that crayfish liver POs are unsuitable to evaluate the low level of water pollution. To clarify DEHP concentration inducing the PO proliferation and the reactivity of fishes for DEHP treatment, first we studied the conditions for tissue fixation and for DAB reaction and the morphological characteristics of POs in wild sweet water fishes. We collected 6 species of wild fishes. Liver was cut into small tissue blocks in ice-cold fixative consisting of 0.5-2% glutaraldehyde (GA) and 0.1 M Hepes-KOH buffer (pH 7.4) and treated by microwave for 0.5-3 min at 500 W and further fixed at RT for 1-2h. Tissue slices were incubated in DAB medium consisting of DAB (1-2 mg/ml), 0.001% Triton X-100, 0.01-0.02% hydrogen peroxide and 0.05 M Teorel-Stenhagen universal buffer (pH 6.0-10.0), tissue slices were fixed in 1% reduced osmium tetroxide, dehydrated and embedded in Epon. Ultrastructure of liver PO was well preserved after 1 min-microwave fixation with 1% GA. POs were stained most strongly after incubation in the reaction medium (at pH 10) consisting of 1 mg DAB/ml and 0.01% hydrogen peroxide. Most of POs were round and contained no cores in all species examined. The diameter of POs ranged 0.1 to 1.8 μm depending on species. POs of a loach were smallest (0.1-0.6 μm) and those of a medaka largest (0.5-1.8 μm). Number of POs varied among species. It tended to decrease when lipid droplets in liver cells increased.

P30

ALL-TRANS-RETINOL INDUCES RAPID RECRUITMENT OF TIP47 TO LIPID DROPLETS IN THE RETINAL PIGMENT EPITHELIUM

TSUIKI, E.¹, FUJITA, A.², OHSAKI, Y.², CHENG, J.², IRIE, T.³, SENOO, H.³, MISHIMA, K.¹, KITAOKA, T.¹, and FUJIMOTO, T.²

¹Department of Ophthalmology, Nagasaki University School of Medicine, Nagasaki, Japan ;

²Department of Anatomy and Molecular Cell Biology, Nagoya University Graduate School of Medicine, Nagoya, Japan ;

³Department of Anatomy, Akita University School of Medicine, Akita, Japan. (t-eiko@net.nagasaki-u.ac.jp)

Abstract: PURPOSE: To investigate the effect of light stimulation on lipid droplets (LD) and LD proteins in the retinal pigment epithelium (RPE), and dissect the underlying molecular mechanism.

METHODS: Mouse eyes exposed to flashlight and ARPE-19 cells treated with all-trans-retinol were labeled for immunofluorescence microscopy and the labeling intensity was quantified by image analysis. LDs stained by BODIPY493/503, LD proteins, i.e., Adipocyte differentiation-related protein (ADRP), TIP47, and Rab18, were examined. Immunoelectron microscopy using Lowicryl HM20 sections were done for ADRP in mouse RPE. Localization of mutated TIP47 was examined. Endogenous expression of TIP47 was knocked down by RNA interference (RNAi), and its effect on the retinoids were quantified by HPLC.

RESULTS: Flashlight on mouse eyes and all-trans-retinol on ARPE-19 cells caused rapid translocation of TIP47 from the cytosol to LDs, whereas ADRP distributed constitutively in LDs. The LDs were distributed randomly in the cytoplasm and their identity was confirmed by immunoelectron microscopy. The localization of TIP47 to LDs was abolished when either the amino terminal or the carboxyl terminal half of the molecule was deleted, but enhanced by a short deletion in the carboxyl terminus. Decrease of TIP47 expression by RNAi did not affect the retinyl ester stored in ARPE-19 cells significantly.

CONCLUSIONS: The result corroborated that TIP47 in RPE in vivo is translocated to LDs in response to the increase of all-trans-retinol upon photobleaching. We speculate that this movement of TIP47 may be related to the retinoid cycle in the RPE.

P31

MACROMOLECULAR SYNTHESIS IN MITOCHONDRIA OF DEVELOPING AND AGING MOUSE HEPATOCYTES AS REVEALED BY ELECTRON MICROSCOPIC RADIOAUTOGRAPHY

NAGATA, T.^{1,2}¹*Dept of Anatomy and Cell Biology, Shinshu University School of Medicine, Matsumoto;*²*Dept of Anatomy, Shinshu Institute of Alternative Medicine, Nagano, Japan. (E-mail: nagatas@po.cnet.ne.jp)*

Abstract: The macromolecular synthesis such as nucleic acids (DNA and RNA) and proteins in mitochondria of animal cells was morphologically first demonstrated by the present author by means of electron microscopic radioautography in primary cultured cells of the livers and kidneys of mice and chickens in vitro as well as in vivo. However, the relationship between the nucleic acid and protein syntheses and the aging of individual animals has not yet been clarified. This paper deals with the relationship between the macromolecular synthesis and aging in hepatocytes of mice in vivo at various ages from prenatal to postnatal senescence by means of electron microscopic radioautography. After the injections with nucleic acid (³H-thymidine, ³H-uridine) and protein precursors (³H-leucine) into several groups of litter mice from prenatal day 19 to postnatal day 1 to month 24 (year 2), the liver tissues were fixed, embedded in epoxy resin, sectioned and processed for electron microscopic radioautography. The radioautographs showed that some of the mitochondria in the hepatocytes were labeled with silver grains due to ³H-thymidine, ³H-uridine or ³H-leucine, respectively, showing DNA, RNA or protein syntheses. Quantitative analysis on the number of mitochondria in mononucleate hepatocytes increased from the prenatal day to postnatal month 2-6, reaching the maximum, then decreased to year 1-2. The numbers of labeled mitochondria with ³H-thymidine showing DNA synthesis and the labeling indices increased from prenatal day to postnatal day 14, reaching the maximum, then decreased to year 1, while the numbers of labeled mitochondria and the labeling indices with ³H-uridine showing RNA synthesis as well as ³H-leucine showing protein synthesis also increased from prenatal day to postnatal month 1 (RNA) or day 14 (protein), respectively, reaching the maximum, then decreased to year 2.

P32

SEQUENTIAL APPEARANCE OF GOLGI-STACKING PROTEINS ON NEWLY-FORMED GOLGI APPARATUS

TAMAKI, H. and YAMASHINA, S.

*Department of Anatomy, Kitasato University School of Medicine, Sagamihara, Japan.
(tamaki@kitasato-u.ac.jp)*

Abstract: We found an anti-microtubular agent, nocodazole induced newly formation of Golgi apparatus in rat parotid acinar cell revealed by immunocytochemistry and electron microscopy. Immediately after parotid tissue pieces were incubated in 10 μ g/ml nocodazole at 37 °C, numerous spot-like structures appeared in the area of the rough endoplasmic reticulum (RER). GRASP55, a Golgi-stacking protein, was closely associated on the small spots. Electron microscopy indicated such spots were smooth-surfaced vesicular structures seemed to bud from the RER. At 30 min after the incubation, the vesicular structures were aggregated into small clusters composed of tubules and vesicles and became positive in one another Golgi-stacking protein, GM 130. Immunogold electron microscopy revealed positive reaction for anti-GM130 on such smooth-surfaced membranous clusters. Whereas, no remarkable change could be observed on existent Golgi apparatus. During further incubation, such membranous clusters were increased in size and developed into small Golgi stack in the basal cytoplasm, and the immunoreactivity for functional Golgi proteins, e.g. mannosidase II, β -COP, GBF1 and TGN38, became positive followed by the formation of secretory granules.

Such process of Golgi development was partially inhibited by low temperature. When incubation with the drug was conducted at 25 °C, only GRASP55-positive spots were appeared, but the addition of the other Golgi-resident proteins and the development of the membranous clusters were completely inhibited followed by marked accumulation of GRASP55-positive small vesicular structures throughout the cytoplasm.

These results suggested that the primary form of the Golgi apparatus was GRASP55-associated vesicles growing out from the RER. Addition of GM130 led to formation of cluster by aggregation of the vesicles. Various Golgi-resident proteins were sequentially appeared on the developing Golgi clusters. Finally, Golgi stack with secretory function was established. Intracellular transport at normal temperature is requisite for the newly formation of Golgi apparatus.

P33

TRANSLOCATION OF ALKALINE PHOSPHATASE DURING THE PROCESS OF RESTORATION AFTER COLCHICINE TREATMENT IN CULTURES OF RAT LIVER CELLS

CHIDA, K. and TAGUCHI, M.

Department of Anatomy, School of Allied Health Sciences, Kitasato University, Sagami-hara, Kanagawa, Japan. (chida@ahs.kitasato-u.ac.jp)

Abstract: We examined, in cultures of the synchronous McA-RH 7777 rat hepatoma cell line and fetal rat hepatocytes (FRH), how alkaline phosphatase (ALP) translocates during the process of restoration after colchicine treatment. Each kind of cells was incubated for 1 h in the medium containing colchicine. Cells were fixed for immunofluorescent staining after cultured in the medium without colchicine. Anti- β -tubulin antibody was used for detection of microtubules. For double staining, anti-ALP and anti-mannosidase (MAN: Golgi marker) antibodies were used, and two antigens were simultaneously detected using FITC-labeled and rhodamine-labeled antibodies. For detection of F-actin in FRH, Texas Red-labeled phalloidin was used. After colchicine treatment, microtubular fibers in the cytoplasm disappeared and MAN dispersed throughout the cytoplasm as fine granules. In FRH, ALP showed localization pattern like coarse granules in the cytoplasm but F-actin distributed around bile canaliculus-like structure as well as a control. On the other hand, although ALP in McA-RH 7777 cells also showed granular localization pattern in the cytoplasm, the localization of ALP at the borders between McA-RH 7777 cells did not change. Twenty-four hours after the treatment, microtubular fibers appeared in the cytoplasm but MAN held fine granular distribution pattern. ALP in most of FRH was localized in granular sites that scattered throughout the cytoplasm. Up to 72 h after the treatment, ALP became to be gradually localized around bile canaliculus-like structure. Meanwhile, in McA-RH 7777 cells, ALP returned to the same localization pattern as a control 24 h after the treatment. The present study reports that translocation of ALP after colchicine treatment is different between McA-RH 7777 and FRH.

P34

PROTEASES INDUCED INTRACELLULAR Ca^{2+} DYNAMICS OF SMOOTH MUSCLES OF ARTERIOLES VIA PAR1 AND 2

SATOH, Y., MISAKI, T. and SATINO, T.

Iwate Medical University, Morioka, Japan. (yisatoh@iwate-med.ac.jp)

Abstract: [AIM] Protease-activated receptors (PARs) mediate cellular responses to various proteases in diverse cell types, including smooth muscles and endothelium of blood vessels. PARs may play important roles in microcirculation in the tissue/organs. Here we examine whether stimulation of PARs induce responses of smooth muscles of arterioles. [MATERIALS AND METHODS] Arterioles were taken from brain and testis of rats. We used arteriole specimens which kept essential structural integrity. Intracellular Ca^{2+} ($[Ca^{2+}]_i$) dynamics and nitric oxide (NO) production during PARs stimulations were evaluated by confocal microscopy (Nikon RCM/Ab), because $[Ca^{2+}]_i$ and NO are key factors in the maintenance of strain in blood vessels. Localization of PARs1 and 2 were immunohistochemically examined. [RESULTS] Thrombin and PAR1-agonist peptide (AP) induced oscillatory fluctuations of $[Ca^{2+}]_i$ of brain arteriole smooth muscles. The response was independent of extracellular Ca^{2+} , but depletion of intracellular Ca^{2+} store suppressed the response. Small arterioles (< 50 μ m in diameter) showed conspicuous oscillations, but larger those not. Any changes of endothelium were not verified. Trypsin and PAR2-AP induced faint oscillatory fluctuations and evident decrease of $[Ca^{2+}]_i$ level. It might be possible that activation of PAR2 induce NO production of endothelium, which in turn depressed $[Ca^{2+}]_i$ level of smooth muscle. However, NO production during PAR2 stimulation was not detected, and NO-synthase inhibitor did not suppressed PAR2 -AP induced $[Ca^{2+}]_i$ decrease. NO showed no decrease of $[Ca^{2+}]_i$ level. PAR3- and PAR4-AP had no effect. In contrast to brain arterioles, smooth muscles of testicular arterioles showed neither oscillatory fluctuations during PAR1 activation nor decrease of $[Ca^{2+}]_i$ level during PAR2 stimulation. In accordance with those, localization of PARs 1 and 2 were immunohistochemically verified in smooth muscles of brain arterioles. [CONCLUSION] Proteases in various pathological conditions control microcirculation via PARs of arteriole smooth muscles in a NO-independent manner, although there may be organ-specificity.

P35

GENESIS OF SECRETORY GRANULE WITH CHROMOGRANIN A-GFP TRANSFECTION: A CYTOCHEMICAL APPROACH

INOMOTO, C.¹, UMEMURA, S.¹, EGASHIRA, N.¹, MINEMATSU, T.¹, TAKEKOSHI, S.¹, ITOH, Y.², ITOH, J.², TAUPENOT, L.³, O'CONNOR, D.T.³, and OSAMURA, R.Y.¹

¹Department of Pathology and ² Cell Science, Teaching and Research Support Center, Tokai University School of Medicine, Kanagawa, Japan, and ³Department of Medicine, University of California at San Diego, CA, USA. ([cisophia@is.icc.u-tokai.ac.jp](mailto:sisophia@is.icc.u-tokai.ac.jp))

Abstract: Chromogranin A (CgA), a member of granin family, is one of the major soluble proteins of the secretory vesicles of the neuroendocrine cells, is also known to interact with several other integral membrane proteins of secretory granules. The chromogranins have recently been demonstrated to play granulogenic roles, inducing secretory granule formation even in non-neuroendocrine cells. CgA may be a model protein for the studies of protein targeting into the regulated pathway of secretion. This study is aimed at to elucidate whether GFP tagged CgA gene construct could serve as a marker protein to follow the synthesis of CgA in the non-endocrine cells via granulogenesis. To elucidate the granulogenesis effect of human CgA, we transfected CgA-GFP expression vector into non-neuroendocrine COS-7 cells and investigated the localization of chimeric protein CgA-GFP using confocal laser scanning microscopy. The transfected COS-7 cells induced granule formation which was interpreted as secretory granule in the cells. The expression of chimeric protein with granular structure was detected in the cytoplasm. Immunocytochemically, the chimeric proteins are focally positive chromogranin A. These results further suggested the possibility that CgA induces the genesis of secretory granules.

P36

ATP INDUCED INTRACELLULAR Ca^{2+} DYNAMICS OF MAST CELLS BUT NOT EXOCYTOSIS

NAKAMURA, Y., OOSAKA, M., SATINO, T. and SATOH, Y.
Iwate Medical University, Morioka, Japan. (yisatoh@iwate-med.ac.jp)

Abstract: [Background/Aim] Adenosine triphosphate (ATP) is a fundamental transmitter in various tissues, as well as intracellular energy source. Previous studies indicated that ATP induced histamine discharge from mast cells which possess many secretory granules, and the discharge was simply thought as exocytosis. It is well known that intracellular Ca^{2+} ($[Ca^{2+}]_i$) increase as a key event in exocytosis in various cells including mast cells, but nobody observed whether ATP induces $[Ca^{2+}]_i$ changes of mast cells, and whether ATP-induced histamine discharge is true exocytosis. [MATERIALS AND METHODS] Rat peritoneal mast cells were collected and loaded with Indo-1/AM or Fluo-4/AM for measuring of $[Ca^{2+}]_i$. The exocytosed granule matrices were stained by sulforhodamine B (SFRMB). The fluorescent images of the cells stimulated by ATP and/or compound 48/80 were consecutively acquired by confocal microscopy (Nikon RCM/Ab or Zeiss 510). [Results] ATP and ADP induced $[Ca^{2+}]_i$ increase but not exocytosis. Adenosine and AMP has no effect, indicating that ATP-induced $[Ca^{2+}]_i$ changes were mediated by P2 receptors, but not P1. UTP (P2Y_{2, 4, 6} agonist) did not induced $[Ca^{2+}]_i$ changes, and removing of extracellular Ca^{2+} abolished ATP-induced $[Ca^{2+}]_i$ changes. These suggested that mast cells possess ion channel type receptors responding to extracellular ATP (i.e., P2X). DBzATP (P2X₇ agonist) elicited prominent $[Ca^{2+}]_i$ increase, but α , β -meATP (P2X_{1, 3} agonist) did not any responses. Intracellular non-exocytosed granule matrices were stained by SFRMB by high dose of dBzATP, indicating increasing plasma cell membrane permeability. Interestingly, after the ATP-induced $[Ca^{2+}]_i$ changes, compound 48/80 induced exocytosis were inhibited. [Conclusions] ATP-induced histamine discharge is not physiological exocytosis, but pharmacopathological conditions in vitro. In tissue, ATP from nerve fibers or other damaged cells may inhibit secretory activity of mast cells.

P37

IMMUNOELECTRON MICROSCOPY OF QUICK-FROZEN AND PHYSICALLY FIXED MEMBRANES REVEALED HETEROGENEOUS GM1 DOMAINS IN THE CELL MEMBRANE

FUJITA, AKIKAZU, CHENG, JINGLEI, and FUJIMOTO, TOYOSHI

Department of Anatomy and Molecular Cell Biology, Nagoya University Graduate School of Medicine, Nagoya, Aichi, Japan, 466-8550 (afujita@med.nagoya-u.ac.jp)

Abstract: Distribution of GM1 and GM3, putative raft molecules in the cell membrane, were examined by immunoEM using rapidly-frozen and freeze-fractured cell specimens. The intensity of immunogold labeling was improved when replicas were prepared by evaporating carbon (C) before platinum (Pt)/C. C (20 nm)-Pt/C (2 nm) replicas and C (2 nm)-Pt/C (2 nm)-C (20 nm) replicas gave equivalent results. By immunogold labeling, GM1 in normal mouse fibroblasts showed clusters of less than 100 nm in diameter. GM1-null fibroblasts were not labeled, but became to show similar clustered labeling when GM1 was added to the culture medium. Upon cholesterol depletion or incubation in the cold, clustering decreased and showed marked regional heterogeneity in a cell. Notably, the average nearest neighbor distance in control cells was almost constant irrespective of the labeling density, but after cholesterol depletion or chilling, it declined as the labeling density increased. GM3 also showed cholesterol-dependent clustering. Clusters of GM1 and GM3 coincided occasionally, but were separated in most cases, suggesting the presence of heterogeneous microdomains. The present method could physically immobilize cell membrane molecules in situ, and demonstrated that GM1 and GM3 make cholesterol-dependent clusters in the living cell membrane.

P38

FOCAL CONTACT ADHESION TO POROUS FILMS; THE AFFECT ON CELL SHAPE, ADHESION, MIGRATION, GROWTH AND SURVIVAL OF HUMAN KERATINOCYTES AND FIBROBLASTS IN CULTURE

MCMILLAN, J.R.^{1,2}, QIAO, H.^{1,2}, TANAKA, M.¹, YAMAMOTO, S.¹, SHIMOMURA, M.¹ and SHIMIZU, H.²

¹*Creative Research Initiative "Sousei" (C.R.I.S.) Faculty of Science, Hokkaido University;*

²*Department of Dermatology, Hokkaido University, Graduate School of Medicine, Sapporo, Japan. (jrm57@med.hokudai.ac.jp)*

Abstract: Unsupported autologous keratinocyte grafts provide clinical benefits and wound coverage but are fragile. We are therefore developing grafts using keratinocytes and fibroblasts grown on biocompatible, poly (EPISILON-calprolactone), hexagonally-packed, porous films. Human epidermal keratinocytes and dermal fibroblasts were cultured on porous films with various sized pores (ranging 3-20 microns and including flat films). Cultured human keratinocytes failed to form proper keratin-hemidesmosomal structures but instead adhered using actin-focal contacts (containing vinculin and talin) on all porous membranes. Furthermore, the smallest-pore (3 micron) membranes provided the best surface on which keratinocytes could attach, adhere, divide and survive in culture. Keratinocyte talin and vinculin expression levels correlated with cell adhesion and survival on small pores films but inhibited the rapid spreading and migration of keratinocytes and induced them to form a more spherical shape. Conversely, fibroblast adhesion, migration, growth and survival were less affected by film porosity and showed highest levels on 5 micron porous films. Keratinocytes, the most discerning of the two cell types assembled the majority of focal contacts around the pore edge, immediately adjacent to the pore rim. Taken together both keratinocytes and fibroblasts attach to small pore films due to the greater pores numbers, increases in pore edge and increases in surface area over which cells can adhere. Small pores also inhibit cells from crossing the film but will allow them to maintain underlying matrix communication together and diffusion of soluble nutrients/factors from the wound. These characteristics are important in developing grafts for use in the treatment of human skin wounds.

P39

**DISTURBED CELL-CELL ATTACHMENT BY
OVEREXPRESSION OF PKC η** OHBA, M.¹, AKAHANE, T.¹, KOHNO, Y.², and KUROKI, T.³

¹*Institute of Molecular Oncology, Showa University, Tokyo, Japan;* ²*Dept. of Oral Pathology, Showa University, Tokyo, Japan;* ³*Gifu University, Gifu, Japan. (moba@pharm.showa-u.ac.jp)*

Abstract: Protein kinase C- η (PKC η) is a key regulator in growth and differentiation of epithelia. Overexpression of PKC η results in the morphological changes of keratinocytes along with epithelial-specific growth inhibition and induction of transglutaminase 1 activity. In present study, we report that overexpression of PKC η disturbed the cell attachment and cell polarity. In PKC η -transgenic mice (TG η), epidermal keratinocytes exhibited the narrower intercellular space and lower electron density of the cell membrane. Desmosomes were significantly smaller and immature and tonofilaments were assembled to lower extent than normal cells. Shape and size of the intestinal epithelial cells of TG η were not uniform and the cell-cell boundary was indistinct. The junctional complex including tight junction and adherence junction exhibited loose structures. E-cadherin existed scattered in TG η indicating the aberrant adherence junction. In cultured human keratinocytes, overexpression of PKC η also disturbed cell-cell adhesion. Expression level E-cadherin was not affected by PKC η but its regular recruitment to cell-cell border was inhibited. These data suggest that PKC η regulates the localization of cell adhesion molecules and polarity of epithelial cells.

P40

IMMUNOCYTOCHEMICAL ANALYSIS OF OSTEOPONTIN FUNCTION IN OSTEOCLAST FORMATION

SUZUKI, K.¹, SODEK, J.² and YAMADA, S.¹¹*Department of Pharmacology, School of Dentistry, University of Showa, Tokyo, Japan,*²*CIHR Group in Matrix Dynamics, Faculty of Dentistry, University of Toronto, Toronto, Canada. (suzukik@dent.showa-u.ac.jp)*

Abstract: Osteoclasts (OC) are the multinucleated cells which is responsible for the bone resorption in both physiological bone metabolism and pathological bone destruction, including osteoporosis, rheumatoid arthritis and tumor bone metastasis. Precursors of OC need to migrate and fuse together to form the multinucleated mature cells, which is an important step in OC formation. That osteopontin (OPN) has a prominent role in bone resorption was first indicated by the demonstration that it colocalizes with the ALPHA ν BETA3 integrin and mediates the attachment of OC to the bone. We have previously shown that OPN is required for the fusion of OC precursors and resorptive activity, using bone marrow cells derived from OPN-null mice. To further clarify this, we examined the OC generated from bone marrow mononuclear precursors by laser scanning confocal microscopy in combination with fluorescent labeling. The results are: 1) In prefusion OC and in motile multinucleated OC, staining for OPN colocalized with CD44 and BETA3 integrin, which are the OPN receptors, in cell processes. 2) OPN was also found to colocalize with Cdc42 and Rac1 in filopodia and ruffled membranes, respectively. 3) OC derived from OPN-null and CD44-null showed diminished perimembranous staining for CD44 and OPN, respectively, indicating a mutual interdependency of these proteins for their localization at cell surfaces. 4) OC generated from these mutant mice showed reduced cell spreading, limited protrusion of pseudopodia and impaired cell fusion compared to wild-type controls, consistent with the putative role of the OPN and CD44 in mediating cytoskeletal rearrangements. In conclusion, these studies indicate that OPN colocalizes with CD44 within osteoclast cell processes, and that OPN may be important in regulating CD44-mediated cytoskeletal changes associated with OC migration, fusion and resorption.

P41

MORPHOLOGICAL VARIABILITY OF SYMBIOTIC BACTERIA, BUCHNERA, IN BACTERIOCYTE DEPENDING ON THE MORPH OF THE HOST INSECT

NISHIKORI, K., KUBO, T., and MORIOKA, M.

The University of Tokyo, Tokyo, Japan., (ijnek@biol.s.u-tokyo.ac.jp)

Abstract: The endosymbiosis in the aphid bacteriocyte represents one of the typical mutually obligate relationships between prokaryotic and eukaryotic cells. The symbiotic bacteria, Buchnera sp. APS, are maternally transmitted through generations of host aphid, *Acyrtosiphon pisum* (Harris) during 100-200 million years. This long-lasting of symbiosis may have been established based on the precise mutual control between the symbiont and host insect as well as on the variability of the bacteriocytes, that contain symbionts, depending upon the physiologic state of the host insect. In the present study, we focused on the later event because this interesting insight had been overlooked.

To analyze the relationship between the morph of host insect and morphological variability of Buchnera within bacteriocytes, histology of Buchnera in the alatae and apterae aphid was examined. Paraffin sections from each morph of some ages were prepared and stained with hematoxylin-eosin (HE). As a result of light microscopic observation, bacteriocytes of any specimen were uniformly filled with thousands of Buchnera. Exceptionally, Buchnera of alatae at 0 day after the final ecdysis (day-0), was sparsely distributed in bacteriocyte, suggesting the temporal disintegration of symbiosis. To understand the molecular mechanisms that underlie this temporal disintegration of symbiosis, protein expression patterns in bacteriocyte were compared between day-0 alatae and apterae using 2-dimensional polyacrylamide gel electrophoresis. Two spots were detected selectively in day 0 alatae, suggesting that these proteins might be involved in the temporal disintegration, which also intimates morphological variability of the bacteriocyte depending on the physiologic state of the host insect.

P42

IMMUNOLocalIZATION OF NG2 PROTEOGlyCAN IN MYOFIBROBLASTS AND SMOOTH MUSCLE CELLS OF MOUSE AND HUMAN INTESTINES

TERADA, N., OHNO, N., SAITO, S., FUJII, Y., and OHNO, S.
University of Yamanashi, Yamanashi, Japan. (e-mail: nobuot@yamanashi.ac.jp)

Abstract: Intestinal subepithelial myofibroblasts (ISEMFs) are widely located in the lamina propria under epithelial cells of various animal tissues. While ISEMFs are thought to play an important role in protecting and maintaining the integrity of the epithelial cell layer, and also in the process of wound healing, neither proteoglycans nor other membranous proteins associated with ISEMFs have been directly examined until now. In this study, we have investigated the immunolocalization of the membrane-bound chondroitin sulfate proteoglycan, NG2, in mouse and human intestines.

Using specific antibodies against ectodomain of NG2 proteoglycan, the routine immunohistochemistry with light and electron microscopy was performed for the adult C57BL/6 mouse or informed-consented human small and large intestines. The short-term paraformaldehyde fixation was used to achieve the strongest immunoreactivity against NG2.

The NG2 was immunolocalized in the ISEMF layer of mouse or human small and large intestines, with similar intensity of immunoreactivity from the crypt to top of villi. It was also immunolocalized along cell membranes of smooth muscle cells at the intestinal muscle layer. However, skeletal and cardiac muscle tissues were not immunostained for NG2, indicating its selective expression. By electron microscopy, the NG2 immunoreactivity was strongly detected along the cell membrane of ISEMFs, with slight diffusion of immunoreaction products into the neighboring matrix, showing the presence of some "shed" NG2.

In conclusion, we have found that the NG2 is abundantly immunolocalized in the ISEMFs and intestinal smooth muscle cells. These findings of NG2 proteoglycan expression by ISEMFs provide some insight into features of the transdifferentiation of fibroblasts, myofibroblasts, and smooth muscle cells. To further confirm our idea, we are currently examining if generally called myofibroblasts, which are thought to play an important role in the tissue remodeling, also express such NG2 proteoglycan in various other tissues.

P43

PACAP DECREASES ISCHEMIC NEURONAL CELL DEATH IN THE HIPPOCAMPUS

SHIODA, S.¹, NAKAMACHI, T.¹, OHTAKI, H.¹, DOHI, K.¹¹*Department of Anatomy, School of Medicine, Showa University, Tokyo, Japan (shioda@med.showa-u.ac.jp)*

Abstract: Pituitary adenylate cyclase-activating polypeptide (PACAP), first isolated from ovine hypothalamus, belongs to the secretin/glucagon/vasoactive intestinal peptide (VIP) superfamily and exists in two amidated forms, PACAP38 and PACAP27. It is reported that PACAP decreases neuronal damage and increases interleukin-6 (IL-6) levels following brain ischemia in the rat. However, the mechanisms underlying neuroprotection are still to be fully elucidated. We designed to investigate the role played by PACAP and IL-6 in mediating neuroprotection following ischemia in a null mouse model. Infarct volume, neurological deficits, and cytochrome c in cytoplasm were higher in PACAP^{+/-} and ^{-/-} mice than in the PACAP^{+/+} animals following middle cerebral artery occlusion (MCAO), although the severity of response was ameliorated by the injection of PACAP38. A decrease in mitochondrial bcl-2 was also accentuated in PACAP^{+/-} and ^{-/-} mice, but this could be prevented by PACAP38 injection. PACAP specific receptor (PAC1-R) immunoreactivity (ir) was colocalized with IL-6-ir in neurons, although the intensity of IL-6-ir in PACAP^{+/-} mice was less than that in PACAP^{+/+} animals. IL-6 levels increased in response to PACAP38 injection, an effect which was cancelled by co-treatment of PAC1R antagonist, PACAP6-38. However, PACAP38 treatment did not reduce the infarct volume in IL-6 null mice. To clarify the signaling pathway associated with the activity of PACAP and IL-6, phosphorylated STAT3, ERK and AKT levels were examined in PACAP^{+/-} and IL-6 null mice following MCAO. Lower levels of pSTAT3 and pERK were observed in the PACAP^{+/-} mice, while a reduction in pSTAT3 was recorded in the IL-6 null mice. These results suggest that PACAP prevents neuronal cell death via a signaling mechanism involving IL-6.

P44

COMPARISON OF MR IMAGES AND HISTOCHEMICAL LOCALIZATION OF INTRA-ARTERIALY ADMINISTERED MICROGLIA IN THE RAT MODEL OF ALZHEIMER'S DISEASE

TOOYAMA, I.¹, SONG, YANG^{1,3}, MORIKAWA, SHIGEHIRO², MORITA, MASAHITO² and INUBUSHI, TOSHIRO²

¹Molecular Neuroscience Research Center and ²Biomedical MR Science Research Center at Shiga University of Medical Science, Setatsukinowa-cho, Otsu 520-2192, Japan; ³Department of Neurobiology, College of Basic Medical Science of China Medical University, China

Abstract: The therapeutic use of microglial cells has recently received some attention for the treatment of Alzheimer disease (AD), but few noninvasive techniques exist for monitoring the cells after administration. Here we present a magnetic resonance imaging (MRI) technology to track microglia cells injected intra-arterially in a rat model of AD. We labeled microglia expressing GFP with super-paramagnetic iron particles (Resovist) using the HVJ-E vector. For a rat model of AD, we micro-injected A β 42 and saline into the left and right hippocampus of rats, respectively. Then, we administered labeled microglia into the carotid artery of the rats. After monitoring exogenously administered microglia using MRI, we compared the MR images and the histochemical localization of administered microglia. MRI revealed clear signal changes attributable to Resovist-containing microglia in A β -injected areas. Histochemistry demonstrated that EGFP-positive microglia accumulated around A β deposits and internalized the peptide. This study demonstrates the usefulness of MRI for non-invasive monitoring of exogenous microglia, and suggests a promising future for microglia/macrophages as therapeutic tools for AD.

P45

NEUROPEPTIDE W –CONTAINING NEURON NETWORK IN THE RAT BRAIN

TAKENOYA F.^{1,2}, KAGEYAMA, H.¹, DATE, Y.³, NAKAZATO, M.³, SHIODA, S.¹

¹Department of Anatomy, School of Medicine, Showa University, Tokyo, Japan; ²Department of Physical Education, Hoshi University School of Pharmacy and Pharmaceutical Science, Tokyo, Japan; ³Department of Internal Medicine, Miyazaki Medical College, University of Miyazaki, Miyazaki, Japan (kuki@hoshi.ac.jp)

Abstract: Neuropeptide W (NPW) is novel neuropeptide which was recently isolated from the porcine hypothalamus. It is an endogenous ligand for GPR7 of G protein-coupled receptor (GPCR). There are two forms of the peptide, designated as neuropeptide W-23 (NPW23) and neuropeptide W-30 (NPW30). GPR7 and GPR8, two structurally related orphan GPCRs, share a high sequence homology to the opioid and somatostatin receptor families. GPR7 and GPR8 are expressed in the brain regions which include feeding behavior. Intracerebroventricular (icv) infusion of NPW into the rat cerebral ventricle increases food intake for 2 h in the light phase and stimulates prolactin and corticosterone release. On the other hand, in the dark phase, the icv infusion of NPW reduces food intake for 48 h with up-regulation of energy expenditure and decrease of body weight. NPW-containing neurons are distributed in the rat brain especially abundant in the hypothalamus. However, the interaction between NPW- and other feeding-regulating peptides-containing neurons has not been clearly identified. Thus, we studied neuron network between NPW-containing neurons and other feeding-regulating neurons in the hypothalamus by double immunostaining methods at the light and electron microscopic level. We found that NPW-containing nerve fibers were in apposition to orexin- and MCH-containing neurons in the lateral hypothalamus. Moreover, NPW- and NPY-containing neurons were contacted with each other in the hypothalamic arcuate nucleus and paraventricular nucleus. These findings suggest that NPW has a function of as well as regulation of feeding in the hypothalamus.

P46

GALANIN-LIKE PEPTIDE PROMOTES FEEDING BEHAVIOR THROUGH ACTIVATION OF OREXINERGIC NEURONS IN THE RAT LATERAL HYPOTHALAMUS

KAGEYAMA, HARUAKI¹, GUAN, JIAN-LIAN¹, TOSHINAI, KOJI²,
DATE, YUKARI², TAKENOYA, FUMIKO^{1,3}, NAKAZATO, MASAMITSU²
and SHIODA, SEIJI¹

¹Showa University School of Medicine, Tokyo, Japan; ²Miyazaki Medical College, Miyazaki, Japan; ³Hoshi University School of Pharmacy and Pharmaceutical Science, Tokyo, Japan

Abstract: Galanin-like peptide (GALP) is implicated in the neural control of feeding behavior. GALP-producing neurons exist at the hypothalamic arcuate nucleus. While centrally administered GALP into rat is known to stimulate feeding behavior, the feeding behavior stimulating pathway have not been clarified. The goal of this study was to determine features of the GALP-mediated neuronal feeding pathway in rat. We investigated the neuronal interactions and functional relationship between GALP and two orexigenic peptides, orexin/hypocretin and melanin-concentrating hormone (MCH), located in the lateral hypothalamus (LH). c-Fos immunoreactivity was expressed in orexin/hypocretin-positive neurons but not in melanin concentrating hormone-positive neurons in the LH 90 min after intracerebroventricular (i.c.v.) infusion of GALP. Double immunofluorescence experiments showed that GALP immunoreactive fibers were in direct contact with orexin/hypocretin immunoreactive neurons in the rat LH. At the ultrastructural level, GALP-immunoreactive axon terminals were found to make synapses on orexin/hypocretin immunoreactive perikarya and dendritic processes in the LH. Furthermore, to determine whether GALP physiologically regulates feeding behavior via orexin/hypocretin neurons, the feeding behavior of rats was studied following GALP i.c.v. injection with or without anti-orexin A and B immunoglobulin (IgG) pretreatment. Following the central administration of control IgG, GALP-stimulated food intake was not significantly different at the 2 hours time point. Pretreated with anti-orexin A and B IgGs significantly attenuated GALP-induced hyperphagia to 50% that of the level in the rats administered control IgG. These results strongly suggest that orexin/hypocretin-containing neurons in the LH are targeted by GALP, and that GALP-induced hyperphagia is mediated through orexin/hypocretin neurons in the LH.

P47

HISTOCHEMICAL ANALYSIS OF THE NERVE REGENERATION IN THE GOLDFISH SPINAL CORD

TAKEDA, A.¹ and FUNAKOSHI, K.¹*¹Yokohama City University School of Medicine, Yokohama, Japan
(funako@med.yokohama-cu.ac.jp)*

Abstract: In contrast to mammals, spontaneous nerve regeneration after lesion of the spinal cord may occur in fishes. We examined tissue remodeling and axon regeneration after spinal hemisection in the goldfish by means of immunohistochemistry. Within two weeks after the hemisection of the cord, the open wound was attached with the fibrous tissue, in the center of which a small cavity was formed. The fibrous scar was demarcated from the nervous tissue by the basement membrane immunopositive for laminin. Many neurons containing 5-hydroxytryptamine (serotonin) were lined along the basement membrane. Three weeks after the hemisection, the laminin-positive basement membrane protruded into the fibrous scar, making a tube-like structure. The glial fibers immunopositive for glial fibrillary acid protein (GFAP) entered the tube, and serotonin neurons were lined with the tube. Then, the tube joined with another tube protruding from the opposite side of the scar, making a tunnel penetrating the fibrous scar, and many regenerating axons passed through the tunnel. The fibrous scar was gradually reduced. On the other hand, the number of axons passing through the tunnels was increased by the day 6 weeks after the hemisection. The descending axons from the locomotion center in the midbrain to the spinal motoneurons were also restored. This might produce the recovery of swimming ability of the goldfish.

P48

IMMUNOHISTOCHEMICAL CHARACTERIZATION OF TOLL-LIKE RECEPTOR 2 EXPRESSION IN MOUSE LUMBAR DORSAL ROOT GANGLIA.

RODELLA, L.F., BORSANI, E., RICCI, F., ALBERTINI, R.,
STACCHIOTTI, A. and BIANCHI, R.

*Department of Biomedical Sciences and Biotechnologies, Unit of Human Anatomy, University
of Brescia, Brescia, Italy.(rodella@med.unibs.it)*

Abstract: Toll-like receptors (TLRs) are transmembrane proteins that play a crucial role in mammalian immune recognition detecting the presence of infectious agents and initiating a set of endogenous signals. TLR2 is a member of this family implicated in the recognition of various microbial products, in the induction of antigen presenting cell activation and pro-inflammatory cytokine production. TLR2 is expressed by monocytes and other myeloid cells as well as by vascular endothelial cells, adipocytes, cardiac myocytes and intestinal epithelial cells. Recently, TLR2 has been found in central nervous system (both in neurons and glia) and in Schwann cells of the peripheral nervous system suggesting that it may sustain the inflammatory response in these areas. Inflammation and cytokines are involved in pain modulation and neuropathic pain pathogenesis. Moreover it has been shown an involvement of TLRs in pain transmission. Since the ganglia represent the first gate in pain signalling and the role and the distribution of TLR2 in ganglia has not been clarified, the aim of this work was to evaluate immunohistochemically its distribution in dorsal root ganglia (DRG) of mouse. The experiments were carried out on 6 C57BL/6 mice. The animals were perfused with 4% paraformaldehyde and the lumbar DRGs (L4-L6) were removed. Frozen serial transverse sections of DRGs were collected and treated for TLR2-immunohistochemistry. We found, in all lumbar DRGs, an intense cytoplasmatic staining in several small- and large-sized neurons. The immunostaining was ranging from light to heavy and it is not linked to the neuron size. The immunoreactivity was not restricted to neurons but also found in the satellite cells. In addition, some TLR2 immunoreactive fibers of various diameters were found. In this work we showed, for the first time, the TLR2 localization in sensitive DRGs. Its peculiar localization could suggest an involvement of TLR2 in pain processing at DRG level.

P49

LOCALIZATION OF FIBROBLAST GROWTH FACTOR-1 (FGF1) IN CHOLINERGIC NEURONS INNERVATING THE RAT LARYNX

OKANO, H.^{1,2}, TOYODA, K.^{1,2}, BAMBA, H.², HISA, Y.², OOMURA, Y.³, IMAMURA, T.⁴, FURUKAWA, S.⁵, KIMURA, H.¹ and TOOYAMA, I.¹

¹Shiga University of Medical Science, Shiga, Japan; ²Kyoto Prefectural University of Medicine, Kyoto, Japan; ³Kyusyu University, Fukuoka, Japan; ⁴National Institute of Advanced Industrial Science and Technology (AIST), Ibaraki, Japan; ⁵Gifu Pharmaceutical University, Gifu, Japan.

Abstract: We have recently discovered a splice variant of choline acetyltransferase (ChAT) mRNA, and designated the variant protein pChAT because of its preferential expression in peripheral neuronal structures. Using antibodies against the conventional ChAT (cChAT) or pChAT, we have demonstrated cholinergic neurons in the laryngeal nervous system. In this study, we investigated the localization of fibroblast growth factor-1 (FGF1), a neurotrophic molecule, in cholinergic neurons innervating the rat larynx by immunohistochemistry and tracer experiments. In the medulla oblongata, FGF1-positive neurons were observed in the dorsal motor nucleus of vagus (DMNV) and the ambiguus nucleus, but not in the nucleus of the solitary tract. In the DMNV, only 9.4% of cChAT-positive neurons contained FGF1, and 70.6% of FGF1-positive neurons co-localized with cChAT. In the ambiguus nucleus, 100% of cChAT-positive neurons were FGF1-positive. In the intralaryngeal ganglia, all ganglionic neurons contained both pChAT and FGF1. In the nodose ganglia, 66.4% of pChAT-positive neurons were also positive for FGF1, and 89.8% of FGF1-positive ganglionic cells displayed pChAT-immunoreactivity. A tracing study using cholera toxin B subunit (CTb) demonstrated that cholinergic neurons sending their axons from the DMNV and ambiguus nucleus to the superior laryngeal nerve were FGF1-negative and FGF1-positive, respectively. The tracing study also demonstrated that some FGF1-positive cells were labeled with CTb. The results indicate that FGF1 is localized to the motor, postganglionic parasympathetic and sensory neurons but very little expression is seen in the preganglionic parasympathetic cholinergic neurons innervating the rat larynx.

P50

EXPRESSION OF GREEN FLUORESCENT PROTEIN POSITIVE CELLS IN THE OLFACTORY EPITHELIUM AND VOMERONASAL ORGAN OF THE GAD67-GFP KNOCK-IN MOUSE

WATANABE, M.¹, KANAYAMA, T.¹, NAKAMURA, Y.², YANAGAWA, Y.³, OBATA, K.⁴, OKI, K.¹, YABUMOTO, M.⁵, and WATANABE, H.⁶

¹Osaka Medical College, Japan, ²Nara Women's University, Japan, ³Gunma University, Japan, ⁴National Institute for Physiological Sciences, Japan, ⁵Medical Co. Kinshukai, Japan, ⁶Medical Co. Watanabe Hospital, Japan. (an2002@art.osaka-med.ac.jp)

Abstract: Glutamate decarboxylase-green fluorescence protein (GAD67-GFP) knock-in mouse has been successfully introduced to the research of GABAergic neurons and GABAergic cells outside the central nervous system. We investigated GFP-positive cells in the nasal cavity of the GAD67-GFP knock-in mouse, and found that a part of the nasal epithelium corresponding olfactory epithelium contains highly GFP-positive cells. In addition to the olfactory epithelium, highly GFP-positive cells were found in the vomeronasal organ and its adjacent vomeronasal glands. The morphology and histochemical characteristics was examined with fluorescent microscope and confocal laser microscope. Expression of mRNAs of GADs and GABA receptor subunits were analyzed by RT-PCR. All GFP-positive cells exhibited GAD67 immunoreactivity, and the cells in the olfactory epithelium were identified as supporting cells. RT-PCR analysis showed expression of two isoforms of GAD mRNAs (GAD65 and GAD67) in the olfactory epithelium and vomeronasal organ including the glands. Expression of GABA_A receptor RHO1 and RHO2 subunit mRNAs were found in the olfactory epithelium. In the vomeronasal organ including the glands, GABA_B receptor R1b and R2 subunit mRNAs were expressed. These results suggest that GABAergic system might have certain important functional roles in these tissues and organs.

P51

ENDODERMAL ORIGIN OF MOUSE THYROID C CELLS – ANALYSIS OF CX43-LACZ AND MASH1 MICE

KAMEDA, Y.

Department of Anatomy, Kitasato University School of Medicine, Sagamihara, Japan. (kameda@med.kitasato-u.ac.jp)

Abstract: Studies using chick-quail chimeras have reported that the ultimobranchial body of avian species is colonized by neural crest cells. By contrast, in the connexin(Cx)43-lacZ transgenic mice in which neural crest cells are specifically labeled by the β -galactosidase monoclonal antibody, the labeled cells did not populate the ultimobranchial body. Furthermore, the organ revealed no cells immunoreactive for TuJ1, NF 160, nestin, P75^{NTR} and Sox10, markers for neural crest cells. The bHLH transcription factor Mash1 plays a key role in the differentiation of autonomic neurons. The ultimobranchial rudiment develops from the fourth pharyngeal pouch at E 11.5 in mice. Mash1 was expressed in the ultimobranchial body at E 12.5, when the organ was located close to the arch arteries. At E 13.5, it joined with the thyroid lobe and still exhibited intense signal for Mash1. At E 14.5, when the ultimobranchial body began to disperse within the thyroid parenchyma as C cells, Mash1 expression was markedly decreased and immunoreactivities for CGRP, somatostatin and TuJ1 appeared in the C cells. Subsequently, calcitonin immunoreactivity appeared at the late stages of fetal development. Targeted disruption of *Mash1* resulted in the absence of C cells. While the formation and migration of ultimobranchial body were not affected in the *Mash1* null mutants, the organ showed increased numbers of apoptotic cells at E 13.5, resulting in degradation. These results indicate that Mash1 promotes C-cell differentiation and gives the neuronal traits to the endodermal ultimobranchial cells.

P52

DISTRIBUTION PATTERN OF NT-3 AND BDNF DURING THE ONTOGENY OF THE RETINA IN THE LIZARD

YANES C.¹, SANTOS, E.¹, ROMERO-ALEMAN, M.M.², CASAÑAS, N.¹, VIÑOLY, R.¹, de PABLOS, E.¹ and MÓNZON-MAYOR, M.²
¹D. Cell Biology, F. Biology, ULL. ²D. Morphology, FCMS, ULPGC. ^{1,2} Canary Islands, Spain. (cyanes@ull.es)

Abstract: Neurotrophins are molecules that regulate several functions in the developing and regenerating visual system, such as neuron survival, axon outgrowth and neuronal plasticity (Levi-Montalcini, 1987; von Bartheld et al., 1996a). In recent studies show a local expression in the retina, and a function in an autocrine/paracrine manner (Vecino et al., 1998b). Although the pattern of distribution of neurotrophins in the retina has been established in four vertebrate classes –from mammals to fishes–, little is known about the reptilia. However, the species *Gallotia galloti*, is of special interest because of its ganglion cell (RGCs) axons capability of regrowth after axotomy (Lang et al., 1998, 2002). In the present study, our aim was to know, the spatio-temporal localization of NT-3 (Neurotrophin-3) and BDNF (Brain derived neurotrophic factor), in the lacertidian retina throughout ontogeny. We used immunoperoxidase method for BDNF and NT3 (Santa Cruz) in cryostat sections and Western Blot analysis. We found that the expression started early in development for NT-3 (embryonic stage E34) in the inner retina, becoming stronger and widespread around hatching. NT3 expression could be detected in RGCs nuclei and cytoplasm and in scattered cells of the innermost inner nuclear layer. The plexiform layers showed some staining as well. Differently, BDNF seemed to be restricted to RGCs axons and sublaminae of the inner plexiform layer, and was clearly detected from E37 onwards. We also noted that these neurotrophins are still synthesised in adult animals, suggesting a role for them not also during visual system development but also in the maintenance of the retinal environment during the whole life of the animal. Moreover, according to similar studies in fish (Caminos et al., 1999), the presence of BDNF in adult lizards could be related to the regenerating ability of ganglion cells axons after optic nerve transection.

P53

AQUAPORIN WATER CHANNELS IN THE OLFACTORY MUCOSA

TAKATA, K., ABLIMIT, A., MATSUZAKI, T., TAJIKA, Y., AOKI, T., HAGIWARA, H., SUZUKI, T.

Gunma University Graduate Schl of Medicine, Maebashi, Japan. (takata@med.gunma-u.ac.jp)

Abstract: Aquaporins (AQPs) are membrane water channel proteins expressed in various tissues and organs, and serve in the transfer of water and small solutes across the membrane. At least 13 isoforms, AQP0 – AQP12, have been identified in mammalian cells to date. We raised antibodies to AQPs using isoform-specific synthetic peptides and surveyed their expression in the rat nasal olfactory and respiratory mucosae. AQP1, AQP3, AQP4, and AQP5 were detected by immunohistochemical and immunoblotting analyses. In the epithelium, both AQP3 and AQP4 were present in the basal and supporting cells. AQP3 was abundant in the olfactory epithelium and localized in the basal and supporting cells, whereas it was restricted to the basal cells in the respiratory epithelium. AQP4, on the other hand, was abundant in the respiratory epithelium, but its abundance was limited to the basal cells in the olfactory epithelium. No AQP was detected in the olfactory sensory cells. Differential localization of AQP3 and AQP4 in the supporting cells and basal cells may play an important role to generate and maintain the specific microenvironment around the olfactory sensory cells. In the underlying connective tissues, AQP1 was present in the endothelial cells of blood vessels and the surrounding connective tissue cells in the olfactory and respiratory mucosae. AQP1 may be involved in the water transfer across the blood vessel wall. In the Bowman's gland, AQP5 was localized in the apical membrane in the secretory acinar cells, whereas AQP3 and AQP4 were found in the basolateral membrane. Similar localization was seen in its duct cells. AQP3, AQP4, and AQP5 in the Bowman's gland may serve in the secretion to generate the microenvironment at the apical surface of the olfactory dendrites for odorant reception.

P54

IMMUNOHISTOCHEMICAL ANALYSIS OF HISTAMINE H₃ RECEPTOR (H₃-R) IN THE STOMACH OF THE RAT

ABE, M.¹, AJIOKA, H.¹, KITANO, S.¹, NANRI, M.¹, KIRIMOTO, T.¹, HORIE, S.² and OKA, T.¹

¹TAIHO Pharmaceutical Co., Ltd., Pharmacological Research Group, Optimal Medication Research Laboratory, Tokushima, Japan. ²Josai International University, Faculty of Pharmaceutical Sciences, Department of Medical Pharmacy Chiba, Japan. masaaki-abe@taiho.co.jp

Abstract: H₃-R has been reported to be present in enterochromaffin-like (ECL) cells in the stomach, but precise distribution and function have been little elucidated. We tried to elucidate the distribution of H₃-R in the stomach by using immunohistochemical technique.

Rat stomach were stained with hematoxylin-eosin and immunostained with anti-histamine antibody for ECL cells, anti-H⁺, K⁺-ATPase antibody for parietal cells, anti-histidine decarboxylase(HDC) antibody for ECL cells and anti-H₃-R antibody.

ECL cells in the fundic glands stained well by histamine and HDC stainings. Distribution of H₃-R immunoreactive cells were not resemble closely that of HDC immunoreactive cells, but that of H⁺, K⁺-ATPase immunoreactive cells. After pretreatment of human H₃-R recombinant produced by E.coli to anti-H₃-R antibody, immunoreactivity of anti-H₃-R antibody to H₃-R receptor was lost. In addition to Shishido's report, that is, existence of H₃-R in ECL cells, it was appeared that H₃-R exists in parietal cells from our studies. It was appeared that H₃-R in parietal cells plays some important role in acid secretion.

P55

PROTEIN 4.1G EXPRESSION IN SCHWANN CELLS OF RODENT PERIPHERAL NERVOUS SYSTEM

OHNO, N., TERADA, N. and OHNO, S.

University of Yamanashi, Yamanashi, Japan. (daibo@pop12.odn.ne.jp)

Abstract: Myelination in the peripheral nervous system depends upon highly elaborate organization of intermembranous contacts between the Schwann cells and axons (heterotypic junctions) and within the Schwann cells (autotypic junctions). Although many membrane-associated molecules have been reported to be involved in the junctions, little is known about the submembranous cytoskeletal molecules which help form and stabilize the Schwann cell autotypic junctions at Schmidt-Lanterman (SL) incisures, paranodal loops and either inner or outer mesaxons. We have investigated the expression and distributions of 4.1G, a membrane-associated cytoskeletal protein, in rodent sciatic nerve fibers. Northern or Western blot analyses were performed, using the sciatic nerve fibers of adult mice and rats, and a specific probe or antibody against 4.1G. The immunohistochemical staining for light or electron microscopy was performed in adult mouse and rat sciatic nerve fibers with the 4.1G specific antibody, including double immunolabeling of 4.1G with E-cadherin, beta-IV spectrin and connexin 32. Immunolocalization of 4.1G was also examined in developing mouse sciatic nerve fibers. Abundant 4.1G mRNA and protein contents could be detected in the rat sciatic nerve extracts by Northern or Western blot analyses. At light microscopic levels, the 4.1G immunolocalization could be observed in paranodal loops, SL incisures and periaxonal, mesaxonal and abaxonal membranes of rodent sciatic nerve fibers. Another immunoelectron microscopy confirmed the immunolocalization of 4.1G in Schwann cells. In the developing mouse sciatic nerves, it was more diffusely immunolocalized in the cytoplasm of immature Schwann cells and gradually getting concentrated at paranodes, SL incisures and periaxonal or mesaxonal membranes during their maturation. These findings support our idea that the 4.1G plays an important role in the cell membrane expansion and specialization occurring during formation and maintenance of myelin internodes in the rodent peripheral nervous system.

P56

EFFECTS OF STEROID HORMONES ON DENDRITIC MORPHOGENESIS OF CULTURED HIPPOCAMPAL NEURONS

ITOSE, M., NISHI, M. and KAWATA, M.

Department of Anatomy and Neurobiology, Kyoto Prefectural University of Medicine, Kyoto, Japan. (mitose@koto.kpu-m.ac.jp)

Abstract: Many studies have shown that stress and gonadal steroids are involved in learning and memory with modification of excitatory synapses in the hippocampus. Although previous *in vivo* studies have demonstrated that several steroids increase the number of dendritic spines in neurons, it is still unclear whether each steroid has a direct effect on the modulation of the spatio-temporal patterns of dendritic morphogenesis. In the present study, we investigated the steroid-induced morphological changes of dendritic spines and filopodia using cultured hippocampal neurons derived from embryonic mice. The dendritic spines and filopodia were visualized by the transfection with Venus-actin. Time-lapse images were taken by a laser scanning confocal microscope during steroid treatment. Corticosterone swelled the spine head within an hour and this alteration was reversible in response to corticosterone treatment. Testosterone but not estradiol increased the number of dendritic spines/filopodia within four hours. These results suggest that each steroid induces rapid and distinct effects on dendritic morphogenesis of cultured hippocampal neurons.

P57

DYNAMIC BEHAVIOR OF INTRANUCLEAR AGGREGATES OF MUTANT AND WILD-TYPE ATAXIN1

KRAWCZYK, P.M., KROL, H., REITS, E., ATEN, J. A.

*Dept. of Cell Biology and Histology, University of Amsterdam, Amsterdam, The Netherlands.
(P.Krawczyk@amc.uva.nl)*

Abstract: Accumulation of mutant proteins containing expanded polyglutamine stretches is a hallmark of neurodegenerative diseases, such as Huntington's, Parkinson's, Alzheimer's diseases and ataxia. During the ongoing debate about the importance of aggregate formation in neurodegenerative diseases it has been suggested that aggregates could sequester essential proteins leading to impairment of cellular functionality. We have analyzed the dynamics of Ataxin1, aggregate-forming protein associated with spinocerebellar ataxia type 1. Mobility of small nuclear Ataxin1 aggregates depends on the length of the polyglutamine expansion. Furthermore, we demonstrated that the initially small aggregates grow with time and can fuse. The fusion kinetics may depend on the size of aggregates and, interestingly, on the length of the polyglutamine expansion. Additionally we examined effects of hyperthermia and transcription inhibition on the dynamics of the aggregates and their mobility. We have found that hyperthermia dramatically changes the dynamics of wild-type, but not of mutant ataxin1, both for the free nuclear fraction and the fraction in aggregates. These data suggest a link between the dynamics of intranuclear ataxin1 aggregates and the length of the polyglutamine expansion and demonstrate polyglutamine expansion length-dependent effect of hyperthermia on the dynamics of the Ataxin1 protein and Ataxin1 aggregates in the cell nucleus.

P58

HISTONE ACETYLATION/DEACETYLATION ALTERS THE BALANCE BETWEEN HERPES SIMPLEX VIRUS LATENCY AND REACTIVATION

SAWTELL, N.M.¹, HAAS, R.L.¹, and THOMPSON, R.L.²

¹*Division of Infectious Diseases, Cincinnati Children's Hospital Research Foundation; Department of Molecular Genetics, Biochemistry, and Microbiology, University of Cincinnati College of Medicine, Cincinnati, Ohio, USA.,* ²*University of Cincinnati College of Medicine, Cincinnati, Ohio (nancy.sawtell@cchmc.org)*

Abstract: The reactivation of HSV is highly regulated, with less than 0.1% of the latently infected neurons exiting the latent state as measured by the expression of lytic viral protein. The ability to detect and analyze individual neurons undergoing herpes simplex virus reactivation *in vivo* is essential for understanding the molecular mechanisms regulating latency and reactivation. We have developed a strategy to detect and quantify neurons exiting latency *in vivo*. Using this approach, we have tested the hypothesis that histone deacetylation of chromatin associated with the latent viral genome contributes to viral genome silencing. We examined the effect of the deacetylase inhibitor, trichostatin A (TSA) on the reactivation of HSV from latency. TSA treatment resulted in a 10-fold increase in the infectious virus production in the ganglia 22 hrs after the reactivation stimulus. Ganglia were examined to determine whether TSA increased the amount of virus produced from the rare reactivating neurons or increased the number of neurons exiting latency. The later was observed, in that there were 10 fold more neurons expressing lytic viral protein with TSA treatment. This increase was not a result of spread, since blocking viral replication did not block the effect of TSA. Examination of the acetylation state of histones associated with the latent viral genome demonstrated increased acetylation of histones associated with key viral promoters within 30 min post reactivation stimulus. Using promoter reporter viruses, we show that TSA increases the number of latently infected neurons in which key viral promoters are upregulated from the latent viral genome by 10 fold and that this upregulation is independent of replication of the viral genome. These findings indicate that histone acetylation/deacetylation plays a regulatory role in the balance between latency and reactivation.

P61

EXPRESSION OF ALCOHOL DEHYDROGENASE-1 AND RETINALDEHYDE DEHYDROGENASE-1 IN THE RAT ANTERIOR PITUITARY

FUJIWARA, K. and YASHIRO, T.

*Department of Anatomy, Jichi Medical University, School of Medicine, Tochigi, Japan.
(ken_fuji@jichi.ac.jp)*

Abstract: Retinoic acids (RA) play an important role on cell growth and tissue development. RA is also known as a regulating factor of pituitary function. It was reported that RA induced growth hormone (GH) gene expression and GH cell differentiation, and it suppressed thyroid stimulating hormone beta-subunit mRNA expression. RA is synthesized from retinol through two oxidation processes. Dehydrogenases catalyzing the oxidation of retinol and retinal are members of the alcohol dehydrogenase (ADH) family, whereas dehydrogenases catalyzing the oxidation of retinal to RA are those of the retinaldehyde dehydrogenase (RALDH) family. The tissue RA is thought to be synthesized from retinol taken from blood. However, ADHs or RALDHs expression in the anterior pituitary gland is not clear. In this study, we tried to identify expression of these enzymes in the rat pituitary gland. We analyzed mRNA expression of ADHs and RALDHs in the adult rat anterior pituitary gland by RT-PCR and quantitative real-time PCR. The expression of ADH-1 in ADH family and RALDH-1 in RALDH family was detected in the gland. By in situ hybridization method with use the digoxigenin-labeled cRNA probe, we tried to detect ADH-1 and RALDH-1 mRNA expressing cells in the gland. ADH-1 mRNA was expressed in the small number of anterior pituitary cells, while RALDH-1 mRNA was expressed in the large number of those. By the double staining of in situ hybridization for enzymes and immunohistochemistry for pituitary hormones (ACTH, GH, LH beta, Prl, TSH beta), ADH-1 mRNA was expressed in some ACTH cells. On the other hand, RALDH-1 mRNA was mainly expressed in the non-hormone producing cells. The results suggested that RA was synthesized in the anterior pituitary gland.

P62

STUDIES WITH LEPTIN SIRNA PROBES SHOW THAT GONADOTROPES MAY DEPEND ON PITUITARY LEPTIN FOR BASAL AND GONADOTROPIN RELEASING HORMONE (GNRH) STIMULATION OF LUTEINIZING HORMONE (LH) EXPRESSION

IRUTHAYANATHAN, M.J.J., CRANE, C., AKHTER, N., JOHNSON, B. and CHILDS, G.V.

Department of Neurobiology and Developmental Sciences, College of Medicine, University of Arkansas for Medical Sciences, Little Rock, AR. childsgwenv@uams.edu

Abstract: Studies of anterior pituitary (AP) leptin have shown changes in mRNA and proteins during the estrous cycle, with peaks before the LH surge (McDuffie et al, 2004). GnRH, a potent secretagogue for LH, also stimulates AP leptin (Akhter et al 2006) and leptin stimulates LH (Yu et al, 1997). To learn if the expression of LH depends on AP leptin, AP cells from male rats were treated with leptin siRNA probes for 8-15 h with the siPORT NeoFX transfection kit (Ambion, Inc). QRT-PCR assayed a 38% or 59% reduction in leptin mRNA with two of the probes, 19783 ("83") and 19784 ("84"), respectively, and no change with the scrambled siRNA sequence. Parallel cultures treated with these probes were counted after in situ hybridization or immunolabeling. Probes 83 and 84 reduced basal expression of leptin proteins from 35±2% of AP cells to 19±1% or 12±1% respectively (p<.003), and blocked stimulatory effects of GnRH (from 48±2% to 1±0.06 or 10 ±0.6%, respectively, p<.001). Probe 83 had no effect on basal expression of LHβ mRNA (14±1% of AP cells). It blocked GnRH-stimulated increases in LH mRNA (from 24± 1% to 14±1%, p=.009). Probe 84 reduced both basal and GnRH-stimulated LH mRNA cells (to 8, or 9±1%, respectively, p<.001). Probes 83 and 84 reduced the % of immunolabeled LH cells from 13±2% to 8±0.5%, or 4±1% of AP cells, respectively (p<.003), and the % of GnRH-stimulated LH cells from 19±0.6% to 4-5±0.3% (p<.001). These studies demonstrate the feasibility of using the Ambion siRNA probes and transfection kit with primary cultures of AP cells. The reduction in LH in cultures in which leptin mRNA is silenced by 38-59%, suggests that basal and GnRH-stimulated expression of LH may depend on AP leptin. Supported by NSF 0240907 and NIH R03 HD 044875 and COBRE award NCRR RR020146.

P63

E- AND N- CADHERIN DIVERGENCE DURING HISTOGENESIS OF THE RAT ANTERIOR PITUITARY GLAND

KIKUCHI, M., YATABE, M. and YASHIRO, T.

*Department of Anatomy, Jichi Medical University School of Medicine, Tochigi, Japan.
(kikuchim@jichi.ac.jp)*

Abstract: Recently, we showed that hormone-producing cells express N-cadherin (N-cad), while folliculo-stellate cells and marginal layer cells E-cadherin (E-cad) in adult rat anterior pituitary gland. These cells are believed to originate from a single cell population of the pituitary placode. In the present study, we examined divergence of cadherin types during pituitary histogenesis by means of double immunostaining of N- and E- cadherins.

Pituitary glands were excised from Sprague-Dawley rats of embryonic day 11 (E11) through postnatal day 60 (P60). They were fixed in Bouin's fluid or half concentration of sublimated formalin. Paraffin sections of 2 μ m thickness were prepared with normal histological process. E-cad and N-cad were immunostained sequentially using mouse monoclonal and rabbit polyclonal primary antibodies and secondary antibodies conjugated with Alexa Fluoro 488 and Texas Red, respectively.

At E11, E-cad was expressed over oral epithelium, while N-cad limitedly to primordium of Rathke's pouch. When Rathke's pouch was formed at E13, E-cad was broadly expressed in entire cell population and E- and N- cads were co-expressed in layer of cells which faced to the lumen. From E14 through E16, majority of cells co-expressed both cadherins, except for that cell population to be pars tuberalis expressed N-cad but E-cad. From E18 through E20 when many hormone-producing cells appear, number of cells which expressed N-cad alone increased, while some cell populations in anterior lobe and multilayered marginal cells still co-expressed both cadherins. After birth, most of anterior pituitary cells came to express one of cadherin types in clusters.

We may conclude that E-cadherin is consistently expressed in folliculo-stellate cells, while cadherin type shifts from E- to N- in hormone-producing cells during cytogenesis of anterior pituitary cells. These changes in cadherin expression will be discussed in reference to cell proliferation and differentiation.

P64

EMBRYONIC DEVELOPMENT OF COLLAGEN ARCHITECTURE IN CHICKEN ADENOHYPOPHYSIS

NISHIMURA, S., NAGATA, M., TABATA, S., and IWAMOTO, H.
Kyushu University, Fukuoka, Japan. (E-mail: shotaro@agr.kyushu-u.ac.jp)

Abstract: Three-dimensional collagen architecture in the adenohypophysis differs among animal species. Chicken adenohypophysis has very fine collagen meshworks composed of distinct cell cluster walls. In this study, the embryonic development of collagen architecture in chicken adenohypophysis was investigated using immunohistochemical and scanning electron microscopic techniques. The heads of chicken embryos from 8, 12, 16 and 20 days of incubation were frozen with liquid nitrogen and cut into 10 μm thick sagittal sections. HE staining was performed for general observation and collagen type I was detected by serial section immunohistochemically. Cell maceration using 8% of NaOH solution was performed for scanning electron microscopic observation of the three-dimensional arrangements of the collagen fibers. Type I collagen immunoreaction was detected in tissue as early as e8 and was also observed in the stages that followed. However, no parenchymal cells were immunostained with antiserum. In e8, immunopositive collagen septa were observed as elongations from the circumference into the gland with a short branch. Collagen septa were relatively simple in appearance at this stage. In later stages, the septa gradually branched to make smaller compartments for the cell clusters. By SEM observation, a relatively coarse plexus of collagen fibrils was observed in e8 adenohypophysis. The wall of collagen septa was not completed and membrane-like constructions and cord-like structures were intermingled. The density and area of collagen meshwork gradually increased with development. At e20, the collagen architecture in the adenohypophysis was similar to that seen in adult chicken. These results suggest that collagen network formation in chicken adenohypophysis starts at an early stage of embryonic development, increases the membranous septa and finally attains an architecture similar to that of the adult by hatching.

P65

EXPRESSION OF LEPTIN AND LEPTIN RECEPTOR IN BOVINE ADENOHYPOPHYSEAL CELLS

OGASAWARA H., OHWADA, S., NAGAI, Y., TAKETA, Y., WATANABE, K., ASO, H., and YAMAGUCHI, T.

Laboratory of Functional Morphology, Department of Animal Science, Graduate School of Agricultural Science, Tohoku University, 1-1 Tsutsumidori-Amamiyamachi, Aoba-ku, 981-8555 Sendai, Japan. (e-mail address:gto-365@bios.tohoku.ac.jp)

Abstract: Leptin (Lep) is a circulating hormone secreted by adipose tissue and a few other tissues, and regulates a variety of functions. Recent studies have shown that the functions of adenohipophyseal cells are mediated by Lep. Lep and Leptin receptor (LepR) expression have been reported in human and rodent adenohipophysial cells. These suggest that Lep may serve as autocrine/paracrine mediator on the signalling pathway in intercellular endocrine interaction in adenohipophysis. The present study was carried out to detail the cellular localization of Lep and LepR in the bovine adenohipophysis and to examine the intercellular mediator of Lep in adenohipophysis.

Six adenohipophysises were obtained from Holstein of 4 months-old. Immunohistochemical stainings of Lep, LepR and adenohipophyseal hormones were performed by immunofluorescence method using their specific antibodies. For RT-PCR analysis, specific primers of Lep and LepR (OB-Ra and OB-Rb) were used. Lep immunoreactivity (Lep-ir) was found in about 30% of cells in the pars distalis. Immunostainings by Lep and specific hormones using serial sections revealed that Lep was present in 60.4% of somatotrophs, 15.9% of gonatotrophs, 6.5% of mammatrohps, 6.5% of thyrotrophs and 2.4% of corticotrophs. In cotrast, LepR-ir was found in only 2.8% of the adenohipophysial cells and over 50% of LepR-ir cells were gonatotrophs that were distributed in the zona tuberalis. Both Lep-R mRNA of OB-Ra and OB-Rb were expressed in the bovine adenohipophysis.

The findings showed the first that Lep and LepR were expressed in bovine adenohipophyseal cells. The cellular expression of Lep and LepR by bovine adenohipophyseal cells suggest that there is autocrine/paracrine pathway by Lep which may regulate the function of gonatotrophs.

P66

DISTRIBUTION OF NEURAL CELL ADHESION MOLECULE, NCAM, IS ADDITIVE TO N-CADHERIN AND OPPOSITE TO E-CADHERIN IN THE RAT ANTERIOR PITUITARY CELLS

TAKAHASHI, K., KIKUCHI, M. and YASHIRO, T.

Department of Anatomy, Jichi Medical University School of Medicine, Tochigi, Japan.
(k.takahashi@jichi.ac.jp)

Abstract: In the anterior pituitary gland, Yatabe *et al.* showed recently that hormone-producing cells express N-cadherin and folliculo-stellate cells express E-cadherin. Such differential expression of cadherin type may be responsible for that folliculo-stellate cells segregate positionally from hormone-producing cells to form pseudo-follicle in anterior pituitary. In the present study, we examined expression of NCAM by contrast with those of cadherins, through *in vivo* and *in vitro* double immunohistochemistry.

Anterior pituitary glands were excised from 8- to 10-weeks-old male Sprague-Dawley rats. Antibodies against 5 types of hormone, S-100 protein, N- and E-cadherin and NCAM were used. Monoclonal anti-NCAM antibody, which recognizes the protein regardless of polysialic acid oxidation, was employed. Specimens were stained with a routine immunohistochemical procedure and observed by a fluorescence microscope or a confocal laser-scanning microscope.

In vivo, hormone-producing cells generally showed positive signal continuously along the cell membrane, while signal intensity varied remarkably cell to cell. In contrast, folliculo-stellate cells showed no significant expression of NCAM. This localization was confirmed to be synonymous with that of N-cadherin by double immunostaining of cadherins and NCAM. Among hormone-producing cells, ACTH cells showed extremely high intensity of signal, GH cells next to ACTH and other type cells showed weak or negligible signal. These tendencies were comparable in primary cultured cells. Furthermore, *in vitro*, it is confirmed that cells expressing the same adhesion molecules tended to preferentially aggregate and those expressing different ones tended to segregate.

We may conclude that NCAM shows tendency to coexist with N-cadherin but E-cadherin, although no relation was shown between expression levels between NCAM and N-cadherin in each cell. These results suggested cadherin and NCAM play roles additively to construct specific distribution of hormone-producing cells and folliculo-stellate cells in anterior pituitary.

P67

DIFFERENTIAL EXPRESSION OF MYOSTATIN AND ACTIVIN RECEPTOR TYPE IIB IN THE BOVINE ANTERIOR PITUITARY GLAND

TAKETA, Y., ASO, H., NAGAI, Y., OGASAWARA, H., HAYASHI, S., MIYAKE, M., WATANABE, K., OHWADA, S. and YAMAGUCHI, T.

Laboratory of Functional Morphology, Department of Animal Science, Graduate School of Agricultural Science, Tohoku University, 1-1 Tsutsumidori-Amamiyamachi, Aoba-ku, Sendai, Japan, 981-8555 (e-mail: ty1010@bios.tohoku.ac.jp)

Abstract: Myostatin(MSTN), also known as growth and differentiation factor 8(GDF-8), is a member of the transforming growth factor β (TGF- β) superfamily that negatively regulates skeletal muscle mass. Activins that belong to the same member with MSTN stimulate FSH production in gonadotrophs but suppress GH and ACTH production in somatotrophs and corticotrophs, respectively. MSTN binds with high affinity to the receptor serine threonine kinase activin receptor type IIB(ActRIIB), which initiates signalling through a smad2/3-dependent pathway. These findings prompt us to elucidate MSTN action in the endocrine system. The present study was carried out to investigate the expression and localization of MSTN and ActRIIB in the anterior pituitary gland.

The anterior pituitary glands were freshly removed from male Holstein cattle. The mRNA expression of MSTN and ActRIIB were analyzed by RT-PCR and the protein expression of MSTN was examined by Western blotting with immunoprecipitation. Furthermore, immunohistochemical analyses were performed to investigate the localization of MSTN and ActRIIB in the bovine anterior pituitary cells. The antibodies used in the present study were mouse anti-bovine MSTN for immunoprecipitation, rabbit anti-human MSTN (CHEMICON International, Inc) and rabbit anti-human ActRIIB (Santa Cruz) for immunohistochemistry.

The expression of MSTN mRNA and ActRIIB mRNA, and also MSTN protein were confirmed in the bovine anterior pituitary gland. Immunohistochemistry of MSTN and specific hormones revealed that MSTN localized in thyrotrophs and gonadotrophs. About 83% of MSTN immunoreactive cells were identified as thyrotrophs. ActRIIB localized mainly in corticotrophs. Interestingly, we observed a lot of MSTN immunoreactive cells adjacent to the ActRIIB immunoreactive cells. These results first demonstrated that MSTN was produced and ActRIIB was expressed in the anterior pituitary cells. These findings suggest that MSTN may serve as a paracrine mediator among the anterior pituitary cells.

P68

DIRECT CELLULAR EXPRESSION OF C-FOS IN THE RAT ANTERIOR PITUITARY

TAKIGAMI, S.¹ and YASHIRO, T.¹

¹Department of Anatomy, Jichi Medical University, School of Medicine, Tochigi-ken, Japan.
(tshu@jichi.ac.jp)

Abstract: The c-Fos is a proto-oncogene and a transcription factor which is transiently expressed in the activated neuron. It has been used as the molecular marker for mapping of the activated brain region. Although the expression of c-Fos was also reported in the anterior pituitary of stressed animals, a detail of relation between transient c-Fos expression and activity in each hormone-producing cell is not known. To estimate the biological significance of c-Fos expression in hormone-producing cells, we examined c-Fos expression evoked by the exogenous and the endogenous stimulus in the rat anterior pituitary. We focused on ACTH cells which play a critical role in a stress response. The iv injection of CRH was used as the exogenous stimulus, and the immobilization stress was done as the endogenous stimulus. To confirm whether the c-Fos specifically expresses in activated hormone-producing cells or not, we immunohistochemically examined c-Fos expression in the anterior pituitary of rats injected with CRH (2 µg/kg) and immobilized in the plastic tube. CRH was injected through iv cannula in undisturbed rats. The number of immunopositive cells against c-Fos significantly increased in the anterior pituitary of rats injected with CRH. Most immunoreactive cells were identified as ACTH cells by the double staining for each anterior pituitary hormone. Because c-Fos was reported to be involved in regulating the synthesis of ACTH, ACTH cells transiently expressing c-Fos could be regarded as the cells activated by the releasing factor. In immobilized rats, the number of c-Fos-immunoreactive cells markedly increased. Immunoreactivities for c-Fos were detected in most ACTH cells, a part of PRL cells and a few TSH cells. The present results suggest that c-Fos might be a useful molecular marker for activated hormone-producing cells in the anterior pituitary.

P69

DIFFERENTIAL EXPRESSION OF L-SERINE SYNTHETIC ENZYME 3-PHOSPHOGLYCERATE DEHYDROGENASE IN THE FETAL AND ADULT MOUSE EYE

SAKAI, K.¹, FURUYA, S.² and HASHIKAWA, T.¹

*Laboratory for Neural Architecture, Brain Science Institute, RIKEN, Saitama, JAPAN;
2Laboratory of Metabolic Regulation Research, Bio-Architecture Center, Kyushu University,
Fukuoka, Japan, (ksakai@brain.riken.go.jp)*

Abstract: L-serine (L-Ser) is a non-essential amino acid that can be synthesized within the cells from glycolytic intermediate 3-phosphoglycerate and used for synthesizing various biomolecules, such as proteins, membrane lipids and nucleotides. It has recently been elucidated that L-Ser play as a neurotrophic factor for cultured neurons, and that its synthetic enzyme 3-phosphoglycerate dehydrogenase (Phgdh/3PGDH; EC 1.1.1.95) is selectively expressed in the radial glia/astrocyte lineage but not in neurons in the brain. In the eye, L-Ser seems to be important in retinal functions as well. In the present study, we examined its cellular expression in the eye of fetal and adult mice using antibodies for the Phgdh. In the fetal eye, the corneal epithelia, lens epithelial cells, primary fibre cells, retinal pigmented epithelium and anterior neuroretina were strongly labeled. In the adult eye, Phgdh expression was downregulated in lens region. In the retina, on the other hand, the immunoreactivity was detected exclusively in Müller cell soma in internal nuclear layer, being close to internal plexiform layer. Cellular processes were also immunopositive, filling spaces between neurons in internal nuclear layer through nerve fiber layer. Immuno-electron microscopic analysis confirmed the Phgdh expression in Müller cells surrounding retinal neurons and rod spherules. It was suggested that Phgdh in these non-neuronal cells may differentially contribute to various functions between differentiating and differentiated cells in the fetal and adult eye, respectively.

P70

IMMUNOHISTOCHEMICAL DEMONSTRATION OF MONOCARBOXYLATE TRANSPORTERS IN THE IN VITRO AND IN VIVO RABBIT CORNEAL EPITHELIUM

SHINOMIYA, KATSUHIKO¹, KATSUTA, OSAMU¹, HORIBE, YOSHIHIDE², FUJII, SHINOBU², KAWAZU, KOUICHI² and IKUSE, TOSHIMI¹

¹Drug safety and Pathology Group, ² Drug Metabolism Group, Research and Development Center, Santen Pharmaceutical Co., Ltd.

Abstract: Transporters bear the characteristics of efficiently delivering a small amount of drugs or organic chemicals to an object tissue. However, few studies have reported about the transporters in rabbit cornea. We usually use rabbits as laboratory animals in our research of ophthalmologic drugs. In this study, we immunohistochemically, demonstrated the distribution of monocarboxylate transporters (MCTs) in the cultured rabbit corneal epithelial cells (RCECs), rabbit corneal epithelium and liver.

The RCECs, the cornea and liver sampled from normal Japanese white rabbits were fixed in paraformaldehyde in 0.1M phosphate buffer. Four- μ m-thick frozen sections were cut for immunohistochemistry using a cryostat. The sections were incubated with primary antibodies against goat polyclonal MCT1, MCT2, MCT3, and MCT4, respectively (Santa Cruz Biotechnology Inc., USA). Then the sections were incubated with secondary antibody, biotinylated against goat IgG (Santa Cruz Biotechnology Inc.) and horse-radish peroxidase conjugated streptavidin (DakoCytomation, USA), in that order. These stainings were visualized using 3, 3'-diaminobenzidin. For immuno-electron microscopy pre-embedding procedure, the sections were embedded in epoxy resin.

Anti-MCT2 antibody showed marked positive-reactivity in all the layers of both the RCECs and the dissected corneal epithelium with a fine granular pattern. On the other hand, anti-MCT1, -MCT3, and -MCT4 antibodies showed weak positive-reactivity for some of the cells of the surface layers of both RCECs and the dissected corneal epithelium. In the liver, as a positive control, anti-MCT1 and -MCT2 antibodies showed strong positive-reactivity, but anti-MCT3 and -MCT4 antibodies showed weak positive-reactivity. In the immuno-electron microscopy, anti-MCT2 antibody showed positive-reactivity on the microvilli and basal membrane of the dissected corneal epithelium, and the rough endoplasmic reticulum and microvilli of the hepatocytes.

In this study, we confirmed MCTs are localized in the RCECs and corneal epithelium of the rabbit. This is a useful technique for researching the drug delivery system via transporters.

P71

CAPILLARY SUPPLY OF SLOW AND FAST MUSCLES AND ITS REMODELLING AFTER DENERVATION AND REINNERVATION

ERZEN, I.¹, CEBASEK, V.¹, KUBINOVA, L.², JANACEK, J.² and RIBARIC, S.³
¹Institute of Anatomy, ³Institute of Pathophysiology, Medical Faculty, University of Ljubljana, Korytkova 2, 1000 Ljubljana, Slovenia, ²Institute of Physiology, Academy of Sciences of the Czech Republic, Videnska 1083, 14201 Prague 4, Czech Republic (ida.erzen@mf.uni-lj.si)

Abstract: Fiber types in skeletal muscles differ in their contractile and metabolic characteristics. In this paper we address the density and geometry of their blood supply. Soleus (SOL) and extensor digitorum longus (EDL) muscles were excised from control, denervated and reinnervated rat muscles. Animal experiments were approved by the Veterinary Administration of the Ministry for Agriculture, Forestry and Food, Republik of Slovenia (Permit 326-07-285/99). Denervation was performed by cutting the sciatic nerve. Both muscles were excised two weeks later. Reinnervation was studied four weeks after nerve crush. Capillaries were demonstrated with a triple immunofluorescent staining with antibodies against CD31, laminin and Griffonia (Bandeira) simplicifolia lectin. Virtual SLICER test probes in three perpendicular directions were superimposed at random into stacks of perfectly registered optical sections that were captured with a confocal microscope. Length of capillaries adjacent to each individual muscle fiber (Lcap/Lfib) was measured per unit fiber length. Interrelationships among capillaries and muscle fibers were demonstrated with maximal intensity projection. Additionally, capillaries were segmented by the interactive TRACER method and visualized using OpenGL graphics system.

Lcap/Lfib was larger in control soleus than in EDL. No difference was found in control EDL among small, slow oxidative fibers and large fast glycolytic fibers. In denervated SOL Lcap/Lfib was reduced, however, after reinnervation it reached values of control muscles. In contrast, no statistically significant difference was found in EDL among the control and experimental groups.

In the EDL capillaries run parallel to the fiber axes or decline slightly from them whilst in the SOL they form transverse connections along their zig-zag course. After denervation the capillary course in SOL became similar to the one characteristic for EDL. The original pattern was re-established after reinnervation. In EDL, no evident change could be observed after denervation, however, in reinnervated muscle transverse connections were established at least in some muscle fibers.

The results of this study indicate that denervation and reinnervation provoke remodelling of the capillary bed.

P72

COMPARISON OF EARLY WITH LATE ENDOTHELIAL PROGENITOR CELLS IN TUBE FORMING ACTIVITY IN VITRO

MUKAI, N.^{1,2,3}, KOBAYASHI, A.¹, KUWANA, R.¹, AMAGASA, T.², and MORITA, I.^{1,3}

¹Dept. of Cellular Physiological Chemistry, Graduate School, Tokyo Medical & Dental University, Japan; ²Dept. of Maxillofacial Surgery, Graduate School, Tokyo Medical & Dental University, Japan; ³21st Century COE, Tokyo Medical & Dental University, Japan. (mukacell@tmd.ac.jp)

Abstract: There is growing excitement that bone marrow and peripheral blood-derived endothelial progenitor cells (EPCs) can be used to promote revascularization of injured and ischemic tissues. However, the mechanism of promoting revascularization by EPC remains controversial. Here, mononuclear cells (MNC) were isolated from peripheral blood, and differentiated into two kinds of EPCs. Early EPCs were observed from 3 days and isolated by day 5 after culture and late EPCs were formed colony from 14 days and isolated by day 21 after culture. Human umbilical vein endothelial cells (HUVECs) were obtained from enzymatically digested human umbilical cord and used as a control. These EPCs and HUVECs were applied to our novel methods for measuring tube forming activity. The principle is as follows; endothelial cells were cultured onto the fully patterned plates in which capillary net works *in vivo* were reproduced by optical lithography. To form vascular tube, the plate was contacted with Matrigel. It is demonstrated that late EPCs as well as HUVECs exhibited tube formation with similar morphology, whereas early EPCs failed to form any tubes. Moreover, when late EPCs were mixed with HUVECs and applied to the tube forming system, late EPCs were incorporated into the tubes formed. On the other hand, when early EPCs were used in this system, it could not be observed EPC-incorporated tubes. It is interesting that when early or late EPCs were cultured with the tube formed by HUVECs, HUVECs could be substituted by late EPCs, but not by early EPCs. However, sprouting of HUVEC was observed by the addition of early EPCs.

In conclusion, early EPCs promote migration and proliferation of endothelial cells, whereas late EPCs constitute blood vessels. It suggests that circulating EPCs have different roles in neovascularization.

P73

HETEROGENOUS SUCCINATE DEHYDROGENASE ACTIVITIES QUANTIFIED IN SITU IN MUSCLE FIBERS OF LATERAL PTERYGOID MUSCLE ATTACHED TO BONES

MIZUTANI, M.¹, NAKAE, Y.² and OHNO, N.¹

¹Department of Anatomy, School of Dentistry, Aichi-Gakuin University, Japan; ²Department of Oral and Maxillofacial Anatomy, Institute of Health Biosciences, The University of Tokushima Graduate School, Tokushima, Japan. (makmizu@dpc.aichi-gakuin.ac.jp)

Abstract: Quantitative assessment of enzyme activities *in situ* in single muscle fibres is essential for understanding functions of skeletal muscles. Function of the lateral pterygoid muscle is not fully understood because it is a deeply located masticatory muscle and cannot be dissected in an intact configuration. Here we report how to measure the activities of mitochondrial succinate dehydrogenase in single muscle fibres in the lateral pterygoid muscles in sections of rat heads. Unfixed head sections were incubated on the gel films containing SDH substrate and NBT tetrazolium salt. During incubation images of the section due to deposition of the final reaction products formazans were captured at intervals of 10 seconds using a real-time image analysis system for absorbance measurements. We found that the belly of the lateral pterygoid muscle consisted of four areas with different mean activities of SDH. Average initial velocity ($\mu\text{mol cm}^{-3} \text{ min}^{-1}$) was 13.707 ± 0.266 in the upper area, 14.239 ± 0.256 in the lateral area, 11.214 ± 0.257 in the medial area, and 7.531 ± 0.189 in the lower area. The lateral and upper areas of the muscle have similarly high SDH activities. The mean activity of the lower area was the lowest and about half of those of the lateral and upper areas. The mean activity of the medial area was intermediate. These results agree with the hypothesis that the superior head of the lateral pterygoid muscle participates in more continuous contraction and is more resistant to fatigue than the inferior head.

P74

HYPERPLASIA IN DM CATTLE IS DUE TO FAILURE OF MSTN INDUCTION BY HGF

HAYASHI, SHINICHIRO, ASO, HISASHI, OGASAWARA, HIDEKI, MIYAKE, MASATO, WATANABE, KOUICHI, OHWADA, SHYUICHI and YAMAGUCHI, TAKAHIRO

Laboratory of Functional Morphology, Department of Animal Science, Graduate School of Agricultural Science, Tohoku University, 1-1 Tsutsumidori-Amamiyamachi, Aoba-ku, Sendai, Japan, 981-8555 (e-mail address : ty1010@bios.tohoku.ac.jp)

Abstract: Numerous growth factors are thought to influence myogenesis. However the precise mechanisms and interactions of these growth factors remain largely unknown. Myostatin (MSTN), a member of the transforming growth factor- β superfamily, is a negative regulator of skeletal muscle growth. Inactivating mutations of the myostatin gene in double muscled (DM) cattle breeds lead to an increase in muscle mass resulting from mainly hyperplasia. HGF affects myogenesis positively by enhancing myoblast proliferation. In this study, we investigated the interaction between MSTN and HGF using regeneration model of skeletal muscle as well as myoblast culture from normal muscled (NM) and DM Japanese shorthorn cattle breeds. Histochemical analysis revealed that myotube formation was enhanced at the site of regenerating muscle in DM cattle as compared with that in NM cattle. Western blotting, immunohisto-chemistry and in situ hybridization methods demonstrated that MSTN expression was markedly upregulated in regenerating muscle, and both MSTN and HGF were co-expressed in identical myocytes at the regenerating area. In vitro analysis, MSTN was mostly expressed in proliferating myoblasts and differentiated myotubes. The addition of HGF to culture medium promoted the myoblast proliferation and the MSTN mRNA expression in myoblasts from NM cattle, but MSTN did not influence HGF expression. And also, HGF inhibited the formation of myotubes in DM myoblast culture with the enhanced cell proliferation. These findings indicate that the hyperplasia in DM cattle is due to failure of the MSTN induction by HGF that promotes MSTN production in myoblasts of NM cattle.

P75

IMMUNOELECTRON MICROSCOPIC ANALYSIS OF CD11C-POSITIVE DENDRITIC CELLS IN THE PERIAPICAL REGION OF THE RAT PERIODONTAL LIGAMENT

KANEKO, T.¹, ZHAO, L-Y.^{1,2}, OKIJI, T.³, and SUDA, H.¹

¹*Pulp Biology and Endodontics, Graduate School, Tokyo Medical and Dental University, Tokyo, Japan;* ²*Stomatology Hospital of Jilin University, Changchun, P.R.China;* ³*Division of Cariology, Operative Dentistry & Endodontics, Niigata University Graduate School of Medical and Dental Sciences, Niigata, Japan. (tomoendo@tmd.ac.jp)*

Abstract: To understand the structural and phenotypic characteristics of dendritic cells (DCs) in the periapical region of the periodontal ligament (PDL), we performed immunoelectron microscopic analysis by using CD11c antibody as a previously untested DC marker. Five-week-old male Wistar rats were used. The PDL of mandibular first molars, either normal or bacterially challenged by making unsealed pulp exposures for 3 days, were subjected to immunohistochemistry and transmission electron microscopy using CD11c, ED1 (anti-macrophages and DCs) and OX6 (anti-major histocompatibility complex class II molecules). The periapical region of the distal root was subjected to quantitative analysis where ratios of DCs to total immunopositive cells were determined following differential cell count under the transmission electron microscope.

The antibody CD11c clearly recognized DCs, although it also labeled certain macrophage subpopulation(s). In the normal PDL, DCs extended several long cytoplasmic processes from their oval to slender cell body. Their cytoplasm contained mitochondria and rough endoplasmic reticula, whereas lysosomal structures were scarce and typical phagosomes were not seen. After three days of pulp exposure, relatively small DCs with many thin and short cytoplasmic processes, representing newly recruited DCs, were detected predominantly near the blood vessels. The cytoplasm of these cells was sparse in organelles. The ratio of DCs to CD11c+ cells was significantly higher than that to ED1+ and OX6+ cells both in the normal and challenged PDL. The present results suggest that CD11c may be a phenotypic marker for both resident and newly recruited DCs in the rat PDL and useful for discriminating DCs from macrophages. The appearance of newly recruited DCs following pulp exposure may support the notion that the PDL is prepared to induce T cell responses against bacterial challenges from the root canal.

P76

ULTRASTRUCTURAL TRANSFORMATION OF GASTRIC PARIETAL CELLS REVERTING FROM THE ACTIVE TO THE RESTING STATE OF ACID SECRETION REVEALED IN ISOLATED RAT GASTRIC MUCOSA MODEL PROCESSED BY HIGH-PRESSURE FREEZING

SUGANUMA, T., SAWAGUCHI, A., AOYAMA, F., OHASHI, M. and IDE, S.
Department of Anatomy, Ultrastructural Cell Biology, Faculty of Medicine, University of Miyazaki, Miyazaki, Japan. (suganumat@med.miyazaki-u.ac.jp)

Abstract: Cryofixation is currently accepted as the best initial fixation step to preserve not only fine structure but also the antigenicity in biological samples. To elucidate a functional transformation of gastric parietal cells, we have newly developed an isolated rat gastric mucosa model whose parietal cells exhibited a reverting process from the active to resting state of acid secretion. Briefly, the parietal cells were treated with cimetidine following prior stimulation of acid secretion in the model, and cryofixed by plunge freezing for light microscopy or high-pressure freezing for electron microscopy. As a result, immunohistochemistry of H⁺/K⁺-ATPase demonstrated a progressive translocation of H⁺/K⁺-ATPase from the apical to the cytoplasmic region. The ultrastructure of parietal cells at 5 min in the reverting phase was quite similar to that of maximally stimulated one. However, the apical microvilli of intracellular canaliculi (IC) changed bulbous by degrees, resulted in complete occlusion of IC at 60 min in the reverting phase. The apical membranes were subsequently internalized into the cytoplasm forming unique penta-laminar membranes. Interestingly, at 90 min in the reverting phase, the penta-laminar membranes formed a number of multilamellar autophagosomes that were intensely labeled for H⁺/K⁺-ATPase. Then, the parietal cells exhibited well-developed Golgi apparatus and lysosomal compartments involving the multilamellar membranes at 105 min, and mostly reverted to their resting conformation at 120 min in the reverting phase. Corresponding to the ultrastructural changes of microvilli, the immunohistochemistry of ezrin showed a dissociation of ezrin from the apical region at 30 min in the reverting phase. We describe the preparation of new experimental model and fine structures in the reverting process by taking the advantages of cryofixation.

P77

ENDOTHELIN (ET) –1, NITRIC OXIDE (NO) AND INFLAMMATORY MARKERS DURING SEPSIS ARE ALTERED IN THE LIVER IN A TIME-DEPENDENT MANNER

JESMIN, S.¹, ZAEDI, S.¹, MOWA, C.N.², MAEDA, S.¹, MIYAUCHI, T.¹

¹Department of Cardiovascular Medicine and Pharmacology, University of Tsukuba, Ibaraki, Japan, ²Department of Biology, Appalalihan State University, Boone, NC, USA

Abstract: Sepsis is a heterogeneous class of syndromes and septic shock, a severe form of sepsis, is associated with the development of progressive damage in multiple organs. The present study examined the time-dependent alterations of ET-1, NO and inflammatory cytokine, such as TNF- α in liver tissue in a septic rat model. Normal male Wistar rats at age 15 wks were administered with lipopolysaccharide (LPS, 15 mg/kg) and then sacrificed at different time points (1h, 3h, 6h and 10h). Control rats were only given vehicle. Both the systolic and diastolic pressures drastically fell an hour after LPS administration and then gradually normalized, even though at 10 h post-LPS administration the blood pressure was lower compared to control rats. Also LPS induced increase in the serum levels of TNF- α (1200-fold), and ET-1 (25-fold), acute liver injury (infiltration of inflammatory cells, hepatocytic necrosis), and plasma levels of Plasma bilirubin, GOT and GPT, in a time-dependent manner. In the liver, LPS induced increase in levels of ET-1 (A 28-fold after 10hr) and TNF- α (4.5-fold). Although a compensatory increase in NO and eNOS levels were seen in liver tissue, as endotoxaemia progressed, a concomitant induction of iNOS led us to question the availability of functional NO. Initially, during sepsis, hepatic levels of ET_AR were down regulated, but increased with time, while ET_BR showed a time-dependent decrease. We conclude that imbalance of ET-1, NO and inflammatory cytokines, at different time points in septic liver, could, in part, help explain the mechanisms that underlie the pathogenesis of acute liver injury in endotoxemia.

P78

HISTOCHEMICAL STUDIES ON AL IN THE LIVERS OF MICE ADMINISTERED WITH AL BY IMMUNOSTAINING AND X-RAY MICROANALYSIS WITH HIGH VOLTAGE ELECTRON MICROSCOPY

KAMETANI, K.¹ and NAGATA, T.^{2,3}

¹Department of Instrumental Analysis, Research Center for Human and Environmental Science, Shinshu University, Matsumoto, Japan. ²Department of Anatomy and Cell Biology, Shinshu University School of Medicine, Matsumoto, Japan. ³Department of Anatomy, Shinshu Institute of Alternative Medicine, Nagano, Japan. (E-mail: kametani@sch.md.shinshu-u.ac.jp)

Abstract: Quantitative elemental analysis on aluminum (Al) was carried out by immunostaining with metallothionein (MT) and X-ray microanalysis using a high-accelerating voltage transmission electron microscope (HVTEM) equipped with energy dispersive X-ray microanalyzer (EDX). MT was used to detect metal metabolism. HVTEM-EDX was used with high permeability at an accelerating voltage of 300kV using thick samples at 1 μ m thickness obtained from the mice administered with aluminum chloride solution for 3, 9 and 17 weeks. MT immunostaining observed by light microscopy revealed expression of MT which was only found in a few cells surrounding blood vessels in the liver tissues of mice which were administered with excess Al. By electron microscopic observation, ultrastructural changes were widely observed in the lysosomes in the hepatocytes as well as the pinocytotic vesicles in the macrophages in the experimental animals. By EDX, the concentrations of Al in the lysosomes of the hepatocytes and pinocytotic vesicles of the macrophages in the livers of mice administered with Al were measured in relation to those administration periods. Moreover, transitional changes of the hepatocyte lysosome ratios by image analysis and the numbers of macrophage counts in the unit area increased in the liver tissues of mice administered with Al as compared with normal control mice. From the results, it was demonstrated that the hepatocyte lysosome ratio and macrophage count increased in the liver tissues of treated mice during those short-term excessive Al administration periods. It was also clarified that the concentrations of Al in both hepatocytes and macrophages increased as observed by HVTEM-EDX. In conclusion, Al was accumulated in the hepatocytes and in the macrophages at 3 and 9 weeks administration before the expression of MT was increased, and the ultrastructural changes remained in the hepatocytes and macrophages.

P79

DYNAMIC CHANGES OF EXPRESSION OF MOLECULES RELATED TO THE EPITHELIAL-MESENCHYMAL TRANSITION IN THE EARLY PHASE OF LIVER DEVELOPMENT

NAKATANI, K., SAKABE, M., and NAKAJIMA, Y.

Department of Anatomy and Cell Biology, Osaka City University Graduate School of Medicine, Osaka, Japan (kazuki@med.osaka-cu.ac.jp)

Abstract: To elucidate the molecular mechanism of liver morphogenesis, we investigated the expression of several molecules related to the epithelial-mesenchymal transition in the early phase of liver development. We used rat embryos that were 11.5, 12.0 and 12.5 embryonic days, and stained the specimens by immunohistochemical methods. The hepatoblasts, which migrated in the septum transversum, had alpha-fetoprotein and cytokeratin 18, but not vimentin and alpha-smooth muscle actin. E-cadherin expression in the hepatoblasts was strongly decreased, whereas endodermal cells in the foregut clearly expressed it. Hepatoblasts began to express N-cadherin, whereas endodermal cells in the foregut did not. Mesenchymal cells in septum transversum also expressed N-cadherin. Hepatoblasts often had contact with other hepatoblasts and mesenchymal cells, and there were adherence junctions between hepatoblasts. We could not detect either matrix metalloproteinase (MMP) 2 or membrane-type MMP 1, which are correlated with degeneration of the basement membrane, in either the hepatoblasts or the endodermal cells in the foregut. It is suggested that the hepatoblasts, which migrate in the septum transversum, have both epithelial and mesenchymal phenotypes, thus epithelial-mesenchymal transition-like phenomenon takes place in the liver morphogenesis.

P80

DLK-1 EXPRESSION IN THE CALLIPYGE MODEL OF SKELETAL MUSCLE HYPERTROPHY; INTEGRATED IMMUNOHISTOCHEMICAL, TRANSCRIPTOMIC AND PROTEOMIC ANALYSIS.

WHITE, J.D.^{1,2}, GROUNDS, M.D.², TELLAM, R.³, VUOCOLO, T.³, MCDONAGH, M.⁴, KNIGHT, M.⁴, COCKETT, N.E.⁵

¹School of Veterinary Science, University of Melbourne, Parkville, Australia. ²School of Anatomy and Human Biology, University of Western Australia, Perth, Australia. ³CSIRO Livestock Industries, Queensland Bioscience Precinct, Brisbane, Australia. ⁴Primary Industries Research Victoria, Attwood, Australia, ⁵ADVS Dept, University of Utah, Logan, Utah, USA.

Abstract: Dlk-1 is a type 1 membrane glycoprotein and is a member of the Epidermal Growth Factor-like family of homeotic proteins. Members of this family of proteins are typically involved in cell fate decisions and in mice Dlk-1 has been implicated in the control of adipocyte differentiation. The *callipyge* mutation in sheep results in significant skeletal muscle hypertrophy in the hind-quarters, whereas muscle of the forelimb and shoulders do not show significant hypertrophy. The hypertrophy trait is inherited in a pattern described as polar over-dominance; the phenotype is only displayed in progeny that inherit the mutated allele from the paternal side. The hypertrophy is associated with fast glycolytic fibres with an associated decrease in the size and proportion of type 1 fibres. The causative SNP is in an imprinted region of ovine chromosome 18 and is surrounded by a number of protein coding regions including Dlk-1, peg-11 and GTL-2. Quantitative RT-PCR studies show that expression of mRNA for genes in this region is elevated in affected muscles (LD, SM hind limbs) but not unaffected muscles (SS or IS); this is especially true for Dlk-1. There are also a number of associated significant alterations in myosin isoform mRNA expression. Immunofluorescent staining for Dlk-1 protein in *callipyge* muscles shows a pattern of staining which parallels the mRNA data. Staining for Dlk-1 is exclusively associated with fast type myofibres and is totally absent from fibres staining positive for slow type myosins. Furthermore, positive Dlk-1 immunohistochemical staining is associated with (Pax7+) satellite cells in ovine skeletal muscle. This data indicates that increased expression of Dlk-1 underlies the mechanism of skeletal muscle hypertrophy in the *callipyge* phenotype.

P81

**SUBCELLULAR LOCALIZATION OF INJECTED
TECHNETIUM-99M SESTAMIBI IN RAT HEART**ISHIKAWA, Y.¹, SATAKE, O.³, UEDA, T.², KURIHARA, T.¹ and
KAJINAMI, K.³¹Medical Institute, ²Anatomy, ³Cardiology of Kanazawa Medical University, Ishikawa Japan
(ishimaro@kanazawa-med.ac.jp)

Abstract: Technetium-99m Sestamibi (MIBI) is a myocardial perfusion imaging agent for diagnosis in patients with ischemic heart disease. It has been reported that the subcellular site of MIBI in heart is mitochondria. However, it remains uncertain where MIBI localizes in mitochondria.

The aim of the present study was to investigate the localization of MIBI in mitochondria by using LEO 912 AB (energy-filtering transmission electron microscope), which can demonstrate the distribution of the element in the organelle.

Seventy-five MBq of MIBI (kindly provided by Daiichi Radioisotope Labs, Tokyo) was injected into Wistar adult rat (200g) from iliac vein.

The heart was monitored by a gamma camera for the period of between 0 and 120 min after injection. The animals were sacrificed and the hearts were dissected into small blocks. Tissues were fixed with 2.5% glutaraldehyde and embedded in Quetol 651 resin. Ultrathin sections were cut 30×40nm in thickness with LEICA ULTRACUT and observed under a LEO 912 AB.

After MIBI injection, various degree of Technetium accumulation was observed in mitochondria of myocytes. Among them, MIBI was accumulated on the cristae of some mitochondria. On the other hand, the MIBI accumulation decreased in number at 120 min after MIBI injection. Furthermore, the accumulation of MIBI on cristae in mitochondria was markedly decreased at this time.

The present study results indicate that injected MIBI distributes in mitochondria.

P82

SILENCING OR BLOCKAGE OF VEGF IN THE CERVIX OF PREGNANT RATS DOWN REGULATES LEVELS OF OXYTOCIN

MOWA, C.N.¹, LI, T.², FOLKESSON, H.G.², JESMIN, S.³, JOHNSON, E.⁴, LOPEZ, M.⁵, USIP, S.², SMITH, D.⁵, PAPKA, R.E.²

¹*Appalachian St Univ, Boone, NC;* ⁴*North Carolina A & T State Univ, Greensboro, NC;* ²*NE Ohio Univs Coll Med, Rootstown, OH;* ⁵*Univ Akron, Akron, OH;* ³*Tsukuba Univ, Tsukuba, Japan (mowacn@appstate.edu).*

Abstract: A successful and timely passage of fetus at term is preceded by a complex process termed cervical ripening (CR) that is associated with microvascular remodeling. The mechanism(s) underlying CR are not completely understood. Because VEGF is a key architect of microvascular remodeling, VEGF likely plays a vital role in CR. We previously deciphered VEGF-related genes in the cervix of pregnant rats treated with VEGF agents, namely inhibitor or siRNA-generating pDNAs targeting VEGF, using genome-wide DNA microarray analysis. Analysis of the microarray data revealed that the most altered (down-regulated) gene, out of a total of 50,000, was oxytocin. Here, we use histological techniques and real time- and gel based-PCR, to validate the microarray data. Consistent with the previous microarray data, levels of oxytocin were down-regulated, in a dose-dependent manner, in the cervix of pregnant rats treated with VEGF agents compared to control rats. We conclude that VEGF may, in part, influence cervical ripening by regulating levels of oxytocin (Funded by: Appalachian State University URC and NEOUCOM Research Challenge grants).

P83

THE MICROENVIRONMENT OF HUMAN TROPHOBLASTIC CELLS IN EARLY PREGNANCY INFLUENCES CELL SURFACE CARBOHYDRATE STRUCTURE EXPRESSION AND CONTROLS CELL PROLIFERATION

SAITOH, E.^{1,2}, SUZUKI, A.², SUSUMU, N.², TANABE, K.¹ and AOKI, D.²

¹Department of Obstetrics and Gynecology, Tokyo Electric Power Company Hospital and

²School of Medicine, Keio University, Japan. (saitoh.eiko@tepcoco.jp)

Abstract: Carbohydrate structures of complex carbohydrate displayed on the cell surface are related to cellular functions. beta1,4- galactose (Gal) residues on *N*-linked glycans have been reported to have an inhibitory effect on cell proliferation of human fibroblastic cells. We have reported that human placental trophoblast similarly expresses Gal in early pregnancy. As contact with maternal blood or extracellular matrix (ECM) has been proposed to influence the differentiation of human trophoblastic cells in early pregnancy, our aim was to clarify the significance of Gal expression on trophoblastic cells as well as its effects on the surrounding cellular microenvironment and on cell proliferation.

Immunohistochemistry with monoclonal antibody MIB-1, that reacts to Ki-67, and lectin histochemistry with *Ricinus communis agglutinin* (RCA), that preferentially reacts to Gal, were performed on human placental tissue from early pregnancy. As the RCA-binding carbohydrate structures is frequently masked by sialic acid, it was removed by sialidase.

MIB-1 reacted positively with cytotrophoblasts or cell columns, neither of which had any contact with the maternal blood or ECM; in addition, the RCA reaction was negative with or without sialidase treatment in these trophoblasts. In syncytiotrophoblasts (ST), which contacts maternal blood, and in extravillous trophoblasts (EVT), which contacts with ECM, the MIB-1 reaction was negative. The RCA reaction was positive in ST after sialidase treatment and was positive in EVT with or without sialidase treatment.

Our results demonstrate that Gal is not expressed in trophoblastic cells without contact to maternal blood or ECM, and that these cells retained their proliferation ability. In contrast, Gal was expressed in trophoblasts in contact with the surrounding environment, and their cell proliferation was suppressed. Thus, our findings suggest that the microenvironment surrounding trophoblastic cells affects their functional differentiation and that Gal residues play an important role to mediate this process.

P84

IDENTIFICATION OF ESTROGEN RECEPTOR BETA-POSITIVE INTRAEPITHELIAL LYMPHOCYTES AND THEIR POSSIBLE ROLES IN NORMAL AND TUBAL PREGNANCY OVIDUCTS

ULZIIBAT, S.¹, HISHIKAWA, Y.¹, SHIBATA, Y.³, EJIMA, K.¹, AN, S., KITAJIMA, M.², FUJISHITA, A.², ISHIMARU, T.², KOJI, T.¹

¹Div. of Histology and Cell Biology, Dept. of Developmental and Reconstructive Medicine, Nagasaki University Graduate Schl of Biomedical Sciences, Japan; ² Dep.t of Obstetrics and Gynecology, Nagasaki University School of Medicine, Japan; ³ Div. of Oral Pathology and Bone Metabolism, Dept. of Developmental and Reconstructive Medicine, Nagasaki University Graduate Schl of Biomedical Sciences, Japan (dm03052c@stcc.nagasaki-u.ac.jp)

Abstract: Although intraepithelial lymphocytes (IEL) in human oviductal epithelium have been implicated in the regulation of local immunity, the precise kinetics and mechanism of steroid regulation of IEL were largely unknown. We examined the localization of estrogen receptors (ERs) and progesterone receptors (PRs) in 41 human oviducts by immunohistochemistry. These tissues were obtained from various menstrual cycles, also from both postmenopausal women and tubal pregnancies. The expressions of ER BETA mRNA and membrane (m)PR mRNA were examined by *in situ* hybridization and RT-PCR, respectively. Most of the IEL expressed ER BETA at both mRNA and protein levels. The number of ER BETA-positive IEL, which were identified as CD8-positive T lymphocytes and also were membrane PR (mPR) positive, was increased in the late proliferative, the mid and late secretory phases in normally cycling women ($P < 0.05$). Interestingly, in tubal pregnancy, ER BETA-positive IEL were consistently abundant. In addition, we found a high Ki-67 labeling index for IEL, though ER ALPHA was entirely absent in the tubal pregnancy oviducts. These results suggest that the number of IEL fluctuated depending upon the levels of estrogen and progesterone probably through ER BETA and mPR, respectively. ER BETA-positive IEL may be involved in regulating immune tolerance in normal and tubal pregnancy oviducts.

P85

ANTAGONISM OF ENDOTHELIN A RECEPTOR IN DIABETIC ERECTILE DYSFUNCTION REVERSES DOWN REGULATION OF NO/NOS BUT NOT VEGF

JESMIN, S.¹, MOWA, C.N.², ZAEDI, S.¹, MAEDA, S.¹, MIYAUCHI, T.¹

¹Dept of Cardiovascular Medicine and Pharmacology, University of Tsukuba, Ibaraki, Japan,

²Dept of Biology, Appalachian State University, Boone, NC, USA (mowacn@appstate.edu)

Abstract: Erectile dysfunction (ED) affects about 50% of male diabetic patients, possibly due to the vascular and neuropathic complications. The role of Vascular endothelial growth factor (VEGF) signaling in different complications of diabetes has been extensively documented, and we have previously shown that VEGF signaling is greatly diminished in the penis of a rat model of type II diabetes at the insulin-resistant stage. Here, we used streptozotocin (STZ)-induced diabetic (DM) rat (Sprague-Dawley, 450±26 g) model, treated for three weeks (65 mg/kg, IP), to assess the effects of endothelin antagonism on the altered levels of VEGF and NO/NOS in penile tissue. Control rats were administered only citrate saline (vehicle). Diabetes was confirmed by hyperglycemia and, after 1 week of diabetes, animals were separated into groups receiving either: 1) endothelin-A/B (ET-A/B) dual receptor antagonist (SB209670, 1 mg/day/rat), 2) endothelin-A (ET-A) receptor antagonist (TA-0201, 1 mg/kg) or 3) saline, for 2 weeks using osmotic mini pump and then sacrificed. Glucose levels in DM rats significantly increased (405±103 mg/dL) compared to non-DM rats (120±8 mg/dL) and local ET-1 level in DM penis was higher by 20%. A 30% decrease in VEGF expression in penile tissue was seen in DM rats, and ET-A antagonist did not restore the down regulated VEGF. However, ET-A/B dual antagonist tended to further decrease the VEGF levels in DM penis. Phosphorylated Akt (pAkt) was reduced in DM penis by 20% and was unchanged by both types of ET blockers. Penile NO and eNOS levels decreased in DM rats, but were significantly restored by ET-A receptor antagonist. However, they were unchanged or decreased by ET-A/B dual antagonist. iNOS was not significantly changed in penile tissues among non-DM, DM and ET-A antagonist-treated groups. We conclude that ET-A antagonist, but not ET-A/B dual antagonist, is effective in attenuating and reversing the down regulation of NO/NOS, in type 1 DM penis, a critical regulatory system in erectile function. However, both ET antagonist could not block and restore levels of the down regulated VEGF and pAkt.

P86

P53 PHOSPHORYLATION IN MOUSE SKIN AND IN VITRO HUMAN SKIN MODEL BY HIGH-DOSE-RADIATION EXPOSURE

KOHNO, Y.¹, SUGASAWA, J.², KOIKE, A.², KOIKE, M.²

¹Department of Oral Pathology, School of Dentistry, Showa University, Japan, ²DNA Repair Gene Research, National Institute of Radiological Sciences, 4-9-1 Anagawa, Inage-ku, Chiba 263-8555, Japan. (yohko@dent.showa-u.ac.jp)

Abstract: The skin is an external organ that is most frequently exposed to radiation. High-dose radiation initiates and promotes acute radiation injury. Thus, it is important to investigate the influence of high-dose radiation exposure on the skin at the molecular level. The post-translational modification of p53 plays a central role in radiation responses, including apoptosis and cell growth arrest. Although it is well known that ataxia telangiectasia mutated (ATM) kinase and DNA-dependent protein kinase (DNA-PK) can phosphorylate Ser15/Ser18 of p53 *in vitro*, the post-translational modification pattern and the modifier of p53 in the skin after exposure to high-dose X-rays are not yet well understood. Here we show that the phosphorylation of p53 on Ser15/Ser18, as well as the phosphorylation of histone H2AX on Ser139, was detected in the keratinocytes of the mouse skin and human skin models after high-dose X-ray irradiation. Following high-dose X-ray irradiation, both proteins were also phosphorylated in the skin keratinocytes of both ATM gene knockout mice and DNA-PK-deficient SCID mice.

All experiments using animals were approved by the University and Institute Committee in accordance with the Guidelines for Animal Experimentation in Showa University and National Institute of Radiological Sciences.

P87

LOCALIZATION OF MYOSIN AND ACTIN IN THE SKIN, HAIR AND WHISKER OF RAT

MORIOKA, K.¹, MATSUZAKI, T.² and TAKATA, K.²

¹The Tokyo Metropolitan Institute of Medical Science, Tokyo, Japan; ²Gunma University, Maebashi, Gunma, Japan. (morioka@rinshoken.or.jp)

Abstract: The combined effects of myosin II and actin enable muscle and nonmuscle cells to generate forces required for muscle contraction, cell division, cell migration, cellular morphological changes, the maintenance of cellular tension and polarity, and so on. However, except for the case of muscle contraction, the details are poorly understood. We focus on nonmuscle myosin and actin in the formation and maintenance of hair and skin, which include highly active processes in mammalian life with respect to the cellular proliferation, differentiation, and movement. The localization of nonmuscle myosin II and actin in neonatal rat dorsal skin, mystacial pad, hair follicles, and vibrissal follicles was studied by immunohistochemical technique to provide the basis for the elucidation of the roles of these proteins. Specificities of the antibodies were verified by using samples from the relevant tissues and subjecting them to immunoblotting test prior to morphological analyses. The myosin and actin were abundant and colocalized in the spinous and granular layers but scarce in the basal layer of the dorsal and mystacial epidermis. In hair and vibrissal follicles, nonmuscle myosin and actin were colocalized in the outer root sheath and some hair matrix cells adjoining dermal papillae. In contrast, most areas of the inner root sheath and hair matrix appeared to comprise very small amounts of myosin and actin. Hair shaft may comprise significant myosin during the course of its keratinization. These results suggest that the actin/myosin system plays a part in cell movement, differentiation, protection from mechanical stress, sealing or other key functions of skin and hair.

P88

VARIATION OF CAVEOLIN-1 EXPRESSION WITH PHOTOAGING AND CHRONOLOGICAL AGING ON CHINESE SKIN

NOBLESSE, E.¹, KURFURST, R.¹, BIGLIARDI-QI, M.², BIGLIARDI, P.L.², ZHIQIANG, C.³, SCHNEBERT, S.¹, and BONTE, F.¹

¹LVMH Recherche, St Jean de Braye, France; ²Departments of dermatology, Hôpital Beaumont, Lausanne, Switzerland ; ³Chinese Academy of Medical Sciences, Dermatology Institute, Nanjing, PR China. (enoblesse@research.lvmh-pc.com)

Abstract: It is known that caveolin-1 is expressed not only in the epidermis where it is related to the phenomena of differentiation and also in the dermis where it is associated with a senescence phenotype in fibroblasts. Very few data are currently known on the influence of the age and the photoexposure on this protein expression.

The present study investigates the influence of age and sun exposure on caveolin-1 expression on the skin of 30 Chinese women. Patients were divided in a young group (22-30 years old) and an old group (60-69 years old). Skin punch biopsies (3mm) were taken from the anterior surface of the upper arm (protected area) and the posterior surface of the forearm (exposed area). Samples were fixed in formalin and embedded in paraffin. Sections were cut and studied for caveolin-1 immunostaining and quantification was obtained by pictures analysis.

We shown that photoexposure increased the caveolin-1 expression in basal layer keratinocytes (+51% in photoexposed skin in comparison with photoprotected skin). This difference is more important for the youngest group (+69%) than for the oldest (+29.8%). In the photoprotected zone, no difference with aging was observed. In contrast, we noticed a statistical aging influence for the photoexposed zone where caveolin-1 expression is decreased with aging in epidermis. For the dermis part, we observed no significant difference in the caveolin-1 expression between photoprotected and photoexposed zones in average for all the patients. In contrast, we observed significant differences with age. In the photoprotected zone, we observed a weak, non significant increased of caveolin-1 expression with age whereas for the photoexposed zone, the caveolin-1 expression is significantly decreased (-51%). These results showed us that the caveolin-1 expression could, at the same time, be differently regulated by chronological aging but also by photoaging.

P89

ADIPOGENESIS AND ADIPOGENESIS IN OBESITY REVEALED BY A VISUALIZATION TECHNIQUE OF LIVING ADIPOSE TISSUE

NISHIMURA, SATOSHI¹, NAGASAKI, MIKA¹, NAGAI, RYOZO¹, and SUGIURA, SEIRYO²

¹Department of Cardiovascular Medicine, ²The Institute of Environmental Studies, Graduate School of Frontier Sciences, The University of Tokyo. (snishi-tyk@umin.ac.jp)

Abstract: Ample evidences suggest that angiogenesis plays a pivotal role in adipogenesis in obesity, but little is known about the detailed mechanism. We have developed a visualization technique based on laser confocal microscopy that allows us to analyze angiogenesis and adipogenesis in intact living adipose tissue three-dimensionally in detail. We found that there were close spatial and temporal interrelationships between blood vessel development and adipogenesis, and both were augmented in animal models of obesity (db/db mice). Formation of new blood vessels by sprouting from preexisting vasculature was coupled with differentiation of adipocytes, and differentiating small adipocytes were surrounded by peri-vascular cells that presented CD34⁺, CD68⁺, lectin⁺, acetylated low-density-lipoprotein uptake⁺, and CD133⁻ and, suggesting that those cells originated from circulating endothelial progenitor cells. Anti-VEGF treatment inhibited not only angiogenesis but also adipogenesis in the db/db mice, and local interplay among adipocytes and peri-vascular cells via hypoxia, reactive oxygen species production, and humoral factors including VEGF might play essential roles in adipocyte differentiation. In conclusion, our visualization technique provides evidence for the dynamic interactions between adipocyte differentiation and angiogenesis in living adipose tissue in obesity.

P90

DYNAMICS OF CORTICOSTEROID RECEPTORS AND IMPORTINS IN LIVING NEURAL CELLS AND NON-NEURAL CELLS

NISHI, M., FUJIKAWA, K., and KAWATA, M.

Department of Anatomy and Neurobiology, Kyoto Prefectural University of Medicine, Kyoto, Japan (nmayumi@koto.kpu-m.ac.jp)

Abstract: Glucocorticoid receptor (GR) and mineralocorticoid receptor (MR) are transcriptional factors, both of which are translocated from the cytoplasm to the nucleus upon ligand binding. Molecules less than 20-40 kDa can passively diffuse through the nuclear pore complex (NPC) from the cytoplasm to the nucleus, whereas more than 40 kDa are transported through gated-channels of the NPC by active mechanisms. Importin alpha and importin beta are docking proteins for karyopherin-mediated binding of substrate in a nuclear import pathway across the NPC. In the classical nuclear import pathway, importin alpha recognizes and binds to the nuclear localization signal on the cargo protein, and also binds to importin beta, which then docks the NPC and mediates translocation from the cytoplasm to the nucleus. In the present study, we investigated the trafficking of GR and MR, and importin alpha in living cultured hippocampal neurons and COS-1 cells with GFP color variants. We observed that GR and MR were translocated from the cytoplasm to the nucleus in association with importin alpha after ligand binding in living COS-1 cells and primary cultured hippocampal neurons, and found that there should be importin alpha subtype specificities in the nuclear translocation process. Furthermore, we examined the direct interaction of these receptors and importin alpha using fluorescent resonance energy transfer (FRET) technique.

Recent study suggested that importins in neuronal dendrites are involved in the signal translocation from the synapse to the distant nucleus to mediate synaptic plasticity. In this study, we also investigated how the intracellular signal molecules such as transcription factors in dendrites travel through the somatic cytoplasm to reach the nucleus. We examined intracellular trafficking of importin alpha 1, 2, 3 and 4 in living hippocampal neurons with GFP. Our data indicated that these importin alpha subtypes show differences in trafficking and distribution patterns in response to neural activity.

P91

DETECTION AND UTILITY OF TUMOR-SPECIFIC AUTO-ANTIBODY IN SERA OF PULMONARY CARCINOMA PATIENTS

NAGASHIO, R.^{1,2}, MATSUMOTO, T.^{2,3}, KAGEYAMA, T.^{2,3}, SATO, Y.^{2,3} and NAKAJIMA, T.¹

¹Dept. of Tumor Pathology, Gunma University Graduate School of Medicine, Maebashi, Japan; ²Dept. of Molecular Diagnostics, School of Allied Health Sciences, Kitasato University, Sagami-hara, Japan; ³Dept. of Molecular Diagnosis, Kitasato University Graduate School of Medical Science, Sagami-hara, Japan. (ryo1019@mug.biglobe.ne.jp)

Abstract: Purpose: Autoantibodies (AAs) are frequently detected in the sera of cancer patients. A correlation between autoantibodies and the presence and development of tumors has been reported. AAs may be useful for detecting novel sera-diagnostic markers of tumors. In this study, we investigated the presence of AAs in sera from pulmonary carcinoma patients and their utility was immunohistochemically studied with commercially available antibodies.

Materials and Methods: The presence of autoantibodies in 13 sera from pulmonary carcinoma patients was detected by immunoblotting using cell lysates of four cell lines ((LCN1; large cell neuroendocrine carcinoma (LCNEC), N231; small cell carcinoma (SCLC), A549; adenocarcinoma (AD) and RERF-LC-AI; squamous cell carcinoma (SQ)). To identify the antigen recognizing AA, two-dimensional gel electrophoresis was utilized. Two sets of gel, one stained with Coomassie Brilliant Blue (CBB) and the other transferred to PVDF membrane for immunoblotting, were prepared for each serum. After immunoblotting, target spots were picked up from the blotting membrane and/or gel with CBB staining. Then, spots were digested with trypsin and protein identified by mass spectrometry. Identified cytokeratin (CK) 18 and villin were further immunohistochemically confirmed by 124 formalin-fixed, paraffin-embedded pulmonary carcinomas and commercially available antibodies.

Results and Discussion: The presence of many AAs was observed in sera from pulmonary carcinoma patients. Each serum reacted with different proteins to various degrees. CK18 and villin were identified by in-gel and/or on-membrane digestion and mass spectrometry. Positive CK18 immunostaining was observed in almost all cases. On the other hand, villin was only detected in AD, 11/28 (39%) and LCNEC, 7/16 (44%). No positive reaction was detected in SCLC and SQ. Villin may be a useful marker to distinguish LCNEC and AD from SCLC and SQ. This method is simple and reliable to identify tumor-associated molecules in sera from cancer patients.

P92

HIGH RESOLUTION, HIGH SENSITIVITY BAC-FISH ANALYSES OF HUMAN CHROMOSOMES

WEIER, H.-U.G.¹, BAUMGARTNER, A.^{1,2}, ZENG, H.¹, LU, C.-M.^{1,3}, and WEIER, J.F.^{1,2}

¹Life Sciences Division, University of California, E.O. Lawrence Berkeley Natl. Lab., Berkeley, CA, USA; ²Dept. of Obstetrics, Gynecology & Reproductive Sciences, University of California, San Francisco, CA, USA, ³Dept. of Chemical & Material Engineering, National Chin-Yi Institute of Technology, Taichung, Taiwan, Department, ROC. (ugweier@lbl.gov)

Abstract: The detailed cytogenetic analyses of human tumors and cancer tissues, in particular, have revealed the presence of structural chromosome abnormalities in most of cases. The underlying changes are often specific for the type of tumor or cancer and the cells' altered phenotype. Furthermore, investigators could demonstrate a correlation between the type or the extent of chromosome changes, disease progression and outcome. However, many of the laboratory techniques applied in the screening for structural abnormalities are limited with respect to the detection of small, 'cryptic' translocations. For example, Giemsa (G) - banding of metaphase chromosomes or the fluorescence in situ hybridization (FISH)-based techniques of whole chromosome painting (WCP) and Spectral Karyotyping (SKY) analysis typically miss translocations that involve segments of less than 10 Mbp, i.e., about the size of a chromosome band.

Small translocations may exist undetected in the genomes of individuals with a normal phenotype or diseases such as mental retardation, impaired fertility, pre-cancerous lesions or early stage tumors. Knowledge about structural alterations and chromosomal imbalances might help clinicians to make more accurate predictions regarding the onset and course of a disease. We investigated the feasibility to rapidly and inexpensively screen the human genome for the presence of occult cryptic translocations (OCTs). Specifically, we began to develop and test FISH assays using collections of chromosome-specific bacterial artificial chromosomes (BACs) for the detection of OCTs in human cancer cells. With BAC probes spaced on average 0.9 Mbp apart and covering the entire euchromatic part of the human genome, we expect our 'BAC-FISH' assay to lead to greatly increased sensitivity compared to WCP or banding tests. This presentation outlines applications of our innovative assay for sensitive genome-wide screening for translocations with examples from cancer cell lines for which limited information about structural abnormalities is available.

P93

DETECTION OF TOTAL AND PHOSPHORYLATED VEGFR2/KDR IN CELLS AND TISSUES

CHANG, W.S.¹, KAHOU, N.S.¹, MAK, J.², BAGRI, A.² and PEALE, F.¹
Departments of ¹Pathology and ²Tumor Biology & Angiogenesis, Genentech, Inc. South San Francisco, CA 94080, USA. (wesc@gene.com)

Abstract: Recent progress in the development of novel therapeutic agents targeted against protein kinases for the treatment of certain kinds of cancers has led to increased demand for the ability to visualize phosphoproteins as markers of kinase activity *in situ*. Detection of the presence and/or absence of phosphorylated substrates in specific cell types could be used in the selection and enrollment of patients for targeted therapies, and could serve as markers of drug efficacy and pharmacodynamic activity. However, the highly dynamic nature of protein phosphorylation and dephosphorylation in cells and tissues imposes significant limitations on the ability to capture these events with a high degree of fidelity. The goal of this study was to assess the technical feasibility of detecting activated Vascular Endothelial Growth Factor Receptor 2 (VEGFR2) in frozen and fixed tissue specimens using immunohistochemical (IHC) localization with antibodies to phosphorylated VEGFR2 (pVEGFR2). A panel of cell lines expressing a range of VEGFR2 protein levels was characterized using flow cytometry, Western blot, ELISA and immunocytochemistry (ICC) with antibodies to total and pVEGFR2. These cell-based assays were used to (1) identify the most specific antibodies to pVEGFR2, (2) develop appropriate IHC staining procedures and (3) study the time course of VEGFR2 dephosphorylation after stimulation by VEGF-A. Frozen and formalin-fixed, paraffin-embedded (FFPE) cell pellets were prepared from control and VEGFR-stimulated cell lines to determine the level of VEGFR2 expression required for detection of pVEGFR2 using IHC. Frozen and fixed tissues from embryonic and adult mice, as well as normal and neoplastic human specimens, were stained with a variety of methods, with the goal of identifying the most sensitive, specific and reliable procedures for pVEGFR2 detection. Effects of different fixation, target retrieval, blocking and signal amplification strategies on pVEGFR2 detection, and the critical role of appropriate control experiments, will be presented.

P94

THE EXPRESSION OF FOXL2 IN HUMAN PITUITARIES

EGASHIRA, N.¹, TAKEI, M.², TERAMOTO, A.², OSAMURA, R.Y.¹¹Department of Pathology, Tokai University School of Medicine, Kanagawa, Japan;²Department of Neurosurgery, Nippon Medical School, Tokyo, Japan (egashira@is.icc.u-tokai.ac.jp)

Abstract: Many transcription factors play important roles in function and differentiation of the human pituitary adenomas. Forkhead box transcription factor L2, Foxl2, is expressed during mouse pituitary development and co-localizes with expression of the glycoprotein hormone α subunit (α GSU). In addition, FOXL2 regulates expression of the α GSU gene in cell culture. To elucidate the functional role of FOXL2 in human pituitary, we detected the localization and expression of FOXL2 in normal human pituitaries and various types of its adenomas. The human pituitary adenomas were obtained by trans-sphenoidal surgery from 66 patients. Two normal adult pituitaries were obtained from the autopsies of non-endocrine diseases. The localization of FOXL2 and pituitary hormones in these pituitary patients was studied by immunohistochemical staining. The quantitative analysis of FOXL2 protein was detected by using immunoblotting. FOXL2 was localized immunohistochemically in many of Gonadotropin producing adenomas, and in about 20% of normal pituitaries that also co-expressed α GSU. These results are consistent with the idea that FOXL2 plays a role in α GSU expression in human pituitary adenomas. Future studies with gain and loss of function animal models will be important to assess the function of FOXL2 in establishing and maintaining differentiated α GSU expressing cells.

P95

THE IMPROVEMENT OF IMMUNOHISTOCHEMICAL DETECTION FOR PITUITARY TRANSCRIPTION FACTOR IN HUMAN PITUITARY ADENOMA

KAJIYA, H.¹, TAKEKOSHI, S.¹, MINEMATSU, T.¹, EGASHIRA, N.¹, TAKEI, M.^{1,2}, TERAMOTO, A.², OSAMURA, R.Y.¹

¹Department of Pathology, Tokai University School of Medicine, Kanagawa, Japan;

²Department of Neurosurgery, Nippon Medical School, Tokyo, Japan. (hanakoki@is.icc.u-tokai.ac.jp)

Abstract: The functional development of pituitary adenoma may depend on the expression of a combination of transcription factors and co-factors. Immunohistochemical methods were examined for their intensity in the detection of nuclear antigens, pituitary transcription factors (Pit-1, Prop-1, DAX1, NeuroD1, Tpit, GATA-2, SF1) in formaldehyde-fixed and paraffin-embedded human pituitary adenoma. Deparaffinized sections were treated for some heating antigen retrieval method (Microwave heating or autoclave heating) in buffers with different pH values ranging from 3.0 to 9.0. For immunostaining determination, enzyme polymer method and biotin avidin enhanced peroxidase (ABC) method were used. The result of fixation method demonstrated that 10% formalin gave good result for detecting pituitary transcription factors. Further, the ABC method performed using autoclave treatment (121°C for 5min) under these optimal conditions may be potentially applicable for detecting pituitary transcription antigens. But there were immunostaining patterns for pH dependency in heat-induced antigen retrieval which may have related in each antigen's isoelectric point.

P96

DIFFERENTIAL EXPRESSION OF BARRIER-TO-AUTOINTEGRATION FACTOR IN PAPILLARY THYROID CARCINOMA CELLS

MURATA, S.¹, OHNO, N.², TERADA, N.², HARAGUCHI, T.³, IWASHINA, M.¹, MOCHIZUKI, K.¹, NAKAZAWA, T.¹, KONDO, T.¹, NAKAMURA, N.¹, YAMANE, T.¹, IWASA, S.¹, OHNO, S.², AND KATO, R.¹

¹Dept of Human Pathology; ²Dept of Anatomy, University of Yamanashi, Yamanashi, Japan; ³CREST Research Project of the Japan Science & Technology Corp, Kansai Advanced Research Ctr, Communications Research Lab., Kobe, Japan (smurata@yamanashi.ac.jp)

Abstract: Background: Characteristic nuclear feature such as irregular nuclear contour, nuclear grooves, and pseudoinclusions of papillary thyroid carcinoma (PTC) cells is one of criteria in pathological diagnosis. Morphogenesis of the nuclear feature, however, has not been clear. Recently, it was found that barrier-to-autointegration factor (BAF), which bridged between double-stranded DNA molecules and inner nuclear membrane proteins carrying LEM domains, was related to nuclear assembly. To clarify the morphogenesis of the characteristic nuclear features of PTC, we studied the differential expression of BAF in PTC cells.

Materials and Methods: We studied 10 normal thyroids (NT), 4 adenomatous nodules (AN), 6 PTC, which were surgically resected in our university hospital. BAF and Emerin or LAP2 were double-stained using rhodamine-labeled anti-BAF antibody and FITC labeled anti-Emerin or anti-LAP2 antibodies. We took digital images of total 2545 double-stained cells of NTs, ANs and PTCs using laser confocal microscopy and quantitatively analyzed the images by texture analysis. [Results] BAF expression was found in the cytoplasm and intranuclear regions as well as nuclear membrane of the PTC cells, whereas NT and AN cells showed the expression of BAF mainly in the nuclear membrane. On the other hand, Emerin and LAP2 were mainly detected at the nuclear membrane in PTCs cells as well as NT and AN cells. More than half benign and malignant cells showed lower expression of BAF than LAP2 or Emerin, however, in PTCs, cells with higher expression of BAF than LAP2 or Emerin significantly increased in number. Texture analysis showed that BAF expression of papillary carcinoma cells has more heterogeneous spacial distribution on nuclear membrane than that of the benign group.

Conclusion: The differential BAF expression may play an important role in the morphogenesis of the characteristic nuclei of papillary carcinoma cells.

P97

LOW COPY DNA REPEATS ON HUMAN CHROMOSOME 1

ZENG, H.¹, GUAN, J.¹, LU, C.-M.¹, BAUMGARTNER, A.^{1,2}, WEIER, J.F.^{1,2}, and WEIER, H.-U.G.¹

¹Life Sciences Division, University of California, E.O. Lawrence Berkeley Natl. Lab., Berkeley, CA, USA; ²Dept. of Obstetrics, Gynecology and Reproductive Sciences, University of California, San Francisco, CA, USA. (HZeng@lbl.gov)

Abstract: Our laboratory is interested in the oncogenic properties of acquired chromosomal changes in tumors of the thyroid gland, especially childhood papillary thyroid cancers (chPTC) that arose in the years following the Chernobyl nuclear accident in 1986. One of the cell lines in our lab., S48TK, forms rapidly growing tumors in nude or SCID mice. A cytogenetic and molecular genetics analysis of this line is complicated by a large number of unbalanced chromosomal rearrangements. In this cell line, results from Spectral Karyotyping (SKY) and comparative genomic hybridization (CGH) experiments suggested several aberrant chromosomes with breakpoints on the long arm of chromosome 1. Our efforts to map bacterial artificial chromosome (BAC) clones on the proximal long arm of chromosome 1 revealed a region at 1q21, which showed significant levels of homology with regions on chromosome 1p12 and 1p36. Interestingly, all three regions are known to be involved in rearrangements in a variety of solid tumors among them neuroblastoma, breast and thyroid cancers. DNA sequence analyses and DNA sequences database searches using BLAST pointed to a group of low copy number repeats (LCR's) shared by the cross-hybridizing BAC clones. This presentation summarizes approaches and results from our molecular cytogenetic as well as bioinformatics experiments, and discusses the observed chromosomal changes and sequence homologies on their evolutionary context.

P98

USEFULNESS OF HNF-1 β AS AN IMMUNOCYTOCHEMICAL DIAGNOSTIC MARKER OF OVARIAN CLEAR CELL ADENOCARCINOMA IN ASCITES SPECIMENS

HIGASHIGUCHI, A.¹, SUZUKI, A.¹, HIRASAWA, A.¹, TAMADA, Y.¹, SUSUMU, N.¹, SUZUKI, N.², AOKI, D.¹ and SAKAMOTO, M.³

¹Department of Obstetrics and Gynecology, School of Medicine, Keio University, Tokyo, Japan; ²Department of Obstetrics and Gynecology, St. Marianna University School of Medicine, Kawasaki, Japan; ³Department of Pathology, School of Medicine, Keio University, Tokyo, Japan (kmog76ha@mub.biglobe.ne.jp)

Abstract: Objective: Hepatocyte nuclear factor-1 β (HNF-1 β) is specifically expressed in clear cell adenocarcinoma (CCC). The aim of this study is to investigate the usefulness of HNF-1 β as an immunocytochemical diagnostic marker of CCC in ascites specimens, and as a critical determinant in the prognosis of CCC cases.

Methods: (1) Real time PCR was used to quantify HNF-1 β mRNA in ovarian carcinoma surgical specimens. (2) Immunostaining using anti-HNF-1 β antibody was performed on surgically-sampled ascites specimens and surgically-resected specimens of ovarian carcinoma. These specimens were classified into six categories based upon the percentage of HNF-1 β positive cells among all observed malignant cells in the specimen (maximum staining:5, no staining:0). (3) Double immunocytochemical staining using anti-HNF-1 β antibody and HBME-1, a specific marker of mesothelium, was performed on ascitic cytological specimens of CCC cases and an in vitro sample of a CCC cell line mixed with cultured mesothelial cells. The clinical portions of this study were approved by the ethics committee of Keio University.

Results: (1) HNF-1 β presented with statistically higher expression levels in CCCs than in other non-CCC specimens (Mann-Whitney's U test, $P < 0.05$). (2) Immunostaining scores of CCC cases (median:4) were significantly higher than the immunostaining scores from serous adenocarcinoma cases (median:0), mucinous adenocarcinoma cases (median:0), and endometrioid adenocarcinoma cases (median:0) ($P < 0.05$). Immunostaining patterns of HNF-1 β in cytological specimens were similar to those observed in the histopathological ovarian specimens from the same patients. (3) Double immunocytochemical staining revealed HNF-1 β immunopositivity only within the nuclei of CCC cells, whereas HNF-1 β staining was negative in the nuclei of mesothelial cells, which were determined by specific positive cytoplasmic staining with HBME-1.

Conclusions: Our results demonstrate possible clinical applications of HNF-1 β immunocytochemical staining in the differential cytopathologic diagnosis of CCC from non-CCC as well as from mesothelial cells in cytological specimens from ovarian carcinoma patients.

P99

A MOLECULAR CORRELATE TO THE GLEASON GRADING SYSTEM FOR PROSTATE ADENOCARCINOMA

TRUE, L.^{1,2}, COLEMAN, I.³, HAWLEY, S.⁴, HUANG, A.³, GIFFORD, D.³, COLEMAN, R.³, BEER, T.⁶, GELMANN, E.⁷, DATTA, M.⁸, MOSTAGHEL, E.^{3,5}, KNUDSEN, B.⁴, LANGE, P.², VESSELLA, R.², LIN, D.², HOOD, L.⁹, and NELSON, P.^{1,2,3,5}

Depts. of ¹Pathology, ³Urology, ⁵Medicine (Oncology) Univ. of Washington; Div's. of ²Human Biology & Clinical Research; ⁴Public Health Sciences, Fred Hutchinson Cancer Research Ctr.; ⁶Dept. of Medicine (Oncology), Oregon Health Sciences Ctr.; ⁷Dept. of Medicine (Oncology), Georgetown University; ⁸Dept. of Pathology, Emory Univ., Atlanta, GA.; ⁹Inst. for Systems Biology, Seattle, WA (ltrue@u.washington.edu)

Abstract: Adenocarcinomas of the prostate can be categorized into tumor grades based upon the extent to which the cancers histologically resemble normal prostate glands. Since grades are surrogates of intrinsic tumor behavior, characterizing the molecular phenotype of grade is of potential clinical importance. To identify molecular alterations underlying prostate cancer grades, we used laser microdissection to obtain specific cohorts of cancer cells corresponding to the most common Gleason patterns (patterns 3, 4, and 5) from frozen sections of 29 radical prostatectomy samples. We paired each cancer sample with matched benign luminal prostate epithelial cells and profiled transcript abundance levels by microarray analysis using custom, cDNA arrays of 20,000 and 18,000 genes following linear amplification of mRNA. We identified 736 genes with altered expression levels between benign and neoplastic epithelium (false-discovery rate <0.01%). Some of these genes (hepsin, alpha methyl coA racemase) have previously been reported to be overexpressed in prostate cancer. Of this set of genes, we then identified an 86-gene model capable of distinguishing low grade (pattern 3) from high grade (pattern 4 and 5) cancers. This model performed with 76% accuracy when applied to an independent set of frozen sections from 30 primary prostate carcinomas. Using tissue microarrays comprised of >800 prostate samples we confirmed a significant association between high levels of Monoamine Oxidase A expression and poorly differentiated cancers by immunohistochemistry. We also confirmed grade-associated levels of Defender against Death (DAD1) protein and HSD17β4 transcripts by immunohistochemistry and quantitative RTPCR, respectively. The altered expression of these genes provides functional insights into grade-associated features of therapy resistance and tissue invasion. Furthermore, in identifying a profile of 86 genes that distinguish high from low-grade carcinomas, we have generated a set of potential targets for modulating the development and progression of the lethal prostate cancer phenotype.

P100

ESTABLISHMENT OF NEW DIAGNOSTIC MARKER PEPTIDES FOR NEUROENDOCRINE TUMOR OF THE LUNG

MATSUMOTO, TOSHIHIDE¹, NAGASHIO, RYO^{2,3}, KAGEYAMA, TAIHEI¹, SATO, YUISHI^{1,3}, KAMEYA, TORU⁴

¹Dept. of Molecular Diagnosis, Kitasato University Graduate School of Medical Science, Sagami-hara, Japan; ²Dept. of Tumor Pathology, Gunma University Graduate School of Medicine, Maebashi, Japan; ³Dept. of Molecular Diagnostics, Kitasato University School of Allied Health Sciences, Sagami-hara, Japan; ⁴Division of Pathology, Shizuoka cancer center, Shizuoka, Japan, (mm05041e@st.kitasato-u.ac.jp)

Abstract: PURPOSE: Pro-gastrin-releasing peptide (proGRP) is a specific tumor marker peptide in patients with small cell lung carcinoma (SCLC). Large cell neuroendocrine carcinoma of the lung (LCNEC) is the latest member of neuroendocrine carcinoma of the lung. To generate a new specific marker for LCNEC, conditioned medium from LCN1 cells derived from LCNEC was used. We report here that a new neuroendocrine tumor marker different from proGRP was picked up from the conditioned medium of LCN1 cells.

METHODS: An LCN1 sub-line grown on serum-free medium was established. Conditioned medium from LCN1 cells was separated into fractions by reverse-phase high performance liquid chromatography (RP-HPLC). Peptide peaks in the fractions were measured by matrix-associated laser desorption/ionization time of flight mass spectrometry (MALDI-TOF-MS), and proteins were identified by tandem mass spectrometry (MALDI-TOF/TOF-MS). The mRNA expression level of this molecule was detected by RT-PCR and *in situ* hybridization (ISH).

RESULTS and DISCUSSION: Specific peaks in conditioned medium but not in used medium were found by MALDI-TOF-MS. These peaks were then analyzed by MALDI-TOF/TOF-MS, and determined as a fragment of protein existing only in neurons and neuroendocrine cells. The mRNA expression of this molecule was detected in all SCLC and LCNEC cell lines to various degrees. In addition, no expression of this molecule was detected in non-small cell lung carcinoma cell lines. We are now developing antibodies for this molecule. This peptide may be a useful sero-diagnostic marker of neuroendocrine tumor of the lung.

P101

UTILITY OF LC-1 ANTIBODY WHICH REACTS WITH CARCINOMA CELLS AND CANCER STROMAL FIBROBLASTS OF THE LUNG

SATO, Y.^{1,3}, NAGASHIO, R.^{1,2}, MATSUMOTO, T.³, KAGEYAMA, T.³

¹Department of Molecular Diagnostics, School of Allied Health Sciences, Kitasato University, Sagamihara, Japan; ²Department of Tumor Pathology, Gunma University Graduate School of Medicine, Maebashi, Japan; ³Department of Molecular Diagnosis, Kitasato University Graduate School of Medical Science, Sagamihara, Japan, (yuichi@med.kitasato-u.ac.jp)

Abstract: Purpose: The post-translational modification of proteins cannot be predicted from their DNA sequences. For the production of monoclonal antibodies (MoAbs) for proteins with tumor-associated post-translational modifications, they were generated using AMeX-fixed lung cancer cell lines as the immunogen instead of purified peptides. We present here an LC-1 antibody which reacts with tumor cells and their cancer stromal fibroblasts of pulmonary carcinomas.

Materials and Methods: MoAb, LC-1 was established by immunization with AMeX-fixed LCN1 cells derived from pulmonary large cell neuroendocrine carcinoma (LCNEC) and immunohistochemical screening with the same AMeX-fixed cell preparations. The utility of the established LC-1 was confirmed by immunostaining of 74 cases of formalin-fixed and paraffin-embedded pulmonary carcinomas (42 adenocarcinoma, 24 squamous cell carcinoma, 4 large cell carcinoma, 2 small cell carcinoma, 2 LCNEC). Reactivity for 14 sera from patients with pulmonary carcinomas and four healthy donors was also studied. Antigenic protein was determined by 2-dimensional gel electrophoresis and mass-spectrometry.

Results and Discussion: On screening, LC-1 antibody showed cytoplasmic staining in a few LCN1 cells. For immunohistochemistry, almost all pulmonary carcinomas showed cytoplasmic staining in tumor cells and cancer stromal fibroblasts to various degrees. No staining was observed in peripheral lung tissues. LC-1 antibody also reacted with 11 of 12 sera from pulmonary carcinoma patients, but not from healthy donors. Protein recognized by LC-1 antibody was of epithelial cell origin and was localized in special epithelial cells. No study has been reported considering this molecule and tumors. LC-1 is a useful diagnostic marker for early pulmonary carcinomas.

P102

ELEVATED EXPRESSION OF FATTY ACID SYNTHASE (FAS) IN HUMAN ABERRANT CRYPT FOCI (ACF)

PRETLOW, THERESA P., KEARNEY, KATHLEEN E. and PRETLOW, THOMAS G.

Institute of Pathology, School of Medicine, Case Western Reserve University, Cleveland, Ohio, U.S.A. (theresa.pretlow@case.edu)

Abstract: Aberrant crypt foci (ACF), the earliest identified neoplastic lesions in the colon, provide insights into changes that promote and/or accompany the transformation of normal cells to cancer. Fatty acid synthase, the primary enzyme involved in de novo lipogenesis from carbohydrates, is expressed at low levels in most normal human tissues but is elevated in several human neoplasms including colorectal adenomas and carcinomas. To test if this pathway is altered even earlier in the tumorigenic process, 35 human ACF from 21 patients with colon cancer or familial adenomatous polyposis were evaluated for the expression of fatty acid synthase. Paraffin-embedded sections, 5 µm in thickness, were incubated with rabbit polyclonal antibodies (Assay Designs Inc, Ann Arbor, MI) at 1:100 and 1:200 dilution after antigen retrieval in 0.1 M Tris buffer at pH 8.6 at full pressure for 5 min in a pressure cooker. The location of fatty acid synthase was visualized by the addition of biotinylated goat antirabbit IgG, followed by streptavidin-biotinylated horseradish peroxidase and 3,3'-diaminobenzidine. Of these 35 ACF, 30 (86%) had increased expression of fatty acid synthase compared to adjacent normal colonic mucosa. Sections of colon cancer served as positive controls, and normal colonic mucosa distant from cancer or ACF served as negative controls. The expression of fatty acid synthase in ACF was not related to the degree of dysplasia or to the number of crypts in the ACF. The high proportion of ACF over expressing fatty acid synthase suggests this enzyme plays an important role very early in colon tumorigenesis and/or may provide unique insights into the neoplastic process. Supported in part by NIH grants CA66725 and CA43703.

P103

MULTI-DIMENSIONAL STROMAL-COLON CANCER CO-CULTURES: DEVELOPING MODELS FOR DRUG RESPONSE.

DAWSON, D.M.¹, CHASE, R.M.², NAVARRE, W.³

¹Case Western Reserve University/University Hospitals of Cleveland, Institute of Pathology, Cleveland, OH, USA; ²Case Western Reserve University, Department of Hematology/Oncology, Cleveland, OH, USA; ³John Carroll University, University Heights, OH, USA.

Abstract: Background: Developing cost-effective predictive in vitro and in vivo preclinical models to assess treatment outcome is critical to the process of optimizing targeted and specific chemotherapy for epithelial cancers. Xenograft systems have failed to accurately predict response and standard two dimensional monocultures do not incorporate key stromal components.

Methods: To determine the effects stromal elements on colon epithelium, 2D and 3D cultures of five unique benign and malignant colon cell lines with and without fibroblasts (WI-38). Cultures were treated with small molecule inhibitors (AG879 and AG 1478) targeting EGFR and erbB2 respectively. Immunocytochemistry was performed for key activated proteins in proliferation, apoptosis and transdifferentiation markers for myofibroblasts (□smooth muscle actin).

Results: Differential □smooth muscle actin expression at the stromal-epithelial cell interface between the cell lines was noted that could be obliterated with the small molecule inhibitors in a dose dependant manner in both 2D and 3D cultures. There was focal upregulation of EGFR and erbB2 in the presence of fibroblasts. The effect of inhibitors on proliferation and cell death was diminished in co-cultured cell lines.

Conclusions: Smooth muscle actin expression can be induced in fibroblasts with neoplastic colon cell lines. This transdifferentiation may reflect the erbB receptor profile in the individual cell lines and is variably receptive to inhibitors. The presence of stromal elements in epithelial cultures may protect the cells from chemotherapeutic agents. Both 2D and 3D co-cultures can be used as a useful first step and intermediate model to study differential drug response.

P104

ANALYSIS OF FHIT GENE EXPRESSION AND LOSS OF HETEROZYGOSITY IN COLONIC MUCOSA OF IBD AND COLORECTAL CARCINOMA PATIENTS

WIERZBICKI, P.¹, KARTANOWICZ, D.¹, STANISLAWOWSKI, M.¹, WIERZBICKI, M.¹, SOKOLOWSKA, I.¹, ADRYCH, K.², WYPYCH, J.², SMO CZYNSKI, M.², MYSLIWSKI, A.¹, KMIEC, Z.¹

¹Dept. Histology&Immunology ²Dept. Gastroenterology&Hepatology, Medical University of Gdańsk, Gdańsk, Poland

Abstract: Ulcerative colitis (UC) and Crohn's disease, main entities of Inflammatory Bowel Disease (IBD), predispose to colorectal cancer (CRC). The aim of the study was to assess mRNA level of the *fhit* gene and its loss of heterozygosity (LOH) in colonic biopsies of 83 UC, 5 CD, and in 26 CRC adult patients because of *fhit* gene's putative role in the suppression of carcinogenesis. The comparison were made between altered and unaltered mucosal tissue taken from the same patient. For the LOH analysis of *fhit* gene we used 3 pairs of microsatellite markers: D3S1300 D3S1481 and D3S1234. LOH analysis was made in Sequi-Gen Sequencing Cell (Bio-Rad) and the peak intensity was measured using Quantity One software (Bio-Rad). mRNA content was measured by the Real-Time PCR in iQ Cycler (Bio-Rad). Level of *fhit* mRNA was β -actin expression. The presence of FHIT protein in biopsies was assessed by IHC using goat polyclonal antibody (Zymed Lab.). In UC patients we observed general tendency into lowering of *fhit* mRNA content ($p=0,084$). However, in altered mucosal biopsies of 5 CD patients we found increased *fhit* gene. Surprisingly, we found increased level of *fhit* mRNA in CRC ($p=0,045$), confirmed also by IHC in 3/5 assessed tumors. Moreover, the expression ratio was much higher in samples taken from inside the tumor than from its periphery. There was no correlation between LOH and *fhit* mRNA levels in UC, CD and CRC patients. No correlation was found between mRNA level and TMN stage or location of the tumor. The intensity of FHIT protein staining in colonic crypts was lower in the altered mucosa of UC patients. In conclusion, we found opposite expression of the *fhit* gene in CRC and UC patients. Further studies, including hypermethylation analysis of promoter region and sequencing of transcripts will be performed to explain these observations.

P105

EXPRESSION OF SECRETORY PHOSPHOLIPASE A2 MRNA AND PROTEIN IN THE ORAL MUCOSAL DISORDER RELATED TO DENDRITIC CELL MIGRATION.

KOMIYAMA, K.¹, TSURUTA, T.², MUKAE, S.¹, and OKAZAKI, Y.¹

¹Department of Pathology and ²Oral and Maxillofacial Surgery, Nihon University School of Dentistry, Japan. (Komiya@dent.nihon-u.ac.jp)

Abstract: This study designed to elucidate a role of the arachidonic pathway in oral mucosal disorder. Oral mucosal disorder such as dysplasia, precancerous lesion, particular oral lichen planus, characterized numerous DC cell migration into the epithelium. DC cell conducts Th1 and CD8 cells band like infiltration indicated in degeneration of the basement membrane. However, precise mechanism of DC cell migration and functions were not fully characterized yet. We hypothesize epithelial cell synthesize sPLA2 and COX2 result in PGE2 production that induced DC cell maturation in situ. Immunohistochemical analysis of sPLA2 (-IIa, -V, -X), COX2 and s100 were performed 45 cases of oral mucosal disorder including dysplasia (20 case), OLP (15cases), oral cancer (20 case) as well as normal control. In addition, sPLA2 (-IIa, -V, -X) mRNA expression of the mucosal epithelium was identified by in situ hybridization. By immunohistochemistry and in situ hybridization, the epithelial cell of oral mucosal disorder preferentially expressed sPLA2-V and -X, while sPLA-IIa was not identified. Both enzymes were mainly identified in the basal and its above layers. Over expression of COX2 was observed in 80 % of examined oral mucosal disorder and found mostly in the prickle cell layer but not in the basal layer. These sPLA2 and COX2 over expressions were correlated to the number of DC cells migration to the epithelium. As the results, sPLA2 and COX2 localized in the epithelium indicated PGE2 synthesize at the site, which contribute DC cell migration and maturation in the oral epithelium. Over expression of both enzymes may play an important role for developments oral mucosal disorder.

P106

AGLYCONIC MUCIN CORE PROTEINS IN A CASE OF EXTRAMAMMARY PAGET'S DISEASE

SMITH, R. F. and SMITH, A.A.

*School of Graduate Medical Sciences, Barry University, Miami Shores, Florida, USA.
(asmith@mail.barry.edu)*

Abstract: Extramammary Paget's disease is a rare cancer in which the cancer cells are scattered singly in the affected epidermis. These cancer cells contain mucins, which are never found in normal epidermal cells. Many (~50%) of the oligosaccharide side chains of Paget cell mucins end with sialic acid, which is easily detected by zirconyl hematoxylin or alcian blue. The sugars in the oligosaccharide chains can be detected by the periodic acid-Schiff reaction.

Rarely, the diagnosis of extramammary Paget's disease is complicated by the absence of mucin from the Paget cells. We have examined such a case. All of the oligosaccharide side chains, including the sialic acids, are absent. The Paget cells stain with neither zirconyl hematoxylin, nor alcian blue, nor the periodic acid-Schiff reaction. Nevertheless, many of the Paget cells contain gastric surface type mucin (epithelial mucin 5AC) and epithelial membrane antigen (epithelial mucin 1) core proteins, which can be stained by labelled antibodies. Thus, immunohistochemical detection of mucin core proteins may be more reliable than tinctorial detection of mucins in the diagnosis of extramammary Paget's disease.

Our results also show that membrane and secretory proteins are not necessarily glycosylated. Whether this is due to the absence of glycosylation at the beginning of protein synthesis or deglycosylation after synthesis remains to be seen.

P107

SSTR2A IS EXPRESSED IN CLINICALLY NON-FUNCTIONING PITUITARY ADENOMAS.

TAKEI, MAO^{1,2}, KAJIYA, HANAKO², MINEMATSU, TAKEO², EGASHIRA, NOBORU², TAKEKOSHI, SUSUMU², TAHARA, SHIGEYUKI¹, TERAMOTO, AKIRA¹ and OSAMURA, ROBERT Y.²

¹Department of Neurosurgery, Nippon Medical School, Tokyo, Japan, and ²Department of Pathology, Tokai University School of Medicine, Kanagawa, Japan, (s3062@nms.ac.jp)

Abstract: Octreotide, which is one of the somatostatin analogues and mainly interact with somatostatin receptor (SSTR) subtype 2A, is useful for treatment for the patients with GHoma and TSHomas. The aim of this study is to elucidate the expression of SSTR2A in the clinically non-functioning adenomas (NFA) in order to explore the possibility of the targeted therapy with Octreotide. Total 30 cases of the NFA (20 cases of gonadotropin-producing adenomas; Gn-omas, 5 cases of null cell adenomas; NCA, 5 cases of silent somatotroph adenomas; SSA) were subjected to immunohistochemical study and mRNA analysis. The immunoreactivity for SSTR2A on each section was scored according to the percentage of immuno-positive cells and intensity of reaction. The expression levels of SSTR2A mRNA in the NFAs were quantified by real time RT-PCR and then compared with those of GHomas. Immunohistochemically, SSTR2A was interpreted positive when it is localized on the cell membrane. Both immunohistochemistry and real time RT-PCR indicated that the average levels of SSTR 2 expressions in NFA were lower than those of GHoma. However, the percentage of SSA with high expression of SSTR2A was approximately 70%, similar to GHoma. In Gn-oma and NCA, although the percentage of SSTR 2A-positive cases were lower, a few cases highly expressed SSTR 2A. These results suggested that Octreotide is useful for the treatment of SSA as well as GHoma. Furthermore, SSTR2A may be also a candidate for target therapy in some Gn-oma and NCA. Thus, the detection of SSTR2A is recommended in NFAs.

P108

COMPUTERIZED MORPHOMETRIC ANALYSIS OF IMMUNOSTAINED PRION PROTEIN IN TISSUES AND CELLS

MAXIMOVA, O.A.¹, POMEROY, K.L.¹, VASILYEVA, I.², BACIK, I.¹, JOHNSON, B.¹, TAFFS, R.E.¹, CERVENAKOVA, L.², PICCARDO, P.¹, and ASHER, D.M.¹

¹Center for Biologics Evaluation and Research, US Food and Drug Administration, Rockville, MD, USA; ²The Jerome Holland Laboratory, American Red Cross, Rockville, MD, USA. (olga.maximova@fda.hhs.gov)

Abstract: Transmissible spongiform encephalopathies (TSEs or prion diseases) are characterized by a constellation of typical though variable pathological changes in the brain. Deposition of disease-associated abnormal prion protein (PrP^{TSE}) is the pathological feature of TSEs most consistent and accessible for quantification. However, the evaluation of PrP^{TSE} deposits detected by immunohistochemical techniques has been traditionally based on arbitrarily assigned semiquantitative scores. This approach is limited by its subjectivity and bias, yielding considerable variability. We developed a computerized morphometric analysis (CMA) that allowed unambiguous detection of even minimal amounts of immunostained PrP^{TSE} in CNS of hamsters infected with the 263K strain of scrapie agent. CMA values correlated well with semiquantitative scores, providing reproducible quantitative data and objective criteria for analyzing PrP^{TSE} deposition. CMA of PrP^{TSE} immunostaining might be of great practical help to improve diagnoses of TSEs and help to assure the suitability of potential donors of human cadaveric tissues and sources of animal tissue used as ingredients and reagents in the manufacture of biological products. There is a theoretical risk that TSE agents (prions) might accidentally contaminate cell substrates used to prepare biological products. We are using PrP immunohistochemistry, CMA and other immunodetection assays to investigate the ability of cell lines relevant for manufacture of biologics to propagate TSE agents. To date, we have detected normal PrP^C in all cell lines under study using antibodies to various PrP epitopes but no PrP^{TSE} in cell cultures exposed to any TSE inoculum tested at passage levels up to 30. To assure safety further, we will perform infectivity bioassays with transgenic mice and squirrel monkeys and apply CMA of immunostained PrP to evaluate their tissues. CMA provides a simple and reliable method for improved and consistent diagnosis of TSEs that may also be used to quantify other immunostained biomarkers.

P109

FEASIBILITY STUDY FOR AUTOMATING MULTI-TARGETED COLORIMETRIC MOLECULAR HISTOCHEMICAL PROTOCOLS FOR HER-2 DIAGNOSIS

NITTA, HIROAKI¹, FARRELL, MICHAEL¹, KERNAG, CASEY¹, ASHWORTH-SHAPE, JULIA¹, BIENIARZ, CHRISTOPHER¹, CARPENTER, ANNE¹, PESTANO, GARY A.¹, WALK, ERIC¹, MILLER, PHIL¹, and GROGAN, THOMAS M.^{1,2}

¹R&D Discovery, Ventana Medical Systems, Inc., ²Department of Pathology, The University of Arizona, Tucson, Arizona, USA. (hnitta@ventanamed.com)

Abstract: HER-2 immunohistochemistry (IHC) and fluorescent *in situ* hybridization (FISH) are methods for evaluating patient eligibility for Herceptin[®] (trastuzumab) therapy. IHC assays evaluate protein expression levels while FISH assays assess HER-2 gene numbers. In contrast to the IHC method, FISH is complex, time consuming, and requires a darkroom for reading the slides. Automation of colorimetric co-visualization of HER2 gene copy and protein levels on the same slide would provide a standardized, reproducible, and easier to execute diagnostic test for Herceptin[®] eligibility. Our objective was to conduct feasibility studies for automating colorimetric detection of HER2 gene and protein on the same slide. ISH was performed with HER2 probe alone or a combination of HER2 and chromosome 17 probes. IHC was evaluated with the rabbit monoclonal anti-HER2 antibody (clone 4B5). Assays were conducted on formalin-fixed paraffin embedded (FFPE) tissue sections of cell line xenografts, MCF7 (normal HER2 gene and HER2 protein level 0), ZR-75-1 (normal HER2 gene and HER2 protein level 1), and BT-474 (amplified HER2 gene and HER2 protein level 3). All experiments were fully automated on the Ventana BenchMark[®] XT. Signal detection for IHC and ISH was performed with HRP or AP conjugated goat anti-mouse or rabbit antibodies. An optimized protocol was completed in less than 8 hours. Reproducible detection of single copies of HER2 gene in MCF tumor without any signal amplification steps was obtained with 2 hour hybridization. Level 1 HER2 protein and single HER2 genes were co-localized in ZR-75-1 tumors while level 3 HER2 protein and amplified HER2 genes were stained in BT-474 tumors. Triple staining of HER2 gene and protein with chromosome 17 was also possible within the FFPE xenografts. We have demonstrated a successful and sensitive automated protocol for simultaneously detecting HER2 genes, chromosome 17 centromeres, and HER2 proteins on a single glass slide.

P110

EVIDENCE FOR HIV TRANSGENE MODULATION AND IMMUNOCYTOCHEMICAL LOCALIZATION IN A HIV-1 MODEL OF AIDS

DENARO, F.J.^{1,4}, MAZZUCHELLI, R.^{2,3}, CURRELI, S.², BRYANT, J.⁴, RIVA, A.³, GALLI, M.³, GALLO, R.C.², and ZELLA, D.²

¹Morgan State University, Baltimore MD ²Division of Basic Science, Institute of Human Virology, University of Maryland, Baltimore MD, USA; ³Laboratory of the Institute of Infectious Diseases and Tropical Medicine, University of Milan, Italy; ⁴Animal Model Division, Institute of Human Virology, Baltimore, MD, USA (Denaro@umbi.umd.edu)

Abstract: HIV associated neuropathology, and neurological symptoms are some of the most severe symptoms of AIDS. Even HAART treatment is not completely successful in treating them. The mechanism by which HIV causes disease is poorly understood. But, current clinical studies strongly support the toxic effects of HIV gene products (ie TAT, GP-120, Nef). To understand this aspect of AIDS pathophysiology new animal models are required. Preferably a small, non-infectious model would be ideal for neurological studies. This has led to transgenic mouse development. However the levels of these molecules are very low in existing transgenic mouse models. In addition, the levels cannot be influenced by immune status. Therefore, very few models satisfy the requirements of being able to study neurology, neuropathology, behavior, immune modulation and viral molecular biology in a single model. A new transgenic model is now available which is easily maintained, a good size for chronic studies and is non-infectious. This model is the HIV-1 Transgenic rat. Moreover, the TAT gene and other viral genes respond to immune activation by altering their levels. In the HIV-1 Transgenic rat LPS stimulation can cause monocytes to up-regulate TAT. This results in a cascade effect in which the other viral transgenes such as NEF and GP-120 respond by up-regulation. Moreover, inflammatory cytokines levels increase. Because of the ability to modulate the level of these factors in the HIV-1 TG rat, it will be possible to correlate these substances to HIV associated neuropathology. It has been possible to identify the transgene products by immunocytochemistry. Gp-120, TAT and Nef have been identified in immune cells in the brain and other tissues such as kidney, heart, skin, spleen and lymph nodes. The capacity to modulate HIV transgenes and protein levels, together with the ability to immunocytochemically identify the transgene products, is an important experimental advantage.

P111

X-CHROMOSOME INACTIVATION IN INVASIVE CYTOTROPHOBLASTS FROM HUMAN PLACENTA

WEIER, J.^{1,2}, NGUYEN, H.¹, MAK, W.³, FERLATTE, C.¹,
BAUMGARTNER, A.^{1,2}, WEIER, H.² and FISHER, S.^{1,4,5}

¹Dept. Ob/Gyn & Reproductive Sciences, University of California, San Francisco, CA; ²Life Sciences Division, E.O. Lawrence Berkeley National Laboratory, Berkeley, CA; ³Dept of Ob/Gyn, Cedars-Sinai Medical Center, Los Angeles, CA; ⁴Dept. of Cell & Tissue Biology, UCSF; ⁵Dept. Anatomy & Pharm. Chem., UCSF, USA. (weierj@obgyn.ucsf.edu)

Abstract: Human cytotrophoblasts (CTBs) acquire aneuploidies when the cells invade the uterine wall during the early stages of pregnancy. Fluorescence in situ hybridization (FISH) with DNA probes specific for chromosomes 16, X and Y showed half of the invasive CTBs were hyperdiploid. Gains of chromosome X were more frequent than those involving either 16 or Y. The inactivated X chromosome in placental tissues, which is hypo-methylated, can be reactivated. Therefore, we investigated the status of X-inactivation in this unusual subpopulation of CTBs. As to the methods, CTBs, cells at various stages of differentiation/invasion were isolated and assayed for *Xist* mRNA expression and histone H3 trimethylation at lysine 27 (H3K27) by using RNA FISH and immunocytochemistry, respectively. The status of X-inactivation was confirmed by using DNA FISH at chromosome X and the stage of CTB differentiation was assessed by HLA-G immunostaining, which positively correlates with acquisition of an invasive phenotype. Most CTBs isolated from the placentas of female fetuses, including invasive CTBs derived from explant culture, were positive for *Xist* expression showing a single RNA domain. However, the expression of H3K27 on CTBs ranged from 40% to 100% of cells. The majority of HLA-G-positive CTBs was H3K27-positive compared to approximately one third of HLA-G-negative cells (76% vs. 30%). These findings suggested that invasive CTBs accumulated H3K27 expression, which is associated with the inactivated X chromosome. In conclusion, invasive CTBs isolated from the placentas of female fetuses are positive for *Xist* RNA expression, and X-inactivation is maintained by H3K27 methylation.

P112

THE EXPRESSION OF PROINFLAMMATORY CYTOKINES IN RADICULAR CYSTS

KARTANOWICZ, D.¹, LOS, D.², DIJAKIEWICZ, M.², MYŚLIWSKI, A.¹ and KMIEC, Z.¹

*1*Dept. Histology&Immunology, *2* Dept. Dental Surgery, Medical University of Gdańsk, Poland

Abstract: Odontogenic cysts belong to bone-destroying lesions of the maxillofacial skeleton, with radicular cysts occurring most often. It has been recently suggested that cytokines may play a role in the development of radicular cysts. The aim of the study was to determine the possible involvement of three proinflammatory cytokines, IL-6, IL-8, and TNF in the development of radicular cysts by measuring the relative levels of cytokines' mRNA and concentration of cytokines in cysts' fluid. We examined 43 patients with radicular cyst (24 women and 19 men, mean age 45 ± 5.4 y, respectively) and 15 gingival biopsies of healthy patients who had 8th tooth extracted. Total RNA was isolated from cyst and gingival tissue and subjected to reverse transcription. mRNA levels were determined by measurements of PicoGreen®-fluorescence of PCR-amplification products and related to the amount of β -actin mRNA in the same tissue. Concentration of cytokines was determined by ELISA (Biosource). Routine blood examination was carried out before the cystectomy. Histopathological examination confirmed the clinical diagnosis. The relative amount of IL-6, IL-8, and TNF mRNA in radicular cysts was $51.4\pm 25\%$, $100.1\pm 63\%$, and $63.6\pm 40\%$ (mean \pm SE) as compared to β -actin gene expression. The levels of IL-8 mRNA were lower in gingival biopsies than in cyst tissue, whereas the relative amounts of IL-6 and TNF were similar. In all patients cytokine fluid levels were at least twice higher in men as compared to women. We observed positive correlation between ESR (Erythrocyte Sedimentation Rate) and TNF, and IL-8 concentration in cyst fluid ($r=0.64$, $p<0.05$ for both cytokines). We conclude that TNF, IL-6 and IL-8 are involved in the pathogenesis of radicular cysts.

P113

NOVEL FEATURES OF THE PALATINE TONSILS IN IGA NEPHROPATHY. - A ROLE OF THE MUCOSAL IMMUNE SYSTEM

NAGURA, H.^{1,2}, HOTTA, O.³, TAGUMA, Y.³ and HOZAWA, K.⁴

¹Department of Athletics and Nutrition, Sendai Collage, Sendai, Japan; Divisions of ²Pathology, ³Nephrology and ⁴Otolaryngology, Sendai Shakaihoken Hospital, Sendai, Japan. (nagura@sendai-shaho.com)

Abstract: IgA nephropathy (IgAN) is defined as a form of glomerulonephritis in which IgA, particularly J-chain-linked IgA1 in an immune complex form dominate or codominate within the glomular deposits. Moreover, the body's synthesis of IgA exceeds that of all other immunoglobulin classes combined. That is, we consider a view of IgAN as a form of immune complex diseases which mucosally derived antigens elicit mucosal antibody synthesis to generate pathogenic immune complexes. Clinically upper respiratory infection and inflammation including tonsillitis often precede IgAN, and tonsillectomy is effective for the treatment of this disease. In the present study, palatine tonsils removed from IgAN patients were immunohistologically analyzed, and compared with those from patients with chronic recurrent tonsillitis.

Palatine tonsils from IgAN patients were rich in germinal centers, and their size and distribution were irregular and the outline of follicular areas was hazy. The interfollicular T cell area was much broader and infiltrated by more B cells than those from chronic recurrent tonsillitis. The HLA-DR⁺ reticulated sponge-like epithelial layer of tonsillar crypts contained many B cells (surface CD20⁺ IgM⁺ B7⁺), T cells (CD4⁺ CD80⁺ CD86⁺) and plasma cells (IgA⁺ or IgG⁺), macrophages, and also interdigitating dendritic cells (S-100⁺). By high dose steroid therapy, germinal centers became smaller or disappeared, and B cells and plasma cells almost disappeared in the crypt epithelial layer. From this present study, we strongly favor the view that the development of IgAN to be a consequence of altered and dysregulated mucosal immune responses, and the tonsil seems to be a unique organ causing initial and / or progressive events to generate glomerular deposited immune complexes in IgAN.

P114

MELATONIN: A NOVEL PROTECTIVE AGENT AGAINST DRUG'S OXIDATIVE INJURYBONOMINI, F.¹, TENGATTINI, S.¹, REITER, R.J.², REZZANI, R.¹ and BIANCHI, R.¹

¹Department of Biomedical Sciences and Biotechnology, Division of Human Anatomy, University of Brescia, Italy; ² Department of Cellular and Structural Biology, University of Texas Health Science Center, San Antonio, TX, USA. (rezzani@med.unibs.it)

Abstract: Melatonin is a derivative of the essential amino acid tryptophan and it is best known as being produced in the pineal gland. It is known that melatonin reduces free radical damage by acting directly as a free radical scavenger and, indirectly, by stimulating antioxidant enzyme activities after its binding to specific membrane receptors (MT1, MT2). This study was designed to examine the beneficial effects of melatonin on Cyclosporine A (CsA)-induced cardiotoxicity. Additionally, we investigated the ability of melatonin to protect the heart via melatonin receptors.

For this study we used five groups of Wistar rats treated for 21 days: the control group treated with olive oil subcutaneously (sc), the second one treated with CsA (15 mg/kg/day sc), the third one treated intraperitoneally (ip) with melatonin (1 mg/kg/day), the fourth one melatonin was administered concurrently with CsA and in the last group melatonin was injected with CsA and luzindole, an antagonist of melatonin receptors. After the end of treatment the rats were killed and the hearts were removed. We evaluated heart morphology by sirius red staining, the expressions of: a protein involved in oxidative stress (Hsp70) and the antioxidant enzymes such as catalase and glutathione by immunohistochemical and biochemical methods.

The co-administration of melatonin increased the antioxidant enzyme levels reduced by CsA treatment and normalized altered cardiac morphology. Moreover the CsA-induced high Hsp70 expression was normalized by melatonin.

In conclusion our study shows that melatonin significantly reduces CsA-induced cardiotoxicity and this reduction was mediated by the binding of melatonin to its membrane receptors.

P115

MITOCHONDRIAL MOSAICS IN THE LIVER OF PATIENTS WITH PEARSON EN ALPERS-HUTTENLOCHER SYNDROMES

ROELS, F.¹, VERLOO, P.², SENECA, S.³, MEERSSCHAUT, V.⁴, EYSKENS, F.⁵, DE CONO, N.², SMET, J.², MARTIN, J.J.⁶, PRAET, M.¹ and VAN COSTER, R.²

¹Pathology, Ghent University, ²Pediatrics, Ghent Univ. Hospital, ³Ctr. for Medical Genetics, Free University VUB Brussels, ⁴Radiology, Ghent University Hospital, ⁵Metabolic Unit Antwerp, ⁶Neurology, University Antwerp, Belgium. frank.roels@ugent.be

Abstract: Mitochondrial heteroplasmy has previously been visualized by cytochrome oxidase staining (COX) in muscle, but not in liver. We studied 2 patients, a girl 2.5 y old with Pearson syndrome (PS)(pancytopenia and exocrine pancreatic failure), and a boy aged 14 m with Alpers-Huttenlocher syndrome (APS)(myoclonal epilepsy, onset at 11 m, and hepatic disease). Both patients showed mitochondria with weak or absent COX activity in many liver parenchymal cells that otherwise looked viable; and strong mitochondrial staining in adjacent hepatocytes. COX activity was localized by DAB with and without cytochrome c after glutaraldehyde fixation, for light and electron microscopy. Mitochondrial staining was positive in bile duct epithelium, endothelium, Kupffer cells, vascular smooth muscle and neutrophils. In the Alpers patient mtDNA of skeletal muscle was depleted for 3/4 as seen by real time PCR. In blood of the girl with PS a deletion of 4091 bp located between positions 5969 and 10060 was found in 50 % of the mtDNA. In her liver decreased protein and activity of complex IV, and subcomplexes of complex V were detected by blue native PAGE. Both patients had increased plasma lactate, but no ragged red fibers in muscle. OXPHOS activities were normal in muscle, fibroblasts and blood cells. Brain MRI of the PS patient demonstrated in the white matter of both frontal lobes a large cavitation with absence of the lactate MR spectrum. MRI of the AHS patient initially showed only slight diffuse cortical atrophy, which has become more obvious while intractable convulsions persisted. The boy died at 3 years of age.

These results demonstrate the merit of liver biopsies and COX staining for fast diagnosis of oxidative phosphorylation defects, and as a clue to their phenotypic variation.

P116

PROTECTIVE EFFECT OF RED WINE POLYPHENOLIC COMPOUNDS, PROVINOLS™, AGAINST DRUG NEPHROTOXICITY THROUGH ITS ANTIOXIDANT AND ANTI- APOPTOTIC PROPERTIES

TENGATTINI, S.¹, BONOMINI, F.¹, PECHÁNOVÁ, O.²,
ANDRIANTSITOHAINA, R.³, BIANCHI, R.¹ and REZZANI, R.¹

¹Dept of Biomedical Sciences and Biotechnology, Division of Human Anatomy, University of Brescia, Italy; ²Institute of Normal and Pathological Physiology, Slovak Academy of Sciences, Bratislava, Slovak Republic; ³Biologie Neuro-Vasculaire Intégrée, UMR INSERM 771 - CNRS 6214, School of Medicine, Angers, France. (rezzani@med.unibs.it)

Abstract: The beneficial effects of fruits, vegetables or red wine may be in part explained by the presence of polyphenols which have a multitude of biological activities including antioxidant and free radical scavenger properties. The aim of the present study was investigate whether a polyphenol extract obtained from red wine, Provinols™ (PV), protects against cyclosporine A (CsA)-induced nephrotoxicity and this through its antioxidant and anti-apoptotic activity. For this study, we used male Wistar rats treated for 21 days and divided into four groups: one control group treated subcutaneously (sc) with olive oil; one group treated with PV (40 mg/kg/day by oral administration in tap water); two groups treated with CsA (15 mg/kg/day by subcutaneous injections) and with CsA plus PV respectively. After the end of treatment, the rats were killed and the kidneys were removed. We evaluated kidney morphology by standard staining, the expression of superoxide dismutase (SOD), glutathione (GSH) and caspase 3 by immunohistochemical and biochemical methods. SOD and GSH play important roles as antioxidant enzymes whereas caspase 3 is involved in apoptotic pathways.

Our results showed that co-administration of CsA and PV greatly re-established the normal renal morphology and the levels of SOD and GSH. Moreover, co-administration of CsA and PV decrease the high level of caspase 3 expression induced by CsA treatment.

In conclusion, these results suggest that PV prevents renal damage associated with CsA and this is associated with both reduction of oxidative stress through an increase of the restoration of antioxidant enzymes and decrease of proteins involved in apoptosis. These results provide a further pharmacological basis for the beneficial effects of plant-derived polyphenols against CsA-induced renal damage in addition to their anti-inflammatory properties reported in our previous studies.

P117

SUBCUTANEOUS INJECTION OF EPIGALLOCATECHIN GALLATE INTO DYSTROPHIN-DEFICIENT MDX MICE AMELIORATES MUSCULAR DYSTROPHY

NAKAE, Y.¹, HIRASAKA, K.², GOTO, J.², NIKAWA, T.², SHONO, M.³,
YOSHIDA, M.⁴, and STOWARD, P.J.⁵

¹Dept. of Oral & Maxillofacial Anatomy, ²Dept. of Nutritional Physiology & ³Support Centre
for Advanced Medical Sciences, Institute of Health Biosciences, University of Tokushima
Graduate School, Tokushima, Japan; ⁴National Centre of Neurology and Psychiatry, Japan;
⁵School of Life Sciences, University of Dundee, UK. (ynakae@dent.tokushima-u.ac.jp)

Abstract: Duchenne muscular dystrophy is a fatal degenerative disorder of human muscles caused by the lack of a cytoskeletal protein, dystrophin. At present the causal mechanism of the disease is still unknown and there is no effective therapeutic treatment. Previously, we found that dystrophin-deficient muscles suffer more oxidative damage than normal controls and have hypothesised that oxidative stress is related to the pathology of muscular dystrophy (Nakae et al. 2004, 2005). The aim of the present study was to investigate the effects of an anti-oxidant, epigallocatechin gallate (EGCG) purified from green tea extracts, on dystrophin-deficient skeletal muscles in *mdx* mice. Five mg EGCG/kg body weight dissolved in physiological saline was injected subcutaneously daily into the backs of *mdx* and normal mice four times a week for 8 weeks after birth. *Mdx* and normal controls were injected with saline only. At the end of this time, diaphragm, soleus and lingual muscles and blood were removed. The high activity of serum creatine kinase of *mdx* mice was reduced to about a fourth by the EGCG administration. However, the EGCG treatment did not affect the maximum intensities of the specific tetanic force of *mdx* and normal soleus muscles, but the half-relaxation time from the maximum tetanic force of *mdx* muscles, but not normal muscles, became 1.8 times longer. The expression of a dystrophin homologue, utrophin, was increased in the subsarcolemmal region in myofibres in the diaphragm and lingual muscles of the EGCG-injected *mdx* mice. Western blotting of homogenates of *mdx* diaphragm muscles also suggested a slight increase in utrophin expression. In contrast, EGCG did not significantly affect the amount of utrophin mRNA in *mdx* diaphragm muscles as determined by real-time PCR analysis. Our results suggest that EGCG improves dystrophin-deficient skeletal muscles by up-regulation of utrophin protein compensating for lack of dystrophin.

P118

CLINICOPATHOLOGICAL EXAMINATION OF FOUR CASES OF HUMAN ALLOGRAFT RECIPIENTS(A KIDNEY, A LIVER, A HEART, AND A PART OF AORTA)

TANNO, MASATAKA¹, HAYAKAWA, KINNYA², IZUMI, HIROSI, KUME, KEIKO, FUKUMURA, YUKI and SUDA, KOICHI³

¹Department of the Clinicolaboratory ,JR Tokyo Hospital, ²Daito University ³Juntendo University

Abstract: Allograft transplantations are relatively rare in Japan. We have experienced 4 allograft recipients in our hospital since 1996, we reported them clinicopathologically. Among the 4 cases, the recipients of kidney, heart and aorta will be reported mainly from the findings of autopsy. As to the recipients of liver, biopsy findings are focused on.

Case 1 (Kidney); The patient, 54 years old male, received kidney transplantation because of chronic renal failure. Despite of transplantation, he expired 4 years after surgery. In autopsy, mesangial proliferative nephritis (MPGN)-like change and arterio-arteriosclerosis were marked in transplantation kidney, indicated chronic rejective reaction.

Case 2 (Liver); The patient, 70 year old male, received liver transplantation because of liver cirrhosis. Biopsied material taken 5 years later, of transplantation, and with no rejective reaction will be shown in the conference. The patient is now good health.

Case 3 (Heart); 7year old boy had heart transplantation in France because of the transposition of the great vessels (TVG), when he was one years old. Seven years later, he died due to acute heart failure in our hospital. With autopsy, marked fibrous thickening of coronary arteries were recognized, suggesting chronic rejection.

Case 4(Aorta); Patients, 63-year old man was received allograft transplantation because of abdominal aortic aneurysm due to infection. He was expired a months after the aortic transplantation. With autopsy, allograft showed little or no change, by thanks to the chemical treatment of the allograft.

Summary

We reported four recipients of allograft of several organ/tissue. The important of arterial lesions are suggested in seeing chornic rejective changes.

P119

MORPHOLOGICAL ALTERATIONS OF SUBMANDIBULAR GLANDS CAUSED BY CYCLOSPORIN A IN RAT

SAGA, T., NISHIMURA, H., KITASHIMA, S., YAKEISHI, A., YOSHIDA, M., YAMAKI, K.

*Department of Anatomy, Kurume University, School of Medicine, Fukuoka, Japan.
(saga@med.kurume-u.ac.jp)*

Abstract: Cyclosporin A (CSA) is a T-lymphocyte-selective immunosuppressant. While the adverse effects of CSA such as nephrotoxicity, hepatotoxicity and pancreatotoxicity have been reported, the detailed mechanisms of its cytotoxicity remain unclear. CSA is also known to accumulate in the salivary glands and secrete in saliva. In this study, ultrastructural changes of rat submandibular glands after CSA treatment were examined. Adult male Wistar rats received oral administration of CSA at 50, 100 and 150mg/Kg/day and 5 days after beginning administration, submandibular glands were removed and observed by light and electron microscopy. Moreover, some of the rats after 5 days administration of 100mg/Kg/day CSA, withdrew from CSA administration for 2 weeks and the submandibular glands were observed. Dose-dependent morphological alternation was observed in rat submandibular glands, and shrinkage of the cytoplasm and swelling of mitochondria occurred in acinar and granular duct cells. Moreover, a decrease in the number of mature secretory granules of granular duct cells was found in submandibular glands treated with every dose of CSA. The degrees of these changes became prominent in the animals that received higher doses of CSA. Two weeks after CSA treatment, the fine structures of the submandibular glands were almost restored; consequently, mitochondrial dysfunction might be due to the direct toxic effects of CSA. Furthermore, we consider that disturbance of protein synthesis and secretion might be induced by a secondary cytotoxic action of CSA.

Index (Author, Page number)

ABLIMIT, A. 94
ADRYCH, K. 143
AKAHANE, T. 80
AKHTER, N. 101
ALBERTINI, R. 89
AMAGASA, T. 111
AN, S. 61, 123
ANDRIANTSITOHAINA, R. 155
AOKI, D. 122, 137
AOKI, T. 94
AOYAMA, F. 115
ARAKI, ASUKA 67
ASHER, D.M. 147
ASHWORTH-SHAPE, JULIA 148
ASO, H. 104, 106
ASO, HISASHI 113
ATEN, J. A. 98

BACIK, I. 147
BAGRI, A. 132
BAMBA, H. 90
BARKER, P.E. 47
BARKER, PETER E. 57
BARROSO, MARGARIDA 40
BASKIN, D. G. 6
BAUMGARTNER, A. 45, 131, 136, 150
BEER, T. 138
BIANCHI, R. 89, 153, 155
BIENIARZ, CHRISTOPHER 148
BIGLIARDI, P.L. 127
BIGLIARDI-QI, M. 127
BLASIC, JOE 57
BONOMINI, F. 153, 155
BONTE, F. 127
BORSANI, E. 89
BOUTTE, ANGELA 32
BRYANT, J. 149
BUTLER, L. 46

CAMPBELL, D. 36
CARPENTER, ANNE 148
CASAÑAS, N. 93
CEBASEK, V. 110
CERVENAKOVA, L. 147
CHANG, W.S. 132
CHASE, R.M. 142
CHEN, I. 5
CHEN, T.C.S. 5
CHENG, J. 68, 69, 71
CHENG, JINGLEI 78
CHIDA, K. 74
CHILDS, G.V 101

COCKETT, N.E. 119
COLEMAN, I. 138
COLEMAN, R. 138
CONCHELLO, J-A. 14
CONCHELLO, JOSÉ-ANGEL 12
CRANE, C. 101
CURRELI, S. 149

DATE, Y. 86
DATE, YUKARI 87
DATTA, M. 138
DAWSON, D.M. 142
DE CONO, N. 154
de PABLOS, E. 93
DE WITT HAMER, P.C. 38
DENARO, F.J. 149
DEUTSCH, E.W. 36
DIJAKIEWICZ, M. 151
DOHI, K. 84

EGASHIRA, N. 7, 76, 133, 134
EGASHIRA, NOBORU 146
EJIMA, K. 123
EL-HUSSEINI, A. 5
ERZEN, I. 110
EYSKENS, F. 154

FARRELL, MICHAEL 148
FEIG, JONATHAN E. 9
FERLATTE, C. 150
FERNANDEZ-SUAREZ, M. 5
FISHER, EDWARD A. 9
FISHER, S. 150
FOLKESSON, H.G. 121
FUJII, SHINOBU 109
FUJII, Y. 49, 83
FUJIKAWA, K. 129
FUJIMOTO, T. 68, 69, 71
FUJIMOTO, TOYOSHI 78
FUJIOKA, A. 63
FUJISHITA, A. 123
FUJITA, A. 68, 69, 71
FUJITA, AKIKAZU 78
FUJIWARA, K. 100
FUKUMURA, YUKI 157
FUNAKOSHI, K. 88
FURUKAWA, S. 90
FURUYA, S. 108

GALLI, M. 149
GALLO, R.C 149
GAO, X. 47
GARDNER, H. 23
GELMANN, E. 138
GERROW, K. 5
GIFFORD, D. 138
GOTO, J. 156

GOTO, T. 50
GREGER, K. 13
GROGAN, THOMAS M. 37, 148
GROUNDS, M.D. 119
GUAN, J. 136
GUAN, JIAN-LIAN 87

HAAS, R.L. 99
HAGIWARA, H. 94
HAILEY, DALE 1
HARADA, TAKAYUKI 67
HARADA, Y. 42
HARAGUCHI, CELINA M. 66, 70
HARAGUCHI, T. 135
HASHIKAWA, T. 108
HAWLEY, S. 138
HAYAKAWA, KINNYA 157
HAYASHI, S. 106
HAYASHI, SHINICHIRO 113
HELL, S.W. 11
HENMI, A. 8
HIGASHIGUCHI, A. 137
HIGUCHI, N. 54
HIRASAKA, K. 156
HIRASAWA, A. 137
HIRATA, SHUJI 66
HIROSE, KENZO 4
HIROTA, S. 22
HISA, Y. 90
HISHIKAWA, Y. 61, 123
HITOMI, T. 42
HOLDEN, MARCIA 57
HONDA, E. 63
HONMA, T. 8
HOOD, L. 138
HORIBE, YOSHIHIDE 109
HOSHI, KAZUHIKO 66
HOTTA, O. 152
HOWARTH, M. 5
HOZAWA, K. 152
HUANG, A. 138

IDE, S. 115
IKUSE, TOSHIMI 109
IMAMURA, T. 90
INADA, K. 53
INOMOTO, C. 76
INOUE, S. 51
INUBUSHI, TOSHIRO 85
IRIE, T. 71
IRUTHAYANATHAN, M.J.J. 101
ISHIKAWA, G. 50
ISHIKAWA, Y. 55, 120
ISHIMARU, T. 123
ITOH, J. 34, 48, 76
ITOH, Y. 76
ITOSE, M. 97

IWAMI, J. 54
IWAMOTO, H. 103
IWASA, S. 135
IWASHINA, M. 135
IZUMI, HIROSI 157

JANACEK, J. 110
JESMIN, S. 116, 121, 124
JOHNSON, B. 101, 147
JOHNSON, E. 121
JOHNSON, E.M. 28
JONKER, A. 38

KAGEYAMA, H. 86
KAGEYAMA, HARUAKI 87
KAGEYAMA, T. 130, 140
KAGEYAMA, TAIHEI 139
KAHOUD, N.S. 132
KAJINAMI, K. 120
KAJIYA, H. 134
KAJIYA, HANAKO 146
KAMEDA, Y. 92
KAMETANI, K. 56, 117
KAMEYA, TORU 139
KAMEYAMA, Y. 54
KAMOSHIDA, S. 53
KANAYAMA, T. 91
KANEKO, T. 114
KARTANOWICZ, D. 143, 151
KATOH, R. 135
KATSUTA, OSAMU 109
KAWATA, M. 97, 129
KAWATA, MITSUHIRO 39
KAWAZU, KOUICHI 109
KEARNEY, KATHLEEN E. 141
KEENER, M.J. 46
KELLER, P.J. 13
KERFOOT, CHRISTOPHER A. 59
KERNAG, CASEY 148
KIKUCHI, M. 102, 105
KIM, PETER 1
KIMURA, H. 90
KINOUE, T. 48
KITAJIMA, M. 123
KITAOKA, T. 71
KITASHIMA, S. 158
KLOCKE, B.J. 18
KMIEC, Z. 143, 151
KNIGHT, M. 119
KNUDSEN, B. 138
KOBAYASHI, A. 111
KOHNO, Y. 80, 125
KOIKE, A. 64, 125
KOIKE, M. 64, 125
KOJI, T. 61, 123
KOJI., T. 35
KOMATSU, K. 8

KOMIYAMA, K. 144
KONDO, T. 135
KRAWCZYK, P.M. 98
KROL, H. 98
KRULL, D.L. 46
KUBINOVA, L. 110
KUBO, T. 82
KUME, KEIKO 157
KURFURST, R. 127
KURIHARA, T. 120
KUROKI, T. 80
KUWANA, R. 111

LANGE, P. 138
LEENSTRA, S. 38
LEVENSON, RICHARD 26
LI, T. 121
LIEBLER, DANIEL 32
LIN, C.W. 5
LIN, D. 138
LINEBAUGH, BRUCE 58
LIPPINCOTT-SCHWARTZ, JENNIFER 1
LIU, A.Y. 36
LOPEZ, M. 121
LORENTZ, HOLGER 1
LOS, D. 151
LU, C.-M. 131, 136

MABUCHI, TADASHI 66
MAEDA, H. 54
MAEDA, S. 116, 124
MAK, J. 132
MAK, W. 150
MANSFIELD, JAMES R. 59
MARTIN, J.J. 154
MARUYAMA, RIRUKE 67
MATSUMOTO, T. 130, 140
MATSUMOTO, TOSHIHIDE 139
MATSUNO, A. 34
MATSUZAKI, T. 94, 126
MAXIMOVA, O.A. 147
MAZZUCHELLI, R. 149
MCDONAGH, M. 119
MCMILLAN, J.R. 79
MEERSSCHAUT, V. 154
MEYER, TOBIAS 2
MINEMATSU, T. 76, 134
MINEMATSU, TAKEO 146
MISAKI, T. 75
MISHIMA, K. 71
MIURA, MASAYUKI 31
MIYAKE, M. 106
MIYAKE, MASATO 113
MIYAUCHI, T. 116, 124
MIYAWAKI, A. 15
MIZUTANI, M. 112
MIZUTANI, Y. 53

MOCHIZUKI, K. 135
MOFFATT, P. 44
MOIN, KAMIAR 58
MONTINE, KATHLEEN S. 32
MONTINE, T. 10
MONTINE, THOMAS J. 32
MÓNZON-MAYOR, M. 93
MORI, M. 50
MORIGUCHI, K. 54
MORIKAWA, SHIGEHIRO² 85
MORIOKA, K. 126
MORIOKA, M. 82
MORITA, I. 111
MORITA, MASAHITO 85
MOSTAGHEL, E. 138
MOWA, C.N. 116, 121, 124
MUKAE, S. 144
MUKAI, N. 111
MURAKAMI, Y. 54
MURATA, S. 135
MYSLIWSKI, A. 143
MYŚLIWSKI, A. 151

NAGAI, RYOZO 128
NAGAI, T. 15
NAGAI, Y. 104, 106
NAGASAKI, MIKA 128
NAGASHIO, R. 130, 140
NAGASHIO, RYO 139
NAGATA, M. 103
NAGATA, T. 56, 60, 72, 117
NAGURA, H. 152
NAKAE, Y. 112, 156
NAKAJIMA, T. 130
NAKAJIMA, Y. 118
NAKAMACHI, T. 84
NAKAMURA, H. 54
NAKAMURA, N. 135
NAKAMURA, Y. 77, 91
NAKANISHI, Y. 8
NAKANO, AKINOBU 67
NAKANO, K. 42
NAKATANI, K. 118
NAKAZATO, M. 86
NAKAZATO, MASAMITSU 87
NAKAZAWA, T. 135
NANCI, A. 44
NAVARRE, W. 142
NELSON, P. 138
NEMOTO, N. 8
NGUYEN, H. 150
NIIOKA, M. 48
NIKAWA, T. 156
NISHI, M. 97, 129
NISHIKORI, K. 82
NISHIMURA, H. 158
NISHIMURA, SATOSHI 128

NISHIMURA, S. 103
NITTA, HIROAKI 37, 148
NOBLESSE, E. 127

OBATA, K. 91
O'CONNOR, D.T. 76
OGASAWARA H. 104
OGASAWARA, H. 106
OGASAWARA, HIDEKI 113
OHASHI, M. 115
OHBA, M. 80
OHIRA, AKIHIRO 67
OHNO, N. 49, 54, 83, 96, 112, 135
OHNO, S. 49, 83, 96, 135
OHSAKI, Y. 68, 69, 71
OHSUMI, YOSHINORI 19
OHTAKI, H. 84
OHWADA, S. 104, 106
OHWADA, SHYUICHI 113
OKANO, H. 90
OKAZAKI, Y. 144
OKI, K. 91
OKIJI, T. 114
OLEA, M. T. 60
OLSOFKA, CLAIRE 65
OMORI, H. 51
OOMURA, Y. 90
OOSAKA, M. 77
OSAMURA, R.Y. 7, 34, 76, 133
OSAMURA, R.Y.¹ 134
OSAMURA, ROBERT Y. 146
OUDES, A. 36

PAMPALONI, F. 13
PAPKA, R.E. 121
PAQUETTE, S.M. 27
PASCAL, L. 36
PATTERSON, GEORGE 1
PEALE, F. 132
PECHÁNOVÁ, O. 155
PERIASAMY, AMMASI 40
PESTANO, GARY A. 148
PETERSON, R.A. 46
PETRICOIN, EMANUEL F. 21
PICCARDO, P. 147
POMEROY, K.L. 147
PRAET, M. 154
PRETLOW, THERESA P. 141
PRETLOW, THOMAS G. 141

QIAO, H. 79

RASCH, E.M. 62
RAY, P. 47
RAY, R. 47
REITER, R.J. 153
REITS, E. 98

REZZANI, R. 153, 155
RHEINHARDT, J. 23
RIBARIC, S. 110
RICCI, F. 89
RICHARD M. 59
RIVA, A. 149
ROBINSON, J.M. 50
RODELLA, L.F. 89
ROELS, F. 154
ROMERO-ALEMAN, M.M. 93
ROSA-MOLINAR, E. 14
ROTH, K.A. 18, 29
ROYSAM, B. 41
RUDY, DEBORAH 58

SADO, Y. 51
SAGA, T. 158
SAITO, N. 3, 25
SAITO, S. 83
SAITOH, E. 122
SAITOH, S. 49
SAKABE, M. 118
SAKAI, K. 108
SAKAMOTO, M. 137
SAMENI, MANSOUREH 58
SANTOS, E. 93
SASANO, HIRONOBU 20
SATAKE, O. 120
SATINO, T. 75, 77
SATO, Y. 130, 140
SATO, YUISHI 139
SATO, Y. 75, 77
SAWAGUCHI, A. 115
SAWTELL, N.M. 99
SCHNEBERT, S. 127
SEKI, T. 8
SENECA, S. 154
SENOO, H. 71
SERRANO-VELEZ, J.L. 14
SHACKA, J.J. 18, 29
SHI, SHAN-RONG 52
SHIBATA, M. 18
SHIBATA, Y. 61, 123
SHIGEYOSHI, Y. 63
SHIMIZU, H. 79
SHIMOMURA, M. 79
SHIMOMURA, R. 53
SHINOMIYA, KATSUHIKO 109
SHIODA, S. 84, 86
SHIODA, SEIJI 87
SHIOGAMA, K. 53
SHODA, TOMOKO 66
SHONO, M. 156
SLAVOFF, S. 5
SLOANE, BONNIE¹ 58
SMET, J. 154
SMITH, A.A 145

SMITH, D. 121
SMITH, R. F. 145
SMOCZYNSKI, M. 143
SNYDER, J.A. 65
SODEK, J. 81
SOKOLOWSKA, I. 143
SONG, YANG 85
STACCHIOTTI, A. 89
STANISLAWOWSKI, M. 143
STELZER, E.H.K. 13
STOWARD, P.J. 156
SUDA, H. 114
SUDA, KOICHI 157
SUGANUMA, T. 115
SUGASAWA, J. 125
SUGITANI, M. 8
SUGIURA, SEIRYO 128
SUN, CHI-KUANG 17
SUSUMU, N. 122, 137
SUZUKI, A. 122, 137
SUZUKI, K. 81
SUZUKI, N. 137
SUZUKI, T. 94
SUZUKI, TAKESHI 24

TABATA, S. 103
TAFFS, R.E. 147
TAGUCHI, M. 74
TAGUMA, Y. 152
TAHARA, SHIGEYUKI 146
TAJIKA, Y. 94
TAKAHASHI, K. 105
TAKAMATSU, T. 16, 42, 43
TAKASHIMA, N. 63
TAKATA, K. 94
TAKATA, K.² 126
TAKEDA, A. 88
TAKEI, M. 133, 134
TAKEI, MAO 146
TAKEKOSHI, S. 7, 34, 76, 134
TAKEKOSHI, SUSUMU 146
TAKENOYA F. 86
TAKENOYA, FUMIKO 87
TAKESHITA, T. 50
TAKETA, Y. 104, 106
TAKIGAMI, S. 107
TAKIZAWA, T. 50
TALATI, RONAK 40
TAMADA, Y. 137
TAMAKI, H. 73
TANABE, K. 122
TANAKA, M. 79
TANI, T. 15
TANNO, MASATAKA 157
TAUCHI-SATO, K. 68
TAUPENOT, L. 76
TAYLOR, CLIVE R. 52

TELLAM, R. 119
TENGATTINI, S. 153, 155
TERADA, N. 49, 83, 96, 135
TERAMOTO, A. 133, 134
TERAMOTO, AKIRA 146
THOMPSON, R.L. 99
TING, A.Y. 5
TOMONO, Y. 51
TOOYAMA, I. 85, 90
TORRES-VASQUEZ, I. 14
TOSHINAI, KOJI 87
TOYODA, K. 90
TRUE, L. 138
TRUE, L.D. 36
TSUIKI, E. 71
TSUIKI, E.¹, FUJITA, A. 71
TSURUTA, T. 144
TSUTSUMI, Y. 53
TUNG, CHING 58

UCHIYAMA, Y. 18, 30
UEDA, T. 55, 120
ULZIBAT, S. 123
UMEMURA, S. 7, 76
UNGER, E. R. 33
USIP, S. 121

VAN COSTER, R. 154
VAN NOORDEN, C.J.F. 38
VASILYEVA, I. 147
VERLOO, P. 154
VESSELLA, R. 138
VIÑOLY, R. 93
VUOCOLO, T. 119

WALK, ERIC 148
WALLRABE H. 40
WATANABE, H. 91
WATANABE, K. 104, 106
WATANABE, KOUICHI 113
WATANABE, M. 91
WATANABE, T. 48
WAZEN, R.M., 44
WEIER, H. 150
WEIER, H.U.G. 45
WEIER, H.-U.G. 131, 136
WEIER, J. 150
WEIER, J.F. 45, 131, 136
WHITE, J.D. 119
WIERZBICKI, M. 143
WIERZBICKI, P. 143
WOLTJER, RANDALL 32
WYPYCH, J. 143

XIAO, Y. 47
XIAO, YAN 57

YABUMOTO, M. 91
YAKEISHI, A. 158
YAMADA, S. 81
YAMAGUCHI, T. 104, 106
YAMAGUCHI, TAKAHIRO 113
YAMAKI, K. 158
YAMAMOTO, S. 79
YAMANE, T. 135
YAMAOKA, Y. 16, 42, 43
YAMASHINA, S. 73
YANAGAWA, Y. 91
YANES C. 93
YASHIRO, T. 100, 102, 105, 107
YASUDA, M. 7
YATABE, M. 102
YOKOTA, SADAHI 66, 70
YOSHIDA, M. 156, 158
YOSHIMURA, F. 54

ZAEDI, S. 116, 124
ZELLA, D. 149
ZENG, H. 131, 136
ZHAO, L-Y. 114
ZHIQIANG, C. 127
ZHOU, LI 67
ZWINDERMAN, A.H. 38

Leader in Developing Novel Labeling and Detection Systems since 1976

For 30 years Vector Laboratories has been supplying the research and diagnostic markets with the highest quality labeling and detection systems for a variety of applications.

- Peroxidase- and Alkaline Phosphatase-based Detection Systems including VECTASTAIN® ABC Reagents
- NEW ImmPRESS™ Peroxidase "Micropolymer" Reagents for Immunohistochemistry
- Mouse on Mouse (M.O.M.™) Immunodetection Kits
- Streptavidin and Avidin Conjugates
- Chromogenic, Fluorescent, and Chemiluminescent Enzyme Substrates
- Labeling Reagents (Biotin, Fluorochromes, Haptens, Sugars) for Proteins, Nucleic Acids, Carbohydrates
- Lectins
- Primary and Secondary Antibodies
- Pathology Reagents and Specialty Products



Vector Laboratories, Inc.
30 Ingold Road • Burlingame, California 94010
Tel: 650-697-3600 • Order Dept.: 800-227-6666 • Fax: 650-697-0339
Email: vector@vectorlabs.com • www.vectorlabs.com

SPECIALIZING IN SECONDARY ANTIBODIES



Jackson ImmunoResearch
LABORATORIES, INC.

www.jacksonimmuno.com

Digital Samples. Fast. Safe. Ahead of Our Time.

Mirax Scan. Superior in Digital Pathology.



- Digital samples with outstanding image quality
- Greater efficiency through fully automated cycles, even at high throughput
- Worldwide availability of data and easy long-term archiving
- The automated system solution for digital pathology

Mirax Scan from Carl Zeiss
Designed for the future

Carl Zeiss Microimaging, Inc.
1.800.233.2343
www.zeiss.com/mirax



We make it visible.

N.A.C.C.

Nippon Automatic Control Company



Innovative solutions for cancer diagnostics

- IHC antibodies
- IHC detection kits and reagents
- CISH™ Probes
- MaxArray™ Tissue Microarrays

www.invitrogen.com/pathology

 invitrogen

EMD | Life Sciences

www.invitrogen.com

Seeing life in a new light.



cri

Dramatically improve your images.



Nuance™ Multispectral Imaging System

- Immunohistochemistry
- Tissue microarray screening
- High-content screening
- Brightfield or fluorescence microscopy
- Remove contrast-robbing autofluorescence
- Improve sensitivity
- Detect and separate multiple signals, even when spatially colocalized
- Achieve results in seconds

Contact us to learn more
about Nuance by calling
1.800.383.7924 or by visiting
www.cri-inc.com/nuance.

Experience the Pathology Lab of Your Future



Experience
Ventana

Experience the improvement in productivity and patient care afforded by the seamless integration of our innovative and proven workflow, diagnostic, and customer care solutions.

- Workflow Solutions
- Diagnostic Solutions
- Customer Care

800-227-2155

www.ventanamed.com

Innovations in Science and Medicine



Nikon

YOUR MICROSCOPY

SOURCE FOR HISTOLOGY



www.nikonusa.com

1-800-52-NIKON



Life Imaging Services

LIFE SUPPORT...



Integral Temperature Control

Gas & Humidity Control

Special Mechanics,
Electronics, Optics

Full Custom Design

for every light
microscope
(widefield
confocal
inverted
upright
etc.)



...FOR LIVE IMAGING

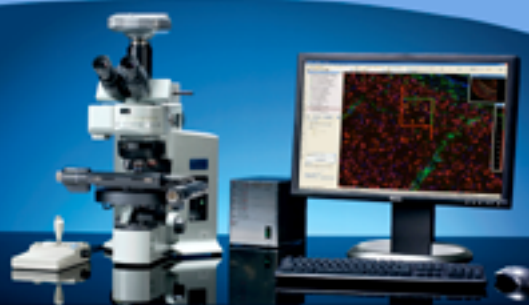
Life Imaging Services GmbH
CH-4153 Reinach Switzerland
info@lis.ch www.lis.ch +41 61 7116461

mbf
BIOSCIENCE

MicroBrightField, Inc.

The Foremost Systems
for
Stereology
Neuron Tracing
Serial Reconstruction
Morphometry
Virtual Microscopy

Trusted Solutions for Research
for more than 19 years



1.802.288.9290
www.mbfbioscience.com

The Best Microscopy Imaging Software Just Got Better

Introducing Imaris 5.0 for the Mac and PC



Interactive Visualization, Quantification, Tracing and Tracking. Imaris gets results fast.

Imaris is the leading software for interactive image analysis for 3D+4D microscopy. Through constant innovation it has shaped the way microscopists work with images for the past 12 years. Imaris 5.0 leverages these years of experience to bring this best in class software to the Macintosh Platform. Imaris seamlessly links visu-

alization and quantification enabling much faster interpretation of even huge data sets and allows researchers to produce results worthy of publication in the top journals. There is no longer a need to improvise, Bitplane offers customers a complete solution.

www.bitplane.com ussales@bitplane.com 1-888-3D-BITPX (332-4879)

the image revolution starts here.



BITPLANE
SCIENTIFIC SOLUTIONS